UNIVERSITÀ DEGLI STUDI DI UDINE

Dottorato di Ricerca in Scienze e Biotecnologie Agrarie

Ciclo XXIV

Coordinatore: Prof. Mauro Spanghero

TESI DI DOTTORATO DI RICERCA

BUILDING CATALOGUES OF GENETIC VARIATION IN POPLAR

DOTTORANDA
Sara Pinosio

RELATORE
Prof. Michele Morgante

CORRELATORE
Dott. Fabio Marroni

ANNO ACCADEMICO 2011-2012

Contents

Summary

The work described in the present thesis was carried out in the framework of ENERGYPOPLAR, a EU-funded project aimed at developing poplar trees with enhanced agronomical traits for industrial production of bioethanol. In accordance with the project aims, the work pursued two main objectives: 1) the identification of SNP markers for the selection of trees carrying beneficial alleles for biofuel production, and 2) the characterization of the genome-wide interspecific sequence divergences as potential markers of heterosis.

Lignin is one of the most important limiting factors in the conversion of plant biomass to biofuels (Vanholme *et al.*, 2008) and altering lignin structure or reducing lignin content can improve biofuel production (Jung and Ni, 1998; Li *et al.*, 2008). For this reason we analyzed the natural genetic variation in different genes involved in lignin biosynthesis to identify natural mutations affecting the coding sequence of these genes. First, we studied naturally occurring polymorphisms (SNPs and small indels) in *CAD4* gene (cinnamyl alcohol dehydrogenase) in a large collection of 384 *Populus nigra* individuals originating from various geographical areas in Europe by means of Sanger sequencing (Chapter 2). We identified 45 SNPs (6 non-synonymous), one insertion and 5 deletions. Three of the six non-synonymous mutations had a frequency lower than 1% and would have been difficult to identify in smaller samples. With this analyses we identified carriers of multiple mutations to be assessed for lignin quality and quantity; individuals showing significant alterations in lignin content will then be used in conventional breeding programs.

With the advent of Next Generation Sequencing (NGS), sequencing abilities increased and we extended the study by increasing both sample size and number of candidate genes. We used NGS Illumina technology to study the natural variation in genes involved in the lignin biosynthesis pathway in a larger *Populus* population (Chapter 3). We used pooled multiplexed NGS to screen 768 *Populus nigra* accessions for mutations in five genes involved in lignin biosynthesis (*CAD4, HCT1, C3H3, CCR7* and *4CL3*)

and developed a novel workflow for SNP detection. Applying our workflow to the whole data set, we identified 37 non-synonymous SNPs in five genes involved in lignin biosynthesis, one of which caused a premature stop codon (C243*) in *HCT1* gene. Carriers of the stop codon have been selected for extensive phenotypic evaluation, and will be used in conventional breeding program to obtain offspring with improved lignin composition. Sensitivity and specificity of the method were extremely high, allowing an accurate estimation of allele frequencies and population genetic parameters. We concluded that our workflow based on pooled multiplexed NGS is an efficient and accurate method to screen a large number of individuals for mutations providing the basis for a next generation Ecotilling method (Comai *et al.*, 2004).

To characterize the genome-wide interspecific sequence divergence among poplar parental species, we performed whole genome next-generation sequencing of 18 poplar accessions: 4 *Populus nigra* accessions, 2 *Populus deltoides* and 12 *P. nigra* x *P. deltoides* F1 hybrids. We studied the genetic variation present in the different poplar species, focusing on the detection of two different classes of structural variants (SVs): 1) insertion/deletion polymorphisms related with the transposable elements activity (Chapter 4) and 2) larger copy number variants (CNVs) (Chapter 5).

For the detection of insertions and deletions we exploited the paired-end mapping information generated from next-generation sequencing data by comparing *P. nigra* and *P. deltoides* sequences to the *P. trichocarpa* reference sequence. Overall, we identified 3380 deletions and 5887 insertions corresponding to 14.7 Mb and 23.3 Mb respectively and accounting in total for the 10% of the whole poplar reference genome. According to our results, the insertion of class I LTR retroelements is the major contributor to the overall observed structural variation. We observed relatively few structural variants in transcribed regions compared to intergenic regions.

CNVs were detected by comparing the depth of coverage obtained in *P. nigra* and *P. deltoides* resequenced individuals. We identified 192 regions (~28.4 Mb) with a higher copy number in *P. nigra* than in *P. deltoides* and 154 CNVs (~24.6 Mb) with the opposite signature. In addition, 117 regions, corresponding to a total of 13.9 Mb, exhibited an intraspecific pattern of copy number variation. Our analysis showed that the regions of copy number variation were rich in repetitive sequences and had lower-than-average gene content. However, some classes of genes, such as disease resistance genes, resulted to be over-represented in CNVs with respect to the rest of the genome,

suggesting a relationship between the evolution of these gene families and copy number variants.

In summary, with the present thesis we built an elaborated catalogue of genetic variation in poplar. With the aim of obtaining different sources of information for selecting poplar with favorable agronomical traits, we 1) surveyed single nucleotide polymorphisms in specific target regions of many individuals and 2) investigated the genome-wide distribution of structural variation in a relatively small interspecific poplar pedigree.

1

Introduction

1.1 ENERGYPOPLAR project

The present PhD thesis work is part of the EU-funded project ENERGYPOPLAR. The project, started in May 2008, brings together an interdisciplinary group of ten public and private partners from six European countries with the ultimate goal of developing poplar trees with enhanced agronomical traits for industrial production of bioethanol. With the growing increase in energy demand and rising petrol-based fuel costs, the development of renewable liquid biofuels derived from cellulosic biomass is a strategic priority for the European Union. Liquid biofuels offer an important alternative to reduce Europe's dependence on fossil fuels, to reduce greenhouse gas emissions and to assist rural and agricultural development. Green plants are being used increasingly for production of transportation fuels in Europe and their application is being promoted through different European directives, which aim to achieve 20% of liquid fuel supply by 2020 (EREC, 2008). The achievement of this target requires a step-change in the understanding and manipulation of plant traits and a shift to second generation biofuel crops. In fact, the most common concern related to the current first generation of biofuel systems, such as corn and sugarcane, is that, as production capacities increase, so does their competition with agriculture for arable land used for food production. On the other hand, second-generation biofuels are produced sustainably by using biomass comprised of the residual non-food parts of current crops, as well as other crops that are not used for food purposes, such as poplar trees (Havlík *et al.*, 2010). Trees are attractive as a bioenergy system because they display a wide range of growth habits and can be grown on marginal lands unsuited to other agricultural crops, with reduced input costs and optimized land management.

Among all forest trees, *Populus* was chosen as the ideal perennial plant to work with. In fact, *Populus* is both model and commercial crop, and an extensive genomics toolbox already exists for this plant. This genomic toolkit includes the annotated genomic sequence of the north American *Populus trichocarpa* species (Tuskan *et al.*, 2006), genome-wide expression oligoarrays (Rinaldi *et al.*, 2007), SNP (single nucleotide polymorphisms) arrays (Douglas, 2011) and large global transcriptomics databases where several hundred microarrays expression studies are available for data-mining and in-silico discovery of candidate genes (Sjödin *et al.*, 2006). In addition, from the fifth framework project POPYOMICS, four extensive mapping populations with molecular genetic markers and an electronic database of QTL for biomass quality and quantity are available and electronically linked to the DNA physical sequence of *Populus*. A large natural population of *Populus* is also available from the sixth framework network of excellence EVOLTREE.

Central to energizing a new biofuel industry based on conversion of cellulosic biomass to ethanol is to improve the quality and quantity of biomass feedstock. Current methods to break down biomass into simple sugars and convert them into ethanol are inefficient and constitute the core barrier to produce ethanol at quantities and costs competitive with gasoline. This requires understanding the factors that are key determinants of plant cell-wall chemical and physical structures. Improving feedstock quality will contribute to improved bioethanol production. However trees selected for desired cell wall properties for efficient fuel production must also be productive: yield should be optimized for low input agricultural systems, ensuring sustainability targets such as greenhouse gas mitigation, maintenance of ecosystem services and diversity. Thus, high biomass production needs to be combined with desirable cell wall properties in trees to be used as a source for generation of biofuels. The specific ENERGYPOPLAR objectives that have been pursued in the present PhD thesis are:

1- the development of SNP markers usable for the selection of trees carrying beneficial alleles for biofuel production.

2- the characterization of the genome-wide interspecific sequence divergence among poplar parental species involved in the production of F1 hybrids. An extensive map of the interspecific genetic variation will be of help for the selection of markers of heterosis.

1.2 Detection of SNP markers in lignin biosynthesis genes

The process of cellulosic biofuel production involves three major steps: (1) pretreatment with acid or steam of biomass feedstock to release the polysaccharides; (2) enzymatic hydrolysis of polysaccharides into simple sugars; and (3) fermentation of sugars into ethanol (Hisano *et al.*, 2009). However, the association of lignin with cellulose and hemicellulose has a negative impact in cellulosic ethanol production. In fact, it inhibits the release of polysaccharides from the cell wall during the pretreatment process and absorbs the enzymes used for saccharification or reduces the accessibility of enzymes during the conversion process (Figure 1. 1). For this reason lignin is one of the most important limiting factors in conversion of plant biomass to biofuels (Vanholme *et al.*, 2008) and altering lignin structure or reducing lignin content can improve biofuel production (Jung and Ni, 1998; Li *et al.*, 2008).

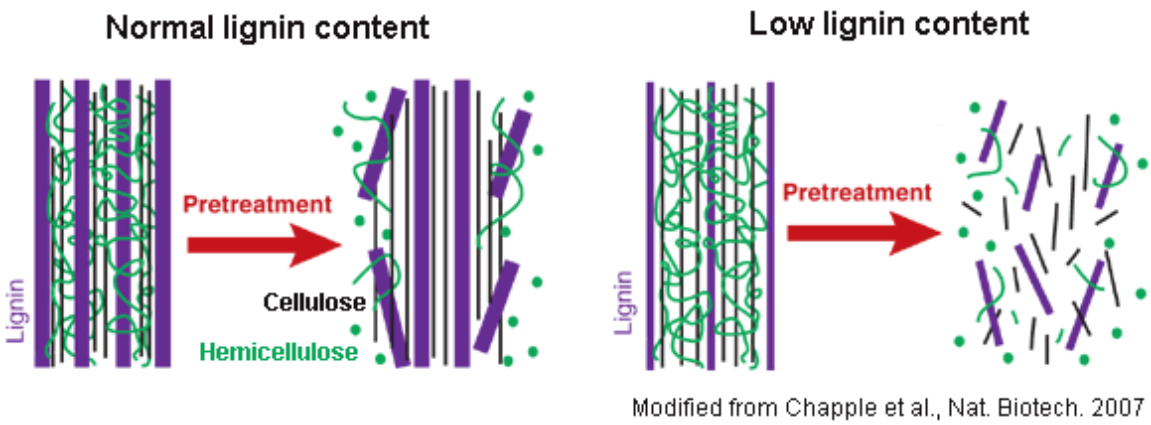

Figure 1. 1 Impact of lignin on the release of polysaccharides from the cell wall. Reduced lignin content can increase yields of fermentable sugars after pretreatment of plant biomass with hot acid and can also reduce or eliminate the need for this step.

Given the impact of lignin structure on biofuel production and the interest in developing SNP markers for the identification of trees carrying beneficial alleles for energy production, the first part of the present thesis focused on genes involved in the lignin biosynthesis pathway. Lignin is a phenolic biopolymer of complex structure, synthesized by all plants. It is an essential component of plant cell walls, playing an important role in mechanical support, water transport, and disease resistance in terrestrial plants (Dixon *et al.*, 2001; Rogers and Campbell, 2004). The biosynthesis of

lignin starts in the cytosol with the synthesis of cinnamic acid from the amino acid phenylalanine by phenylalanine ammonia lyase (PAL). Lignin is composed by three main p-hydroxycinammyl alcohol precursors or monolignols: p-coumaryl, coniferyl, and sinapyl alcohols. These alcohols undergo dehydrogenative polymerizations by peroxidase (PER) and laccase (LAC) to form p-hydroxyphenyl (H), guaiacyl (G) and syringyl (S) lignin, respectively (Weng and Chapple, 2010). The relative proportion of each lignin unit varies with species, plant parts, and maturity. The whole pathway of lignin biosynthesis in higher plants is shown in Figure 1. 2. Many studies have proposed that the following enzymes are required for monolignol biosynthesis through phenylpropanoid pathway: phenylalanine ammonia lyase (PAL); cinnamate 4-hydroxylase (C4H); 4-coumarate-CoA ligase (4CL); cinnamoyl CoA reductase (CCR); hydroxycinnamoyl CoA: shikimate hydroxycinnamoyl transferase (HCT); coumarate 3-hydroxylase (C3H); caffeoyl CoA 3-O-methyltransferase (CCoAOMT); ferulate 5-hydroxylase (F5H); caffeic acid 3-O-methyltransferase (COMT); and cinnamyl alcohol dehydrogenase (CAD) (Weng and Chapple, 2010).

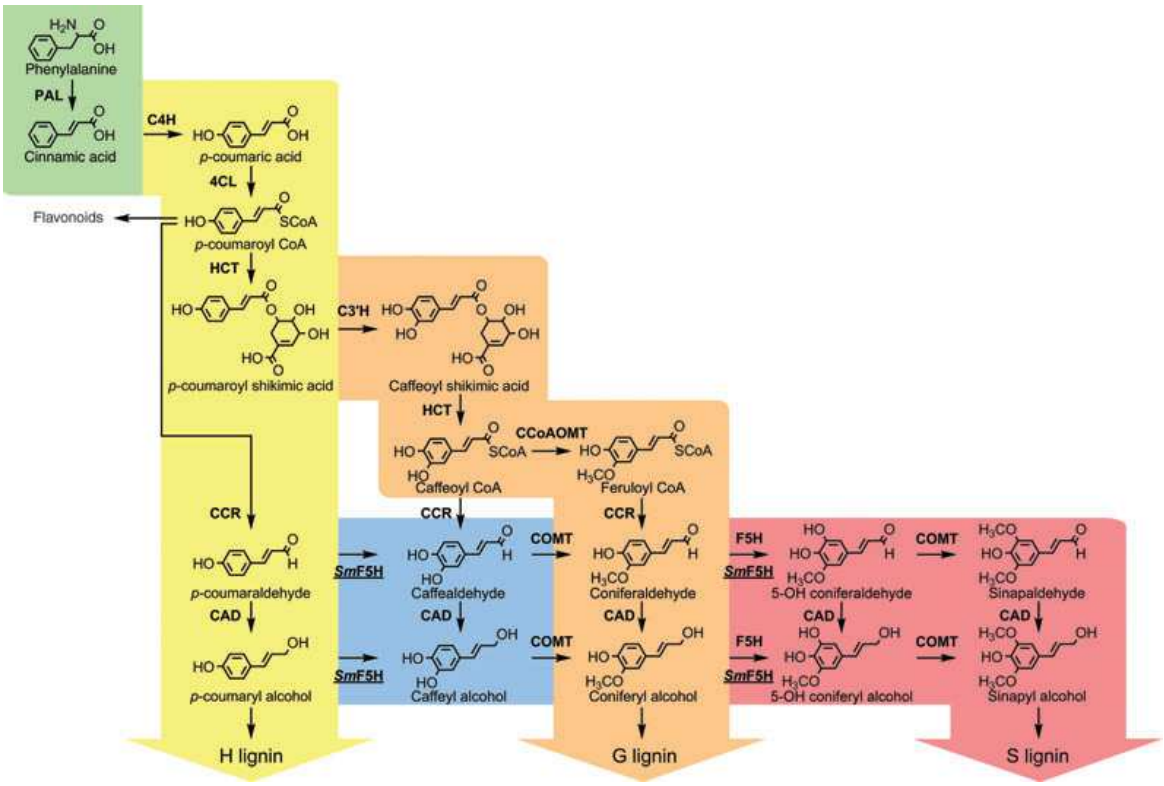

Figure 1. 2 The monolignol biosynthetic pathway (Weng and Chapple, 2010).

The functions of many lignin genes have been well-studied in several plant species, especially in dicot plants using either mutants or transgenic plants. Different studies have reported the possibility to modify or reduce lignin content in biofuel crops by overexpression, down-regulation, or suppression of genes involved in either lignin synthesis, regulation, or polymerization (Li *et al.*, 2003; Chen and Dixon, 2007). The effect on lignin reduction or modification depends on the transgene. For example, the down-regulation of the upstream genes like C3H, HCT, or 4CL leads to reduction in lignin content, while the down-regulation of F5H and COMT resulted in changes of S/G ratio (Weng *et al.*, 2008). However, there are still concerns with the potential environmental impacts of such genetically modified (GM) plants, including gene flow from non-native to native plant relatives. As a result non-GM biotechnologies using 'molecular breeding' remain particularly attractive. An alternative approach to transgenesis is the identification of natural mutations affecting the activity of these genes and the evaluation of the phenotypic effects of such mutations. In fact, the huge reservoir of genetic diversity present in the *Populus* germplasm has so far been poorly exploited because of the inefficiency in identifying natural variants for candidate genes. Functional variants are likely to be rare (Eyre-Walker, 2010) and the identification of rare SNPs requires sample sizes larger than those commonly used in studies aimed at surveying genetic variation. New methods are being developed that allow fast and cheap resequencing of genes and genomes and even the standard Sanger sequencing technology has now become so affordable that gene resequencing can be accomplished on hundreds of individuals (Greenman *et al.*, 2007). For this reason we decided to screen a large population of *Populus nigra* to identify both common and rare functional variants in candidate genes of lignin biosynthesis pathway.

1.2.1 CAD4 Sanger sequencing

We decided to start with the analysis of the natural genetic variation in one of the ten genes involved in lignin biosynthesis: the cinnamyl alcohol dehydrogenase (CAD). CAD is a family of genes involved in lignin biosynthesis in several plants (Walter *et al.*, 1988). In *Populus*, the CAD gene family includes at least 15 candidates (Barakat *et al.*, 2009) (Figure 1. 3). Natural loss-of function CAD mutants have been identified in several plants (Halpin *et al.*, 1998; Sattler *et al.*, 2009); however, no natural loss-of function CAD mutant has been identified in poplar so far. We therefore set out to search

for natural polymorphisms occurring in CAD and obtain a map of genetic variation in the gene.

CAD4 was the first of the CAD genes to be isolated and cloned (Van Doorsselaere *et al.*, 1995). Following the isolation of *CAD4* cDNA, transgenic poplar trees expressing antisense *CAD4* construct were obtained (Baucher *et al.*, 1996). Transgenic poplars with reduced *CAD4* activity showed structural alterations of lignin (Lapierre *et al.*, 1999), thus confirming the importance of *CAD4* in determining lignin composition. Among the members of *CAD* family, *CAD4* is considered to be the most important CAD gene in the poplar lignin biosynthetic pathway based on phylogenetic and expression analyses (Hamberger *et al.*, 2007). A recent study (Shi *et al.*, 2010) showed that *CAD4* (referred to in the study as PtrCAD1) is the only gene of the CAD family showing a substantial expression and a high specificity for differentiating xylem and is therefore likely to be the only gene of the family actively involved in lignin formation in differentiating xylem. Given this background information, *CAD4* was chosen as the most interesting member of the CAD gene family to be investigated in detail.

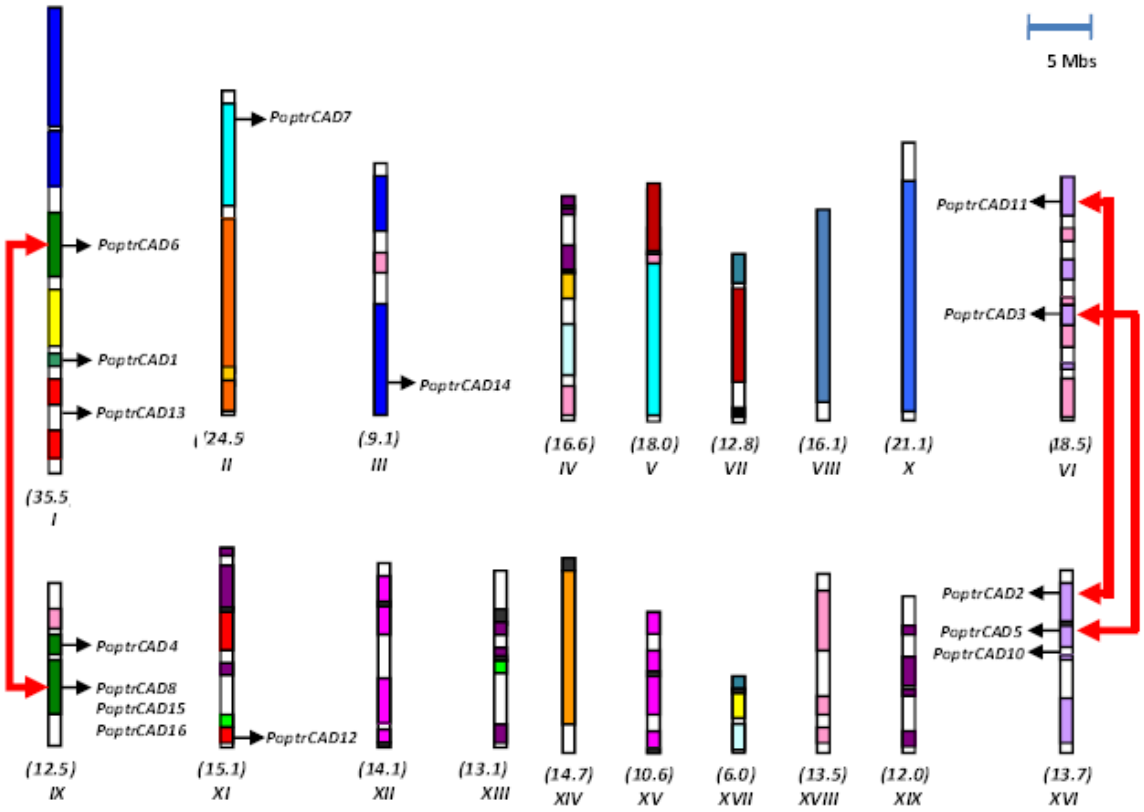

Figure 1. 3 Distribution of CAD genes on *Populus* chromosomes (Barakat *et al.*, 2009). The names of the chromosomes and their sizes (Mb) are indicated below each chromosome. Segmental duplicated homeologous blocks are indicated with the same color. The position of genes is indicated with an arrowhead.

Polymorphisms detected in the protein-coding region of the gene will fall in one of the three functional categories: nonsense mutations (null alleles) which cause a stop codon, and thus lead to a truncated protein; missense mutations which cause an amino acidic change; and synonymous polymorphisms, which have no effect on the amino acidic sequence of the protein. Nonsense mutations are likely to have the strongest effect on lignin content. However, such alleles are likely to be negatively selected, and thus rare (Eyre-Walker, 2010). Missense mutations, causing an amino acidic change, can have an impact on the structure of the enzyme and thus on the efficiency with which lignin is produced. Although synonymous polymorphisms do not affect amino acidic composition of the protein, they can in some instances affect the correct splicing of the gene or they can be in linkage disequilibrium (LD) with some undetected functional variant. Genome-wide and candidate gene association mapping can thus be used to identify the role of such variants (Risch and Merikangas, 1996). Noncoding polymorphism can affect the expression of the gene when located in promoter or in other regulatory regions.

Surveys of nucleotide polymorphisms are customarily performed on less than 50 individuals (Gilchrist *et al.*, 2006; Ingvarsson, 2008; Olson *et al.*, 2010), and are likely to miss SNPs with frequencies equal or lower than 1%. However, functional polymorphisms, if negatively selected, are likely to be rare (Eyre-Walker, 2010) and require larger sample sizes. With this in mind, we set out to identify and study naturally occurring polymorphisms in a large collection of 384 *Populus nigra* individuals originating from various geographical areas in Europe. We screened each genotype for nonsense, missense, and synonymous mutations in *CAD4*.

1.2.2 Pooled multiplex sequencing of CAD4, HCT1, C3H3, CCR7 and 4CL3

With the advent of Next Generation Sequencing (NGS), our sequencing abilities increased and we decided to deepen the study by increasing sample size and increasing the number of candidate genes. To study the natural variation in genes involved in the lignin biosynthesis pathway in a larger *Populus* population, we decided to exploit NGS Illumina technology. We used pooled multiplexed NGS to screen 768 *Populus nigra* accessions for mutations in five genes involved in lignin biosynthesis. We selected the

candidates prioritizing genes for which (a) a known effect on lignin biosynthesis has been documented either in poplar or in other species through the respective orthologs (Vanholme *et al.*, 2008), (b) functional redundancy is less pronounced (Shi *et al.*, 2010), and (c) expression is higher in differentiating xylem compared to other tissues (Shi *et al.*, 2010). The selected candidate genes were *CAD4*, *HCT1*, *C3H3*, *CCR7* and *4CL3*.

1.2.3 Next-generation sequencing technology

In the last few years, the high demand for low-cost sequencing has driven the development of high-throughput sequencing technologies that parallelize the sequencing process, producing thousands or millions of sequences at once. Next-generation sequencing (NGS) allows researchers to obtain a large amount of genetic data in the form of short sequences at an unprecedented rate. NGS platforms share a common technological feature: massively parallel sequencing of clonally amplified or single DNA molecules, spatially separated in a flow cell (Shendure and H., Ji, 2008). This design is a paradigm shift from that of Sanger sequencing, which is based on the electrophoretic separation of chain-termination products produced in individual sequencing reactions. In NGS, sequencing is performed by repeated cycles of polymerase-mediated nucleotide extensions. As a massively parallel process, NGS generates hundreds of megabases to gigabases of nucleotide sequence output in a single instrument run (Mardis, 2008).

One of the most established and widely-adopted NGS technology is the one developed by Illumina. The first Illumina sequencer, introduced in 2006, was the Genome Analyzer. This sequencer was based on the concept of "sequencing by synthesis" (SBS) to produce sequence reads of ~32-40 bp from tens of millions of surfaced-amplified DNA fragments simultaneously (Mardis, 2008). In particular, the Genome Analyzer uses a flow cell consisting of an optically transparent slide with 8 individual lanes on the surfaces of which are bound oligonucleotide anchors (Figure 1. 4 A). Template DNA is fragmented into lengths of several hundred base pairs and end-repaired to generate 5'-phosphorylated blunt ends. A single A base is added to the 3' end of the blunt phosphorylated DNA fragments to allow the ligation of the DNA fragments to specific oligonucleotide adapters, which have an overhang of a single T base at their 3' end. These adapters are complementary to the flow-cell anchors in order to enable the

ligation of the template DNA to the flow cell. DNA templates are then amplified in the flow cell by "bridge" amplification, which relies on captured DNA strands "arching" over and hybridizing to an adjacent anchor oligonucleotide. Multiple amplification cycles convert the single-molecule DNA template to a clonally amplified arching "cluster".

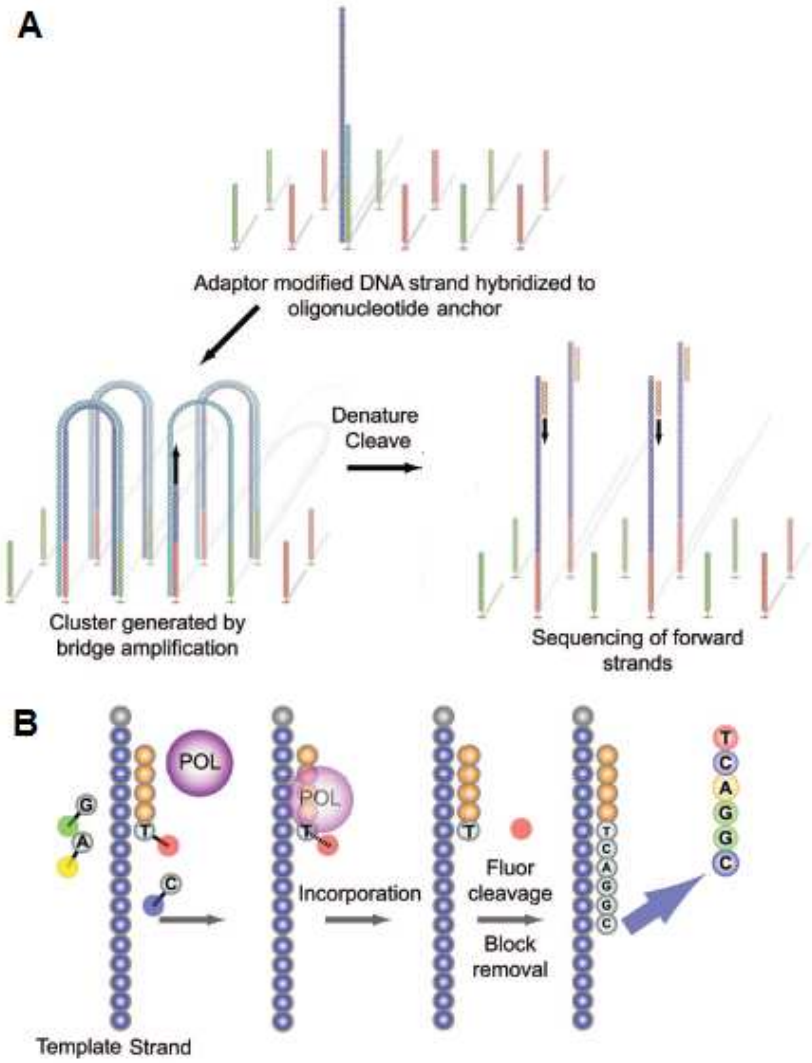

Figure 1. 4 Illumina Genome Analyzer sequencing. Adapter-modified, single-stranded DNA is added to the flow cell and immobilized by hybridization. Bridge amplification generates clonally amplified clusters. Clusters are denatured and cleaved; sequencing is initiated with addition of primer, polymerase (POL) and 4 reversible dye terminators. Postincorporation fluorescence is recorded. The fluor and block are removed before the next synthesis cycle (Shendure and H., Ji, 2008).

Approximately 50 x 10^6 separate clusters could be generated per flow cell. For sequencing, the clusters are denatured, and a subsequent chemical cleavage reaction and wash leave only forward strands for single-end sequencing (Figure 1. 4 B). Sequencing of the forward strands is initiated by hybridizing a primer complementary to the adapter sequences, which is followed by addition of polymerase and a mixture of 4 differently colored fluorescent reversible dye terminators. The terminators are incorporated according to sequence complementarity in each strand in a clonal cluster. After incorporation, excess reagents are washed away, the clusters are optically interrogated, and the fluorescence is recorded. With successive chemical steps, the reversible dye terminators are unblocked, the fluorescent labels are cleaved and washed away, and the next sequencing cycle is performed. This iterative, sequencing-by-synthesis process required approximately 2.5 days to generate read lengths of 36 bases. With 50 x 10^6 clusters per flow cell, the overall sequence output was >1 Gb per analytical run (Bentley *et al.*, 2008). Subsequent to the first Genome Analyzer, new platforms with an improved throughput were launched by Illumina: the Genome Analyzer IIx, which can generate up to 90 Gb per analytical run with read lengths of 150 bp and the latest HiSeq2000 that can produce more than 600 Gb per run with read lengths of 100 bp. Illumina, as other NGS technologies, offers also the possibility to sequence both ends of template molecules (Figure 1. 5 A). Such "paired-end" sequencing provides positional information that facilitates alignment and assembly (Korbel *et al.*, 2007; Campbell *et al.*, 2008) and is emerging as a key technique for assessing genome rearrangements and structural variation on a genome-wide scale. An interesting application of Illumina NGS is the "multiplex sequencing", i.e. the sequencing of different DNA samples in the same lane. Considering the high throughput of the latest sequencing machine, multiplexing is very useful when targeting specific genomic regions or working with small genomes. In fact, pooling samples into a single lane of a flow cell exponentially increases the number of samples analyzed in a single run without drastically increasing costs or time. In the multiplexed sequencing method, DNA libraries are "tagged" with a unique DNA sequence, or index, during sample preparation. Multiple samples are then pooled into a single lane on a flow cell and sequenced together in a single run. An automated three-read sequencing strategy (Figure 1. 5 B) identifies with high accuracy each uniquely tagged sample for individual downstream analysis.

The high-throughput of NGS sequencing technologies enables resequencing of individual genomes, or targeted re-sequencing of a number of selected regions in a large

number of pooled individuals (Ingman and Gyllensten, 2009). NGS can be used to screen large populations for rare functional variants in target genes, and as a follow-up to genome-wide association studies, to extensively sequence regions surrounding associated single nucleotide polymorphisms (Druley *et al.*, 2009). Previous studies have indicated that NGS can reliably detect variants in pooled samples (Druley *et al.*, 2009; Out *et al.*, 2009).

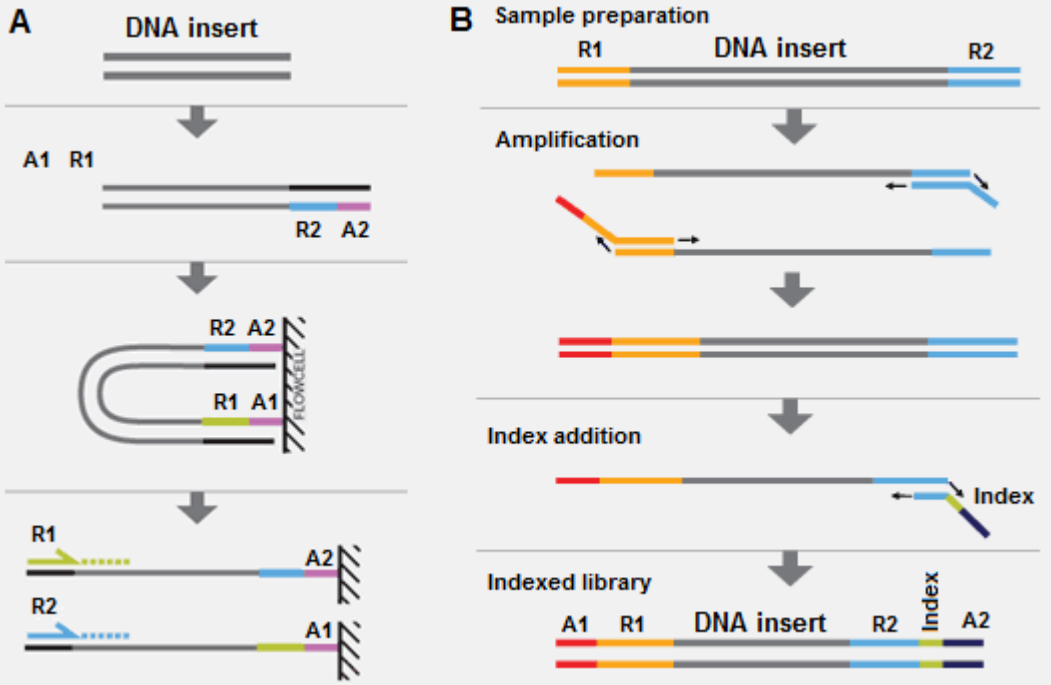

Figure 1. 5 A. **Paired-end sequencing**: adapters (A1 and A2) are ligated onto DNA fragments. Template cluster are formed on the flow cell by bridge amplification and the two ends (R1 and R2) are sequentially sequenced. **B. Multiplex sequencing**. During library preparation, a 6 bp sequence is added to the DNA insert allowing the sequencing of different libraries in the same lane of a flow cell.

1.3 Phenotypic effect of structural variants

High yield is an important phenotypic trait for energy crops. Natural phenotypic variation observed among different genotypes can be partly explained by the presence of genetic variants. Understanding the genetic basis of phenotypic variation is important for the identification of genetic markers usable for the prediction of specific phenotypic traits. In poplar, high yield depends on the successful exploitation of the remarkable

hybrid vigor that is achieved when crossing different species to produce interspecific F1 hybrids. The molecular bases of hybrid vigor remain elusive despite a long history of exploitation of heterosis in breeding and of research on this topic. Recent studies focused on the role of regulatory variation in determining heterosis that finds its basis in DNA sequence variation (Springer and Stupar, 2007). A correlation between genetic distance and heterosis has long been recognized even though it is not a perfect one (Frascaroli *et al.*, 2007). For example, analysis of the genomic variation in maize, a species with pronounced intraspecies hybrid vigor, showed remarkable sequence variation especially outside of transcribed regions (Brunner *et al.*, 2005) that is accompanied by high levels of cis-regulatory variation resulting in differential expression of the two alleles present in the hybrid (Stupar and Springer, 2006). Preliminary analysis of sequence variation among different *Populus* species showed limited levels of variation in transcribed regions, while intergenic regions harbor much more variation, even though still less than that observed in maize (G. Zaina and M. Morgante, unpublished).

To explore the extent of sequence diversity present between different poplar species and get a sense of its possible contribution to phenotypic variation, we set out to study the *P. nigra-P. deltoides* sequence divergence at a genome-wide level by means of Illumina next-generation sequencing. It was long assumed that most of the genome variation arises from single nucleotide polymorphisms. In recent years, the role of another type of genetic variation has been recognized, namely, structural variation (Manolio *et al.*, 2009). Structural variants (SVs) are defined as chromosomal alterations such as insertions, deletions, and other differences in copy-number of genomic regions (CNVs) involving segments of DNA larger than 1 kb (Feuk *et al.*, 2006) (Figure 1. 6). SVs can occur in genomes after large segmental duplications, or as the result of unequal or illegitimate recombination (Achaz *et al.*, 2000), DNA segment inversions (Fransz *et al.*, 2000) or as a consequence of the transposable elements activity (Hughes *et al.*, 2003). SVs presumably contribute to more base-pair differences between individuals than SNPs. Furthermore, it has been recently demonstrated that SVs are quite common in the human genome and may have considerable effects on human phenotypic variation for example altering gene dosage, disrupting coding sequences, or perturbing regulation (Hurles *et al.*, 2008). Little is known about the prevalence of this phenomenon in plants and of its relationship with the origin of intra-specific diversity. In *Arabidopsis thaliana* it has been demonstrated that structural variation may contribute to postzygotic

isolation through the production of genetically deficient hybrids (Lynch and Conery, 2003). Currently, not much interest has been manifested for the detection and consequences of structural polymorphisms in plants, but, although the global impact of structural variation is unknown, it might have dramatic consequences on phenotypic diversity (Weigel and Mott, 2009).

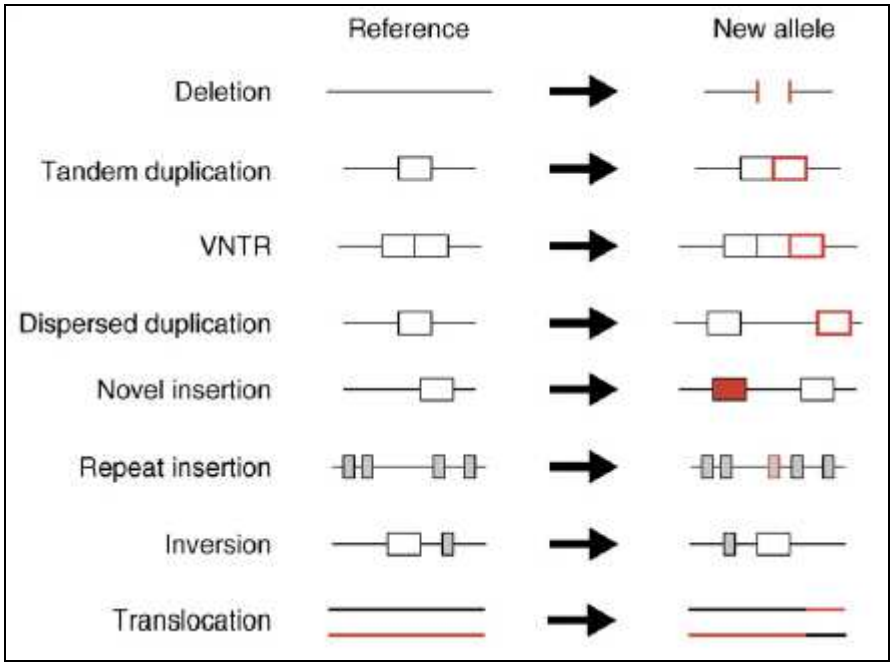

Figure 1. 6 Types of structural variants (Hurles *et al.*, 2008).

SVs can be divided in two groups on the basis of their sequence length: 1) small SVs, when they range from 1 to ~30 kb in size, and 2) large SVs, that can extend from ~30 Kb to few Mb. Many small insertion/deletions are probably due to the recent movement of transposable elements (TEs), that are very active in many plants. In fact, TEs are a tremendous source of genome instability and genetic variation; for example, they impact gene expression via the introduction of alternative regulatory elements, exons, and splice junctions (Ray and Batzer, 2011). In addition, TEs can mediate genome rearrangements through nonhomologous recombination (Eichler and Sankoff, 2003). The molecular basis of the larger SVs, referred also as copy number variations (CNVs), are still not fully understood. However, several recent studies have reported their presence in the human genome (Sebat *et al.*, 2004; Tuzun *et al.*, 2005). The presence of large CNVs has also been reported in maize where a region of ~2.6 Mb present in the

inbred line B73 but entirely absent from the Mo17 inbred line was identified (Springer *et al.*, 2009).

To study interspecific sequence divergence in poplar we performed whole genome next-generation sequencing of 18 poplar accessions: 4 *Populus nigra* accessions, 2 *Populus deltoides* and 12 *P. nigra* x *P. deltoides* F1 hybrids, obtained by crossing two of the four resequenced *P. nigra* and the two resequenced *P. deltoides* with a factorial design. We then took advantage from two different analytical strategies for the detection of the two different classes of structural variants:

1- small variants (deletions and insertions), probably resulting from the movement of TEs, were detected by comparing *P. nigra* and *P. deltoides* sequences with respect to the *P. trichocarpa* reference sequence.

2- larger variants, whose mechanism of origin is not fully understood, were detected by comparing sequences from *P. nigra* with those from *P. deltoides*.

1.4 Methods for SV detection

The earliest methods for discovering structural variants are based on whole-genome array comparative genomic hybridization (aCGH) (Medvedev *et al.*, 2009). Array CGH platforms are based on the principle of comparative hybridization of two labeled samples (test and reference) to a set of hybridization targets to test the relative frequencies of probe DNA segments between two samples (Pinkel *et al.*, 1998) (Figure 1. 7). However the power of this technology in identifying structural variant is limited. In fact, aCGH is limited to detecting only copy number differences of sequences that are present in the reference assembly used to design the probes. Array CGH platforms cannot identify balanced structural variants or, in the case of duplication, specify the location of a duplicated sequence. In addition, the breakpoint resolution of any prediction is correlated with the density of the probes on the array and is usually low (~50 Kb). SNP microarrays have been used for SVs discovery and genotyping (Cooper *et al.*, 2008). These platforms are also based on hybridization and measure the intensity of probe signals at known SNP loci. For this reason, SNP microarrays suffer of the same limitations as aCGH. The advent of next-generation sequencing technologies promises to revolutionize structural variation studies and replace microarrays as the

platforms for discovery and genotyping. However, NGS approaches present substantial computational and bioinformatics challenges. In general, the identification of SVs from NGS data is performed by mapping sequence reads to a reference genome and subsequently identifying signature or patterns that are diagnostic of different classes of SV. In particular, there are two main signatures that can be exploited for the detection of SVs from NGS data: paired-end mapping (PEM) and depth of coverage (DOC) (Medvedev *et al.*, 2009).

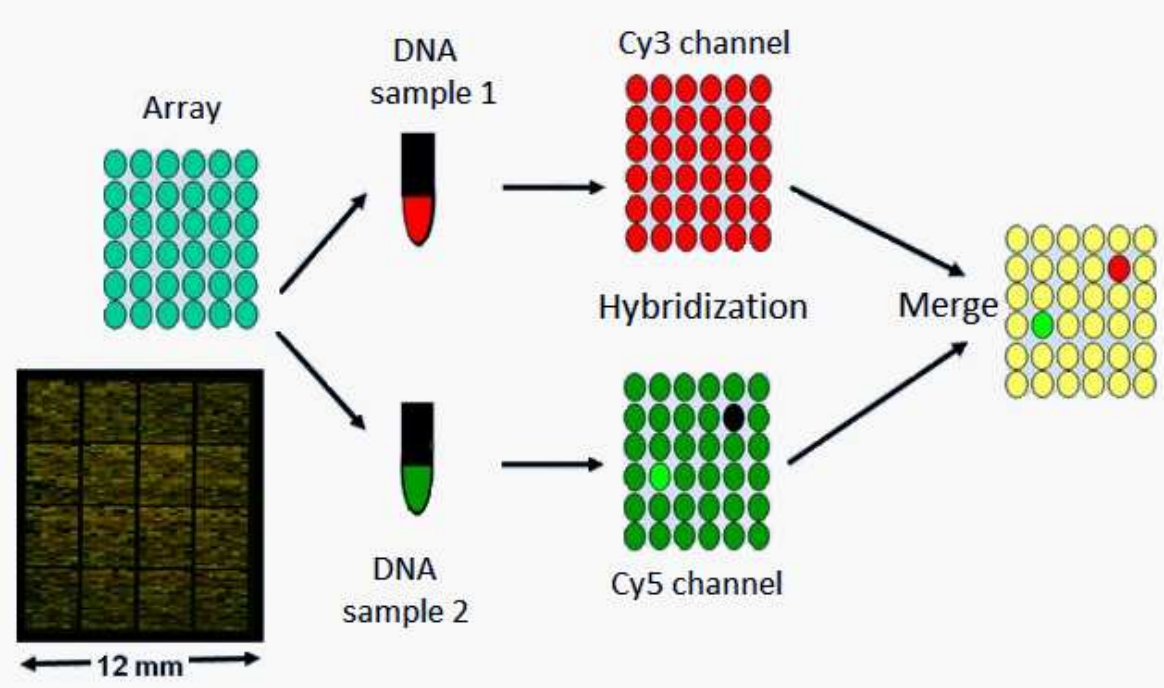

Figure 1. 7 Array CGH technology. DNA from two samples is differentially labelled, using different fluorophores, and hybridized to several thousand DNA probes. Differences in copy number between the two samples are detected as differences in the intensities of the two fluorophores.

1.4.1 Paired-end mapping (PEM) signature

The paired-end mapping signature results from the analysis of the mapping information of paired-end reads aligned against a reference genome. Using this signature, structural variants can be detected with the presence of 'discordant' paired reads, i.e. pairs in which the mapping span and/or orientation of read pairs are inconsistent with the reference genome (Figure 1. 8). Most classes of variation can, in principle, be detected. Deletions can be detected by the presence of read pairs that map to reference genome

with a mapping distance greater than the insert size. Conversely, insertions can be detected by the presence of read pairs with a mapping distance smaller than the expected one. However, basic insertion signature suffer from two main limitations: 1) no signature is detected when the size of the insertion is greater than the insert size of the sequenced fragment and 2) the signature gives no information regarding composition of the inserted sequence. Another variant that leaves a clear PEM signature is an inversion: a paired-read that spans one of the breakpoints of an inversion will map to the reference genome with the orientation of the read, lying within the inversion, flipped (Korbel *et al.*, 2007).

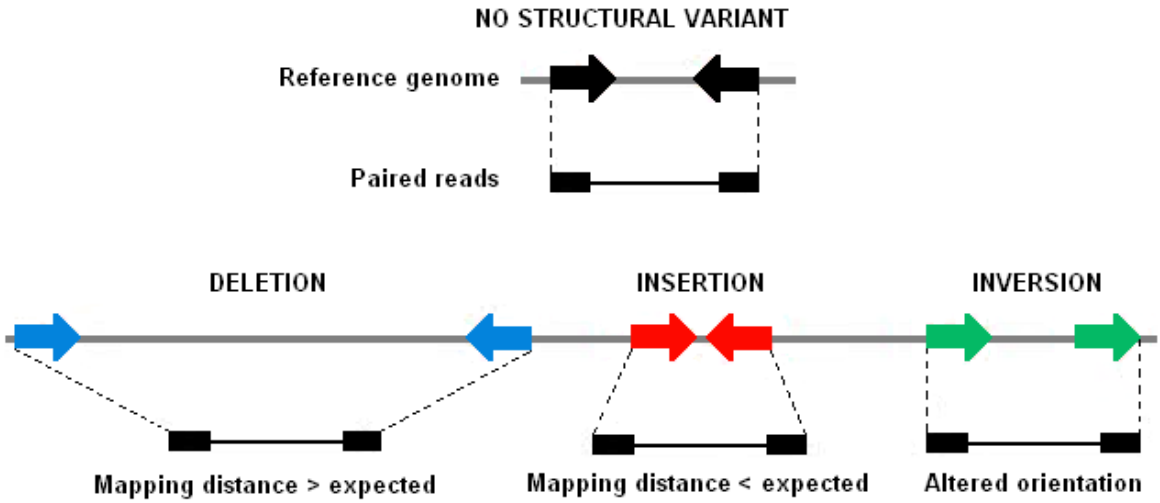

Figure 1. 8 PEM signature. Schematic representation of the paired-end mapping signature usable for the detection of deletions, insertions and inversions.

The read-pair method is the most widely applied approach for the detection of SVs, and was first demonstrated using BAC end sequences (Volik *et al.*, 2003) and subsequently applied with fosmid paired-end sequences (Tuzun *et al.*, 2005). Only later was applied to next-generation sequencing (Korbel *et al.*, 2007). Several computational tools based on PEM signature have been developed for the detection of structural variants from NGS data, including PEMer (Korbel *et al.*, 2009), VariationHunter (Hormozdiari *et al.*, 2010), BreakDancer (Chen *et al.*, 2009) and MoDIL (Lee *et al.*, 2009).

We decided to take advantage from PEM signature for the detection of small deletions and insertions occurring in *P. nigra* and *P. deltoides* sequenced individuals with respect to the *P. trichocapra* reference genome. For the detection of deletions, we decided to

use BreakDancerMax (Chen *et al.*, 2009). On the other hand, for the detection of the insertions, none of the available methods using PEM signature could be employed. In fact, we are interested in the detection of insertions of sequences that are greater than the standard Illumina insert size (~500 bp) and, as a consequence, simple PEM signature cannot be applied. For this reason we decided to develop a custom pipeline for the detection of insertions resulting from the movement of transposable elements.

1.4.2 Depth of coverage (DOC) signature

The high sequence coverage obtained with NGS technologies allows the identification of a completely different type of signature, namely, depth of coverage signature (DOC). Assuming the sequencing process is uniform, the number of reads mapping to a region follows a Poisson distribution and is expected to be proportional to the number of times the region appears in the donor (Medvedev *et al.*, 2009). Thus, the depth of coverage signature can be used for the detection of SVs that alter the copy number of a sequence (Figure 1. 9).

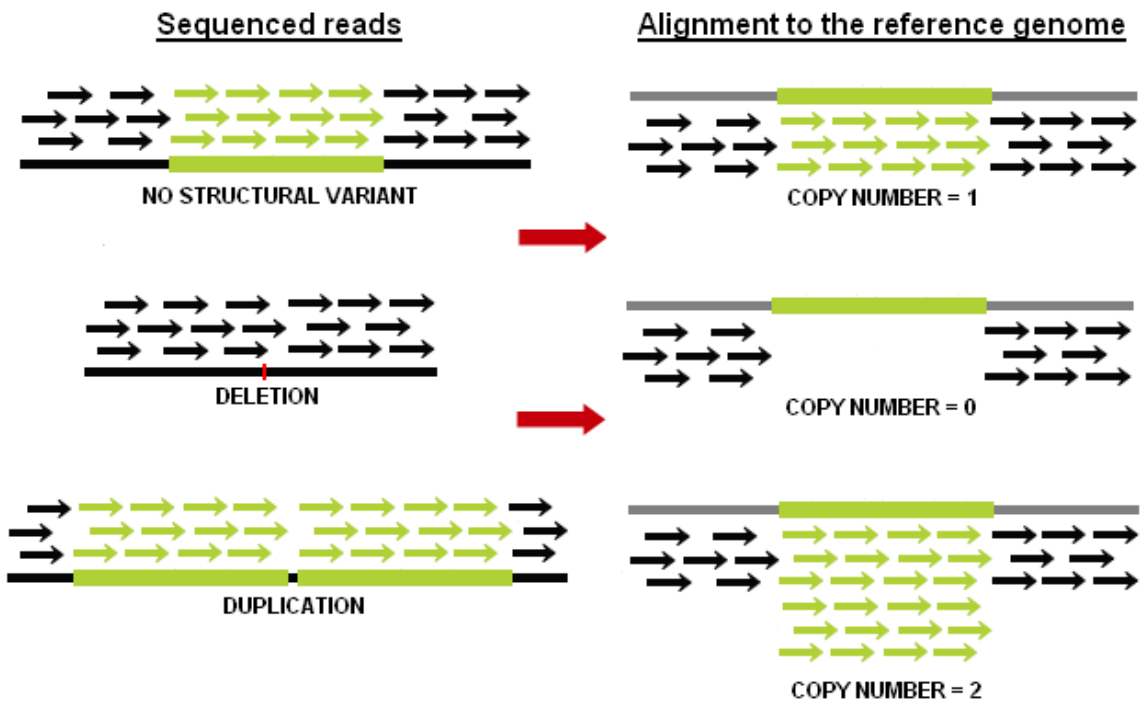

Figure 1. 9 DOC signature. Schematic representation of the depth of coverage signature usable for the detection of deletions and duplications.

In fact, the depth of coverage analysis examines the increase and decrease in sequence coverage to detect duplications and deletions, respectively, and to predict absolute copy numbers of genomic intervals (Alkan *et al.*, 2011; Yoon *et al.*, 2009). Read-depth approaches using NGS data were first applied to define rearrangements in cancer (Campbell *et al.*, 2008) and to build absolute copy number maps of the human genome (Sudmant *et al.*, 2010).

Unlike the PEM insertion signature, the gain DOC signature does not indicate were an insertion occurred, but rather what duplicated sequence has been inserted. The strength of a gain/loss signature is directly related to the coverage of the dataset and to the size of the CNV. In contrast to most PEM signatures, DOC signatures can be used to detect very large events; in fact, the larger the event, the stronger the signature. However, they are not able to identify smaller events that PEM signatures are able to detect; they are also much poorer at localizing breakpoints.

We thus decided to use the DOC signature to detect large regions of copy number variation between the *P. nigra* and *P. deltoides* sequenced individuals in order to determine the level of sequence homology among these two species and to check for the presence of large CNVs as those reported in maize (Springer *et al.*, 2009) and in humans (Tuzun *et al.*, 2005).

2

Genetic Diversity in *CAD4*

The content of this chapter has been published:

Nucleotide diversity and linkage disequilibrium in Populus nigra cinnamyl alcohol dehydrogenase (CAD4) gene. F. Marroni, S. Pinosio, G. Zaina, F. Fogolari, N. Felice, F. Cattonaro and M. Morgante. Tree Genetics & Genomes, 2011.

2.1 Materials and Methods

2.1.1 Subjects and genotyping

Individuals included in the present study were originally collected in five different European nations: France (n=169), Italy (n=103), Germany (n=50), The Netherlands (n=48) and Spain (n=14). In Italy, Germany and Spain trees were collected from one to three locations, while in France and The Netherlands they were collected at several different sites. DNA extraction was performed on dehydrated leaves using the DNeasy plant kit (Qiagen, Inc., Valencia, CA).

Although components of CAD gene family in poplar are now well characterized (Barakat *et al.*, 2009), until a few years ago, researchers focused their efforts on a single gene coding for Cinnamyl Alcohol Dehydrogenase (CAD, EC 1.1.1.195), located on Linkage Group (LG) IX of the *P. trichocarpa* genome (Lapierre *et al.*, 1999). We focused on the same gene, which is now named *CAD4*, and is one of the only two genes of the CAD family which are preferentially expressed in the xylem (Barakat *et al.*,

2009). Primer design was performed using Primer3plus (Untergasser *et al.*, 2007). Table 2. 1 lists the primers used in the experiment. DNA amplifications were performed in a 20 µl volume. The reactions contained on average 15 ng of genomic DNA and the following reagents: 0.3 µM of each primer, 250 µM of each dNTP, 1.5 mM $MgCl_2$, 2% DMSO, 1 unit Amplitaq Gold (Applied Biosystems, Foster City, CA) and 1X PCR buffer II (Applied Biosystems, Foster City, CA). The reactions were performed in the Geneamp 9700 PCR system (Applied Biosystems, Foster City, CA), under the following conditions: 95 °C for 10 min., 35 cycles of 20 sec. at 94 °C, 30 sec. at 60 °C and 1 min. 30 sec. at 72 °C, followed by a final extension of 10 min. at 72 °C. PCR products were analysed on agarose gel and purified using Agencourt Ampure magnetic beads (Beckmann Coulter, Fullerton, CA) using a Biomek FX robot (Beckmann Coulter, Fullerton, CA).

Table 2. 1 Primers used to sequence *CAD4*. F=Forward. **R**=Reverse. **Position**: Position of the first base of the primer relative to *CAD4* consensus sequence.

Primer	Orientation	Position	Sequence
CAD4a	F	5	CCACCACCCGTAAAATATGC
CAD4a	R	880	GATTCAGCAAAGCCTCCTTG
CAD4b	F	742	TGTTGGAGTCATCGTTGGAA
CAD4b	R	1737	CAAGATCAGCTTGCCATCAA
CAD4c	F	1351	TTGTGGTGAGAATTCCTGATGG
CAD4c	R	2244	AAAGCAAAGACAGACGGTCACA

Sequencing was performed using ABI Prism Dye Terminator Cycle Sequencing Ready Reaction kit v3.1 (Applied Biosystems, Foster City, CA) on an ABI3730 sequencer (Applied Biosystems, Foster City, CA). Sequences were trimmed using Lucy (Chou and Holmes, 2001) on the basis of Phred quality scores (Ewing *et al.*, 1998; Ewing and Green, 1998). The trimmed sequences were aligned and visualized using Phrap and Consed (Gordon *et al.*, 1998). SNPs and insertion/deletion polymorphisms (indel) were confirmed by visual inspection of sequence alignments after automated detection with PolyPhred (Nickerson *et al.*, 1997), a program that identifies SNPs by providing the user a confidence score which represents the probability that the call is correct conditional on the site being a SNP (Stephens *et al.*, 2006). Rare variants are likely to occur as singletons in a large sample; to reduce the chance of observing false positives

due to amplification and sequencing errors, we introduced the following quality controls: 1) we included in the present study only SNPs with a confidence score equal to 99; 2) whenever SNP information was available on both strands or in mutliple amplicons, we built a "SNP consensus" integrating information from different reads for each individual; 3) at each SNP position, we considered only individual sequences for which the genotype quality score was higher than 98%. Two multiallelic SNPs were excluded from further analyses. Intron-exon boundaries were defined according to poplar genome versions 1.1 (http://www.jgi.org) and 2 (http://www.phytozome.com), and confirmed using the gene prediction program GeneMark (Lomsadze *et al.*, 2005).
To predict the effect of the amino acid substitutions on protein structure and function we built molecular models of mutants based on the Protein Data Bank structure (http://www.rcsb.org/pdb) of the closely related cinnamyl alcohol dehydrogenase of *Arabidopsis thaliana* (PDB id. 2CF5) which displays 78% identity in sequence. We used the program Swiss-PDB-Viewer (Guex and Peitsch, 1997) for building consensus and all mutant structures. No sidechain refinement was attempted at this stage as only gross features of the models were used.

2.1.2 Statistical analyses

Two measures of LD between pairs of SNPs, r^2 and D', were calculated using the R (http://www.r-project.org) package *genetics*. Since singleton SNPs give no information when calculating LD, we excluded them from LD analyses. The decay of r^2 with distance was fitted using Hill and Weir expectation of r^2 between adjacent sites (Hill and Weir, 1988). In accordance with previous work (Remington *et al.*, 2001), we used the equation:

$$E(r^2) = \left[\frac{10+C}{(2+C)(11+C)}\right]\left[1+\frac{(3+C)(12+12C+C^2)}{n(2+C)(11+C)}\right]$$

where *n* is the sample size and *C*, the parameter to be estimated, represents the product of the population recombination parameter ($\rho=4N_e r$) and the distance in base pairs. The decay of D' was fitted using the equation $E(D')=(1-\theta)^t$, where t, the parameter to be estimated, represents the number of generations since D'=1 (Abecasis *et al.*, 2001). Non-linear least squares, implemented in the R package *nls*, were used to fit equations to our data.

Multilocus haplotype reconstruction was performed using PHASE 2.1.1 (Stephens *et al.*, 2001), which has been shown to provide accurate estimates of haplotype frequencies from population data (Marroni *et al.*, 2005). Haplotypes were reconstructed in the whole dataset assuming a panmictic model and in each individual country of origin. Tajima's *D*, Fay and Wu's *H*, and McDonald-Kreitman tests were performed with DNAsp (Librado and Rozas, 2009). The effect of sample size on population genetics parameter estimates was investigated by sampling subsets of six different sizes (5, 10, 25, 50, 125 and 250 individuals) and calculating nucleotide diversity and neutrality statistics. For each sample size we produced by resampling five subsets.

Some of the analyses required an outgroup; we therefore included two *P. trichocarpa* sequences for *CAD4*, retrieved from Joint Genome Institute (http://www.jgi.org) and National Center for Biotechnology Information (http://www.ncbi.nlm.nih.gov/) web sites.

2.2 Results

We obtained sequences of *CAD4* from 360 trees (GenBank accessions: HM440565 to HM440924). Consensus sequence was 2240 bp long; coding sequence was 1074 bp long, and was formed by five exons (Figure 2. 1). The consensus of *P. nigra CAD4* was aligned using BLAST against the whole *P. trichocarpa* genome. The best hit was *P. trichocarpa CAD4* sequence (locus estExt_Genewise1_v1.C_LG_IX2359 in poplar genome v1.1, locus POPTR_0009s09870 in poplar genome v2), showing 97% identities to the whole length of the query, an expected value of 0 and a score of 3736. The second best hit was on scaffold one, showing 89% identities to a fragment of 886 bases of the query, an expected value of 0 and a score of 1126. These results confirm that produced sequences belonged to the *CAD4* locus.

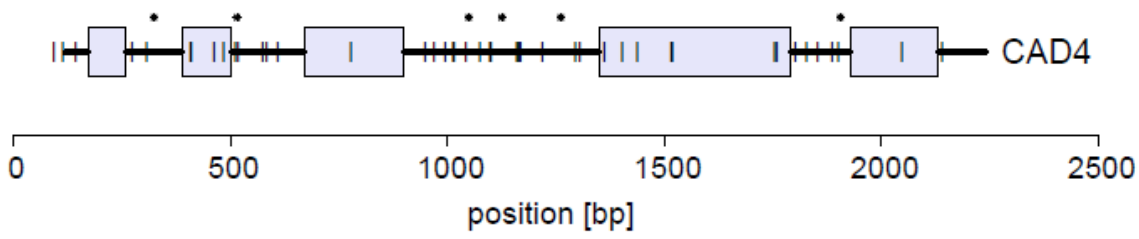

Figure 2. 1 Positions of SNPs (vertical bars) and deletions (asterisks) relative to noncoding sequences (represented as horizontal lines) and exons (boxes).

We identified 45 SNPs, corresponding to one SNP every 50 base pairs. The complete list of the SNPs, together with the corresponding minor allele frequency is presented in supplementary Table S- 1. Thirteen of the 45 SNPs are in *CAD4* coding sequence, and six of them cause amino acid substitutions (Table 2. 2); position of SNPs and indels relative to the coding sequence of *CAD4* are depicted in Figure 2. 1. In addition, we identified 5 deletions and one insertion, all in non-coding regions (

Table 2. 3).

Table 2. 2 Predicted aminoacidic substitutions caused by non-synonymous SNPs. **Consensus (bp):** position of the SNP relative to the consensus sequence. **SNP**: Common allele/rare allele**. Coding (bp):** Position of the SNP relative to the consensus coding sequence**. a.a. change:** amino acid substitution caused by the variant.

Consensus (bp)	SNP	Coding (bp)	a.a. change
409	G/C	109	V37L
484	C/T	184	H62Y
777	C/A	310	N104H
1361	A/G	443	K148R
1515	A/G	597	I199M
1753	G/A	835	A279T

Table 2. 3 Insertions and deletions identified in *CAD4*. **Position (bp):** Position of the insertion or deletion relative to the consensus sequence. **Length:** Length of the indel. **Bases:** inserted or deleted nucleotides.

Type	Position (bp)	Length	Bases
Insertion	324	6	TGTGTA
Deletion	515	1	A
Deletion	1049	1	A
Deletion	1125	1	C
Deletion	1261	2	AA
Deletion	1905	1	T

According to molecular models we built, all amino acid substitutions are far apart from the zinc ion binding catalytic site and thus it is not straightforward to predict any structural or dynamical consequences relevant to enzymatic function. The most interesting mutations are N104H and I199M. N104H is in close proximity to one of the zinc ion binding sites and could thus perturb this structural motif which appears conserved in cinnamyl alcohol dehydrogenases of several plant species (Youn *et al.*, 2006). Moreover the mutation introduces a titratable group that could be in the range of pH of optimal enzyme activity (Sarni *et al.*, 1984). Although it is difficult to predict dramatic effects as a consequence of I199M mutation, unless the protein cannot accommodate the increase in side chain volume, it is worth noting that the residue is contacting the helix entailing C163 which is participating in the catalytic site and could thus perturb the structure and/or the dynamics at the catalytic site. Finally, we identified several subjects carrying more than a single non-synonymous SNP. They were homozygous carriers of N104H, I199M and A279T or composite heterozygous for various combinations of N104H, I199M, A279T and V37L. One subject was homozygous for N104H and carried one I199M allele.

The decay of r^2 with distance was rather fast (Figure 2. 2 A); according to our nonlinear regression, the value of r^2 was decreased by 50% after only 16bp, and decreased to values close to zero (i.e. < 0.05) after 50bp. The pattern for D' was strikingly different, although it still showed a rapid decay (Figure 2. 2 B). D' values were on average higher than r^2 values and the decay of D' with distance was slower than the decay of r^2. Our nonlinear regression showed that the distance at which D' was reduced by 50% was 1294bp.

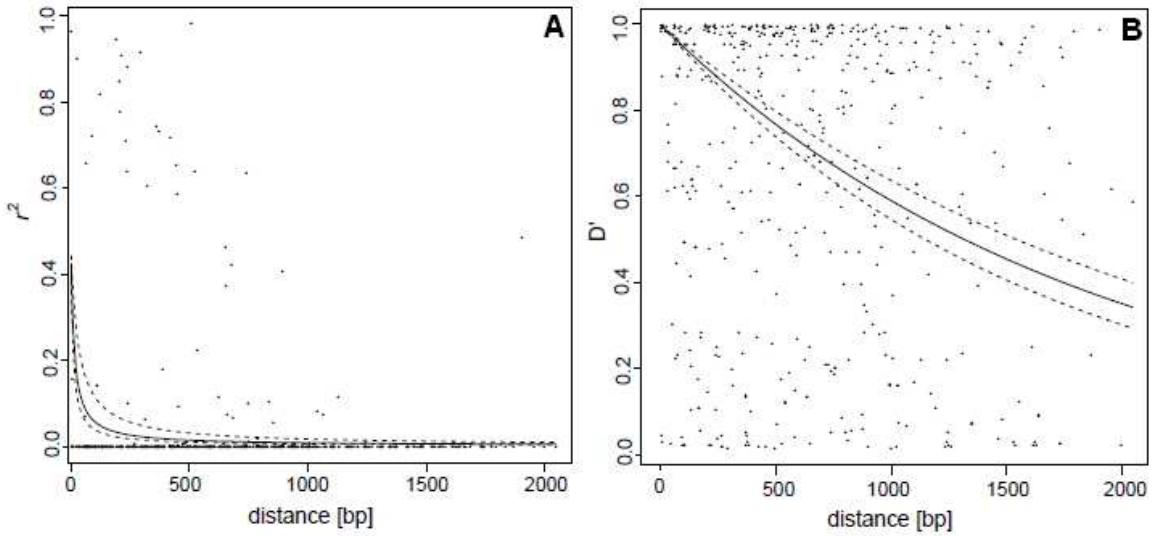

Figure 2. 2 A. Decay of r^2 as a function of distance. Regression line is based on Hill and Weir (1988). Estimated value for the parameter C is 0.152. Dashed lines represent confidence intervals of regression line. **B.** Decay of D' as a function of distance. Regression line is based on Abecasis et al. (2001). Estimated value for the parameter t is 536.25. Dashed lines represent confidence intervals of regression line.

The difference in behavior of the two different measures of LD is emphasized in Figure 2. 3, in which we plot D' as a function of r^2.

Since LD measures, and in particular r^2, depend on allele frequencies, we repeated the analyses applying different minor allele frequency (MAF) thresholds (Table 2. 4). Our results show a positive correlation between MAF and extent of LD measured as the distance in bp to obtain a 50% decay. Nucleotide diversity (π) in *CAD4* was 0.0012. The ratio of non-synonymous to synonymous diversity (π_a/π_s) was 1.05. The ratio of non-synonymous to synonymous nucleotide divergence (K_a/K_s) was 0.091.

Resampling experiments showed that nucleotide diversity estimates were robust with respect to sample size (Table 2. 5).

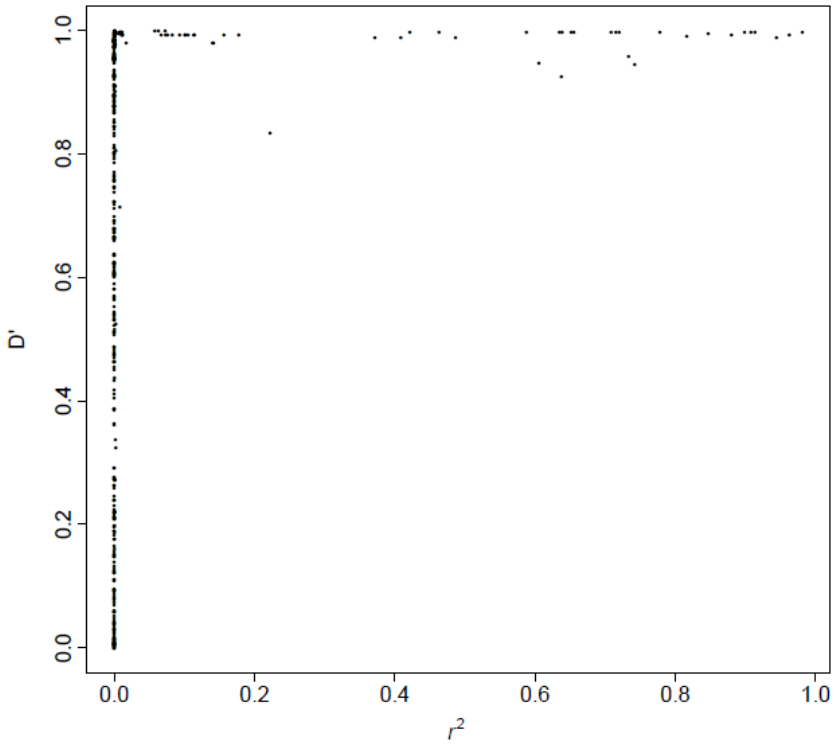

Figure 2. 3 D' as a function of r^2. Each data point shows values of the two LD measures obtained for all pairs of alleles.

Table 2. 4 Variation of LD patterns depending on SNPs minor allele frequencies**. Threshold**: Minor allele frequency (MAF) required to include SNPs in the analyses. **Non-unique**: No frequency threshold applied (MAF>0). **Decay$_{50}$**: Distance (in bp) at which LD is reduced of 50%.

Threshold	Decay$_{50}$ (r^2)	Decay$_{50}$ (D')
Non-unique	16	1294
0.01	64	2236
0.02	69	1655
0.025	59	2845
0.05	93	6750
0.1	491	8695

Table 2. 5. **Variations in estimated population genetics parameters as a function of sample size.** For each parameter mean of the values obtained in five replicates are shown for each subsample. π: nucleotide diversity. π_a: aminoacidic nucleotide diversity. π_s: nucleotide diversity in synonymous positions. π_{snc}: nucleotide diversity in synonymous or non-coding positions. K_a: non-synonymous nucleotide divergence compared to the outgroup. K_s: synonymous nucleotide divergence compared to the outgroup. ***D***: Tajima's *D*. ***D* p-val**: Tajima's *D* p-value. ***H***: Fay and Wu's *H*. ***H* p-val**: Fay and Wu's *H* p-value. **NI**: McDonald-Kreitman Neutrality Index. **NI p-val**: McDonald-Kreitman Neutrality Index p-value. **S**: Number of segregating sites. **Ha**: Number of reconstructed haplotypes.

	Sample Size						
	5	**10**	**25**	**50**	**125**	**250**	**360**
π	0.0011	0.0012	0.0012	0.0012	0.0012	0.0012	0.0012
π_a/π_s	Inf	0.92	2.02	1.13	1.00	1.04	1.05
π_a	0.0007	0.0006	0.0008	0.0007	0.0007	0.0007	0.0008
π_s	0	0.0008	0.0004	0.0006	0.0007	0.0007	0.0007
π_{snc}	0.0013	0.0026	0.0015	0.0015	0.0015	0.0015	0.0015
K_a/K_s	0.095	0.091	0.095	0.093	0.093	0.093	0.091
K_a	0.0029	0.0028	0.0029	0.0028	0.0028	0.0028	0.0029
K_s	0.0307	0.0308	0.0307	0.0309	0.0309	0.0309	0.0309
D	-0.63	-1.14	-1.13	-1.44	-1.47	-1.38	-1.49
***D* p-val**	0.317	0.141	0.133	0.056	0.04	0.054	0.029
H	1.63	0.24	-2.30	-3.11	-8.12	-6.52	-11.30
***H* p-val**	0.919	0.632	0.248	0.287	0.024	0.043	0.006
NI	2.36	2.01	2.16	2.41	3.48	2.68	4.08
NI p-val	0.660	0.688	0.590	0.518	0.391	0.489	0.240
S	8.2	14.4	19.8	27.2	35.4	39	45
Ha	5.4	8.8	13	19	29	38.2	44

Average π ranged from 0.0011 to 0.0012 across all sample sizes. Only extremely small sample sizes led to occasional major departures from the observed value of 0.0012. The same behavior was observed for the K_a/K_s ratio. Neutrality tests are more sensitive to sample size. Mean values obtained with less than 50 subjects are lower than the estimate obtained with the whole sample, and significant departures from neutrality failed to be detected even with as many as 250 subjects. Fay and Wu's *H* seemed to be more affected by sample size than Tajima's *D*.

2.3 Discussion

CAD4 is an essential gene for lignin biosynthesis; natural CAD mutants showing

aberrant phenotype have been identified in maize (Halpin *et al.*, 1998) and in sorghum, (Sattler *et al.*, 2009) while a mutation associated with reduced expression of CAD was mapped in the same region as the *cad* locus in pine (MacKay *et al.*, 1997). Transgenic poplar trees with silenced CAD gene have been obtained, but no natural CAD loss-of-function mutant has been identified. We set out to screen *CAD4* in a large sample in search of functional variants. Functional variants are likely to be rare (Eyre-Walker, 2010), and the identification of rare SNPs require sample sizes larger than those commonly used in studies aimed at surveying genetic variation.

One objective of the present work was to screen a large sample of *P. nigra* individuals to identify non-synonymous SNPs in the *CAD4* gene. In total, we identified 45 SNPs (13 in coding region, 6 of which non-synonymous), one insertion in non-coding region and 5 deletions, also in non-coding region. Three of the six non-synonymous mutations have a frequency lower than 1% and would have been difficult to identifiy using smaller sample size. The mutations likely to have the strongest impact on CAD enzymatic activity are I199M and, to a lesser extent, N104H, but the two substitutions have been identified in *P. tremuloides* (Youn *et al.*, 2006). Individuals carrying multiple occurrences of non-synonymous SNPs are more likely to show altered CAD activity. Only experimental validation, which is however out of the scope of the present investigation, could confirm or rule out this hypothesis. Individuals carrying mutations shown to affect lignin composition might be used in experimental crosses to obtain an offspring with the desired properties.

We investigated decay of r^2 and D' with distance in *CAD4* using the appropriate decay function for each LD statistic. Previous studies observed that LD in different poplar species extends only for few hundred base pairs (Gilchrist *et al.*, 2006; Ingvarsson, 2008). We confirmed the findings, and obtained an even faster decay of LD in *CAD4*. According to our estimates, the distance over which LD (measured as r^2, for comparison with previous studies) is reduced by 50% is about 16 bp while in previous works it was reported to vary between 50 and 500 base pairs. The difference might be due to the different number of loci investigated or to the different sample size. The present study is focusing on a single gene, and LD decay can be different from the decay measured by pooling data from several genes. On the other hand, LD estimates depends on allele frequencies and sample size (Jiang *et al.*, 2009; Terwilliger and Hiekkalinna, 2006; VanLiere and Rosenberg, 2008). Previous studies were investigating sample sizes of less than 50 individuals (Gilchrist *et al.*, 2006; Ingvarsson, 2008). For

such studies, all non-unique SNPs would have a MAF greater than 0.01. LD measures, and in particular r^2, depend on allele frequencies, in that rare alleles tend to lower LD levels and studies which miss rare SNPs will tend to give slightly inflated LD estimates (Hedrick and Kumar, 2001). This is confirmed by the LD analyses that we performed using different MAF thresholds. Increasing the cut-off frequency, we obtained higher average LD values and slower LD decay. Applying a threshold of 1% for MAF we obtained an estimate of 64 bp as the distance at which LD decays of 50%. Increasing the threshold to 5% brought the distance to 93bp. D' decay was slower than r^2 decay, but it showed a similar dependence on allele frequency. The different behavior of D' and r^2 is well-known, and was confirmed by plotting D' as a function of r^2 (see Figure 2. 3). D' suffers from a "ceiling effect", because it reaches its maximum value of 1 whenever one of the 4 possible haplotypes is not observed in the sample (Mueller, 2004). The probability of this happening is fairly high if one (or both) the investigated SNPs has a low MAF. R-square, on the contrary, tends to be low, especially when rare alleles are present (Hedrick and Kumar, 2001), and suffers therefore from what could be named the "floor effect". The combination of floor effect and ceiling effect is evident in Figure 2. 3. The floor effect is witnessed by the presence of several pairwise comparisons with $r^2=0$, irrespective of D' value. The ceiling effect, on the contrary, results in an abundance of pairwise comparisons with D'=1, irrespective of r^2 value.

As a further objective of our work, we estimated diversity indexes, and evaluated their robustness with respect to variations in sample size. We observed negative Tajima's *D* and Fay and Wu's *H* values for *CAD4*. Negative values of Tajima's *D* indicate negative selection, population growth and/or genetic hitchhiking (Tajima, 1989), and negative values of *H* suggest genetic hitchhiking (Fay and Wu, 2000). However, the coexistence of negative values for both *D* and *H* has been related to the demographic history of the population, and might be explained by a bottleneck event (Heuertz *et al.*, 2006); since we investigated only one locus, we cannot determine if negative values of Tajima's *D* and Fay and Wu's *H* are due to selection or to demographic history. In their original work McDonald and Kreitman (McDonald and Kreitman, 1991) found that replacement to synonymous ratio between *Drosophila* species exceeded that measured within a *Drosophila* species and interpreted this as evidence for adaptive fixation of amino acid changes. On the other hand, more recent studies (Nachman *et al.*, 1994; Rand and Kann, 1996) observed instances in which the replacement to synonymous ratio within species was higher than that between species, thus leading to a Neutrality Index (NI)

greater than 1, like in the present study. This can be explained by the nearly neutral theory of evolution, assuming that moderately deleterious polymorphisms are present within species, but in the long range are eliminated by selection and do not contribute to divergence between species. Nucleotide diversity (π) was 0.0012, in agreement with the average nucleotide diversity of 0.0018 observed in nine genes in *P. trichocarpa*, (Gilchrist *et al.*, 2006) but lower than the values of 0.0042 and 0.0110 observed in two previous studies in *P. tremula* (Ingvarsson, 2008). Non-synonymous substitutions are relatively frequent in *CAD4* (π_a/π_s=1.05), but they do not survive enough to become fixed across species (low Ka/Ks), thus suggesting the existence of negative selection on *CAD4*.

Previous studies showed the effect of ascertainment bias on θ and Tajima's *D* (Ramírez-Soriano and Nielsen, 2009); given the availability of a large sample, we investigated the effect of sample size on population genetics parameters and neutrality tests. Resampling experiments showed that accurate measures of nucleotide diversity can be obtained when the sample size is 25 individuals (corresponding to 50 chromosomes) or more, while neutrality tests are quite sensitive to variations in sample size, and deviations from neutrality might fail to be detected even with sample sizes of 250 individuals (Table 2. 5); this is because small sample sizes lead to a relatively large variance of π and hence *D* (Lohse and Kelleher, 2009).

In conclusion 1) we screened 360 *P. nigra* individuals in search of functional variants of *CAD4*. The use of a large set of individuals enabled us to sample most of the genetic variation in *CAD4* and to identify six functional variants. In addition, we identified carriers of multiple mutations to be assessed for lignin quality and quantity; individuals showing significant alterations in lignin content will then be used in conventional breeding programs. Then, 2) we investigated LD structure in *CAD4*; we showed that LD estimates in small samples might be biased, and 3) we studied the robustness of population genetics parameters estimates with respect to sample size. We showed that the use of small data sets might lead to wrong interpretation of neutrality tests.

2.4 Supplementary Material

Table S- 1 Summary statistics of identified SNPs. **Position**: base pair position relative to the consensus sequence. **SNP (1/2)**: Alleles of the SNP (in alphabetic order). **MA**: Minor Allele. **MAF**: Minor Allele Frequency. **O(1/1)**: Observed individuals with genotype 1/1**. O(1/2)**: Observed individuals with genotype 1/2. **O(2/2)**: Observed individuals with genotype 2/2. **HWE**: p-value of Fisher's exact test for deviations from Hardy-Weinberg Equilibrium. Non-synonymous SNPs are shown in bold.

Position	SNP (1/2)	MA	MAF	O(1/1)	O(1/2)	O(2/2)	HWE
93	C/G	G	0.018	297	11	0	1.00
114	A/T	A	0.002	0	1	311	1.00
143	C/G	G	0.005	315	3	0	1.00
273	A/G	A	0.021	0	14	315	1.00
306	A/T	A	0.015	0	10	320	1.00
408	C/T	C	0.008	0	5	325	1.00
409	**C/G**	**C**	**0.008**	**0**	**5**	**326**	**1.00**
462	A/C	A	0.002	0	1	331	1.00
484	**C/T**	**T**	**0.001**	**334**	**1**	**0**	**1.00**
511	A/T	A	0.006	0	4	328	1.00
518	A/T	T	0.003	334	2	0	1.00
574	G/T	G	0.166	10	89	229	0.97
583	A/T	T	0.111	266	42	15	0.00
609	C/T	C	0.002	0	1	330	1.00
777	**A/C**	**A**	**0.157**	**8**	**79**	**216**	**1.00**
948	A/T	A	0.079	7	38	285	0.13
969	C/G	G	0.066	294	34	5	0.19
995	C/T	T	0.001	340	1	0	1.00
1012	C/T	T	0.021	326	12	1	0.84
1015	A/T	T	0.001	340	1	0	1.00
1042	A/T	A	0.009	0	6	333	1.00
1075	A/G	A	0.025	2	13	322	0.38
1098	C/T	T	0.176	221	82	15	0.45
1100	C/T	C	0.024	2	12	318	0.37
1159	A/G	G	0.066	280	32	5	0.19
1163	A/G	A	0.002	0	1	313	1.00
1165	G/T	G	0.010	0	6	307	1.00
1168	A/T	A	0.002	0	1	316	1.00
1219	G/T	T	0.002	313	1	0	1.00

Position	SNP (1/2)	MA	MAF	O(1/1)	O(1/2)	O(2/2)	HWE
1294	G/T	T	0.002	308	1	0	1.00
1305	A/G	G	0.021	292	9	2	0.32
1361	**A/G**	**G**	**0.002**	**309**	**1**	**0**	**1.00**
1402	C/T	C	0.009	0	6	322	1.00
1437	A/G	G	0.029	322	18	1	1.00
1515	**A/G**	**G**	**0.178**	**241**	**67**	**26**	**0.00**
1518	A/G	A	0.021	2	10	328	0.34
1753	**A/G**	**A**	**0.017**	**1**	**8**	**292**	**0.81**
1758	A/G	G	0.007	293	4	0	1.00
1801	C/T	C	0.002	0	1	299	1.00
1827	C/T	C	0.052	3	25	271	0.58
1853	A/T	A	0.002	0	1	297	1.00
1886	A/T	T	0.168	215	39	28	1.97E-006
1900	C/T	C	0.002	0	1	298	1.00
2047	A/C	A	0.007	0	4	300	1.00
2140	A/G	G	0.007	275	4	0	1.00

3

Rare Variants in Lignin Genes

The content of this chapter has been published:

Large scale detection of rare variants via pooled multiplexed next generation sequencing: towards next generation Ecotilling. F. Marroni*, S. Pinosio*, E. Di Centa, I. Jurman, W. Boerjan, N. Felice, F. Cattonaro and M. Morgante. The Plant Journal, 2011.
*First shared authorship

3.1 Materials and Methods

3.1.1 Plant Material

The experimental sample consisted of 768 *Populus nigra* accessions originally collected in different European areas (Smulders *et al.*, 2008; Rohde *et al.*, 2010). A large proportion of trees originated from France (n=631). The remaining trees originated from Italy (n=118), Germany (n=9), Spain (n=9) and The Netherlands (n=1). Latitude ranged from 40.24° N to 51.48° N (median latitude=46.24°N) and longitude from 16.39° E to 0.56° W (median longitude=3.19° E). Altitude above sea level ranged from 35 m to 1699m (median altitude 160m). Approximately 1 gram of leaf material was collected for DNA extraction from each tree.

3.1.2 Amplification and pooling

DNA of 768 *P. nigra* accessions was extracted from dehydrated leaves using DNeasy plant kit (Qiagen, Inc., Valencia, CA). Primer design was performed using the web interface Primer3plus (Untergasser *et al.*, 2007). DNA amplifications were performed in a 15 µl volume, using primer pairs listed in Table 3. 1.

Table 3. 1. Primers used to obtain sequences of candidate genes. **F** = Forward. **R** = reverse.

Primer	Orientation	Sequence
CAD4a	F	CCACCACCCGTAAAATATGC
CAD4a	R	GATTCAGCAAAGCCTCCTTG
CAD4b	F	TGTTGGAGTCATCGTTGGAA
CAD4b	R	CAAGATCAGCTTGCCATCAA
CAD4c	F	TTGTGGTGAGAATTCCTGATGG
CAD4c	R	AAAGCAAAGACAGACGGTCACA
HCT1	F	TCTCCTGGGTTGAGTCCGATA
HCT1	R	TCTGCCTTGCATCAAACCAT
C3H3a	F	TTGTGGAAATTAGAGGGACCA
C3H3a	R	CGTTGGCTAGATGGGTTGAA
C3H3b	F	CAAACATTTTGTCCGATTAGAACG
C3H3b	R	GCATGGTGTGCCATACAAAA
C3H3c	F	GCCAAGCAGCATTTTGTTGA
C3H3c	R	AAGGTTGGAGCAAGCCTTCA
CCR7a	F	CTCCACTTTCCCAGTCACCA
CCR7a	R	TGCACAGAATTTATTGGTTCAGG
CCR7b	F	AAGTCCGACGAGTGGTGTTC
CCR7b	R	CCTTTGGGTCATTCAAAAGC
CCR7c	F	GAGGTGGTGGAAATCCTTGC
CCR7c	R	ACACCTGCACATTGGCATTC
4CL3a	F	ATTCTTCACCAAACGCAACC
4CL3a	R	TGGAACATAGGCAACACACA
4CL3b	F	CGTAGACTCTGCCCCAGATG
4CL3b	R	ATTGGTTTCCAACCCCTTTT
4CL3c	F	CACGTCTCCACCCGGTATCT
4CL3c	R	TTCGGTGGCCTGAGACTTTT
4CL3d	F	ATGGTTGCACACAGGCGATA
4CL3d	R	TGCTGGTGGAACAAATCACC

The reactions contained on average 25 ng of genomic DNA and the following reagents: 0.3 µM of each primer, 250 µM of each dNTP, 1.5 mM $MgCl_2$, 2% DMSO, 1 unit Amplitaq Gold (Applied Biosystems, Foster City, CA) and 1X PCR buffer II (Applied Biosystems, Foster City, CA). The reactions were performed in the Geneamp 9700 PCR system (Applied Biosystems, Foster City, CA), under the following conditions: 95 °C for 10 minutes, 40 cycles of 20 seconds at 94 °C, 30 seconds at 60 °C and 1 minute and 30 seconds at 72 °C, followed by a final extension of 10 minutes at 72 °C. Amplification of *HCT1* was performed substituting 1 unit Amplitaq Gold with 0.3 units of Phusion High Fidelity DNA polymerase (Finnzymes, Espoo, Finland). PCR products were then pooled according to the following schemes:

Phase 1: We amplified *CAD4* in three amplicons, using PCR primers already tested in a different sample (Marroni *et al.*, 2011); for each amplicon, the quantities of the PCR products of 16 random accessions were estimated on agarose gel; the average concentration was taken as an estimate of each amplicon's concentration, and the three amplicons of each individual were combined in equimolar amounts. Experimental samples were pooled in 12 separate groups, each composed by 64 accessions (totaling to 768). A schematic representation of the pooling scheme is depicted in Figure 3. 1. Three amplicons obtained from three control accessions for which Sanger sequencing was already available (Marroni *et al.*, 2011) were added to each pool.

Phase 2: In phase 2, we amplified the CDS of the selected genes using one primer pair for *HCT1*, four for *4CL3* and three for each of *C3H3* and *CCR7*. For each amplicon, the quantities of the PCR products of 16 random accessions were estimated on agarose gel; the average concentration was taken as an estimate of each amplicon's concentration and the eleven amplicons of each individual were combined in equimolar amounts. Experimental samples were pooled in 12 separate groups, each composed by 64 accessions.

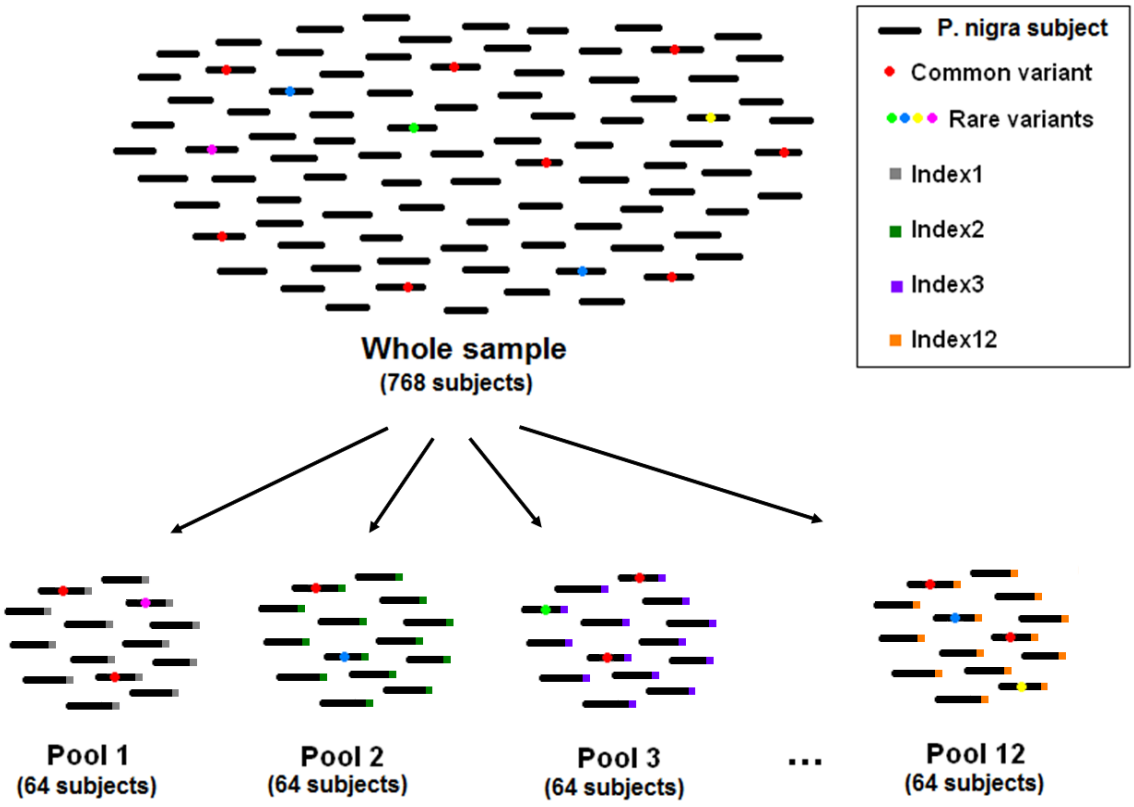

Figure 3. 1 Pooled multiplexed next generation sequencing screening of large populations. Identification of mutation carriers in a pool requires sequencing of the accessions of the corresponding pool.

3.1.3 Sequencing

To prepare NGS libraries, 5 µg of pooled PCR products were randomly fragmented by nebulizing at 60 psi (pound per square inch) for 4 minutes. Libraries were prepared using Illumina reagents, according to manufacturer's specifications (Illumina, San Diego, CA). End repair of fragmented DNA was performed using T4 DNA polymerase and Klenow polymerase with T4 polynucleotide kinase. An "A" base was added at the 3' end using a 3'–5' exonuclease-deficient Klenow fragment, and Illumina indexed adapter oligonucleotides were ligated to the sticky ends thus created. We electrophoresed the ligation mixture on an agarose gel and size-selected fragments at 200 bp.

DNA was enriched for fragments with Illumina adapters on either end by a 16-cycle PCR reaction performed by using the Illumina Multiplexing Sample Preparation Oliogonucleotide Kit according to manufacturer's instructions. A Genome Analyzer

flowcell was prepared on the supplied cluster station according to manufacturer's protocol. In both phase 1 and phase 2 of the experiment, two lanes of the flowcell were used to sequence the 768 accessions. Clusters of PCR colonies were then sequenced on an Illumina Genome Analyzer II platform using a single read run of 44bp coupled with 7bp Illumina indexes sequencing with the Illumina Multiplex Sequencing primer. Images from the instrument were processed using the manufacturer's pipeline software to generate FASTQ sequence files. Sanger sequencing was performed using BigDye ® Terminator v3.1 Cycle Sequencing Kit (Applied Biosystems, Foster City, CA) on an ABI3730 sequencer (Applied Biosystems, Foster City, CA) following manufacturer's instructions.

3.1.4 Data Analysis

In a previous study (Marroni *et al.*, 2011) we obtained a *CAD4* consensus sequence from 360 accessions (GenBank accessions HM440565 to HM440924). This reference was 2240bp long and comprised the complete *CAD4* CDS (1074bp). The *P. nigra* reference sequences for the coding portions of *HCT1* (accession JF693234), *C3H3* (accession JF693232), *CCR7* (accession JF693233) and *4CL3* (accession JF693234) were obtained from Sanger sequencing of eight accessions, using phred (Ewing and Green, 1998), phrap and consed (Gordon *et al.*, 1998).

Illumina sequences were aligned against the *P. nigra* reference with the short reads aligner Novoalign (Novocraft Technologies Sdn Bhd, Kuala Lumpur, Malaysia), which uses full Needleman-Wunsch algorithm with gap penalties. Alignment was performed setting the alignment scoring options *t* (the highest alignment score acceptable for the best alignment) and *g* (the gap opening penalty) in a different way for SNP and small indel detection. For SNP detection the chosen pair of scoring options was t=60 and g=15, while for indel detection t=110 and g=20. Default settings for the remaining alignment scoring, quality control and read filtering options were retained. Coverage statistics were calculated based on alignment performed for SNP detection. Mean Individual per Base Coverage (MIBC) was calculated for each base as R/N, where R is the number of reads covering the position and N is the number of accessions (N=768 for analysis on the whole data set and N=64 for analysis at pool level). Thus, MIBC represents for each base the mean number of reads covering the base in each accession. Mean Individual Coverage (MIC) is calculated as the average of MIBC over the

reference sequence. To evaluate experiment-wide MIC we used the reference sequences of all the studied genes.

SNP and indel detection was performed with Varscan (Koboldt *et al.*, 2009). SNP detection was performed separately on forward and reverse reads of each pool; a SNP was called if the alternative allele was present both in forward and reverse sequences in at least 10 reads per strand. This allowed discarding false positive SNPs due to sequence specific sequencing errors. SNPs called by Varscan with an average variant quality lower than 25 and SNPs identified in regions with a MIBC lower than 50x (corresponding to a total coverage of 3350x) were not considered.

Error distribution in Illumina reads is not uniform; the proportion of errors usually shows an increasing trend from the beginning to the end of the read, with the possibility of observing high error rates in the very first bases (Kircher *et al.*, 2009). In addition, preliminary results of the present study indicated that false positive SNPs can be identified at the 3' and 5' ends of a read when a small deletion/insertion is present near (<10bp) the read ends. To control for this, a specific *a posteriori* quality control was applied. Each read was partitioned in three segments of equal length, and the condition was imposed that each SNP had to be independently identified (using the thresholds shown above) when considering each of the segments of the read separately.

To assess the performance of NGS multiplexed pooled genotyping to identify SNPs, in phase 1 two amplicons (*CAD4b* and *CAD4c*) of two of the twelve pools (pool 5 and pool 9) were sequenced with the Sanger method and SNPs were detected on the obtained individual sequences. Identification of SNPs in Sanger sequences of the training set was performed using polyphred (Nickerson *et al.*, 1997). Sensitivity and specificity of pooled multiplexed NGS were measured using receiver operating characteristic (ROC) curve analysis, considering individual Sanger sequencing as a gold standard. Comparison was performed only on positions in which Sanger coverage was at least 50x.

In ROC curves, the true positive rate (sensitivity) is calculated in function of the false positive rate (1 - specificity) for different cut-off points; each point on the ROC represents a sensitivity/specificity pair corresponding to a particular decision threshold. Area under the ROC curve (AUC) is an overall measure of test performance, with 0.5 indicating random performance and 1.0 denoting perfect performance. The proportion of true Illumina SNPs as a function of the proportion of false SNPs was calculated, using the variant frequency threshold as the test outcome and Sanger genotyping as the

outcome. Best variant frequency threshold was chosen as the one at which the average of sensitivity and specificity was highest, in order to maximize true positives, while minimizing false positives.

The correlation between minor allele frequencies of SNPs identified by pooled next generation sequencing and of those SNPs identified by individual Sanger sequencing was calculated by the Pearson product-moment correlation coefficient. In each pool, minor allele frequency (MAF) for Sanger sequencing was calculated as the number of occurrences of the alternative allele divided by the total number of sequences. MAF for pooled multiplexed NGS was calculated as the number of reads carrying the alternative allele divided by the total number of reads.

Small indel detection was performed separately on forward and reverse reads of each pool, requiring an indel to be called in both forward and reverse strands in at least 2 reads per strand. Indels with an average individual coverage lower than 25x per strand were not considered.

To investigate the effect of sequence coverage on SNP calling and to identify the optimal coverage for variant detection, a total of 1000 simulations, sampling subsets from 1% to 99% of reads generated in phase 1 were run, and the identified SNPs (positives) were compared with those identified using the whole sequence data. The intersection of the two sets represents a conservative estimate of true positives. Positive Predictive Value (PPV) was calculated as the ratio between true positives and positives.

Comparison between SNPs identified by multiplexed pooled NGS and individual Sanger sequencing was repeated in phase 2. The selected test set was composed as follows: all the twelve pools for primer *HCT*, pool 2 for primers *CCR7b* and *CCR7c*, and pool 12 for primer *4CL3b*. The algorithm applied for SNP detection in Sanger sequences was the same as applied in phase 1, while when identifying SNPs in short reads in *HCT1, C3H3, CCR7* and *4CL3* (showing on average half of the coverage of *CAD4*), the number of reads required on each strand and the lower acceptable individual coverage of a region to be used for SNP calling were linearly scaled, and set to five and 25x, respectively.

To investigate the effect of frequency threshold on SNP calling, additional analyses were conducted by varying the MAF threshold frequency from 0 to 1%, removing coverage thresholds and requiring that only one occurrence of the SNP was found on the forward and reverse strand. When the MAF threshold was zero, the number of polymorphic positions corresponded to the number of bases in which an error was

introduced on both strands during the whole sequencing process. The proportion of polymorphic positions was plotted as a function of the variant frequency used to define a polymorphism in each gene.

Nucleotide diversity is the average number of *per site* differences between two randomly chosen DNA sequences (Nei and Li, 1979); here, it was estimated as the sum of unbiased heterozygosity of segregating sites (Tajima, 1989), averaged over all nucleotides. Heterozygosity and its 95% confidence limits were calculated by resampling with replacement all pairs of polymorphic loci with probability corresponding to the frequency of the two alleles, and multiplying by n/(n-1), where n is the sample size of the pool, to obtain an unbiased estimate of nucleotide diversity (Futschik and Schlötterer, 2010); for each polymorphic position 200 resampling experiments were performed, each of size 10000. Neutrality hypothesis was tested calculating Tajima's D (Tajima, 1989); we chose confidence limits for Tajima's D based on the beta distribution for n=1000 DNA sequences, as calculated by Tajima (Tajima, 1989). Statistical analyses were performed in R (www.r-project.org).

3.2 Results

3.2.1 Resequencing

We performed a multiplexed pooling NGS experiment in 768 *P. nigra* accessions divided in 12 pools of 64 accessions each. The experiment consisted of two phases; we list objectives and results of each experimental phase below.

Phase 1 (CAD4)

Aim of phase 1 was to set-up a multiplexed pooled sequencing procedure for SNP detection in *CAD4* in 768 accessions. In addition, two pools (n=128) underwent individual Sanger sequencing to perform a sensitivity analysis and to identify the optimal SNP calling method; we will refer to this subset as the "training set".

In phase 1 of the experiment, about 0.9 Gb of sequence data were generated. Dividing this amount by the number of accessions (n=768) and by the length of the *CAD4* consensus (2240bp), we obtained an experiment-wide Mean Individual Coverage (MIC)

of 486x. The complete consensus sequence of *P. nigra CAD4* was obtained in our laboratory in a previous study (Marroni *et al.*, 2011). The consensus was used as a reference against which short reads were aligned. After removing a) reads which could not be aligned to the reference (8%), b) reads which could not be assigned to an index (4%), and c) over represented reads at amplicon ends (16%), an experiment-wide MIC of 350x was obtained (Figure 3. 2). MIC was variable across pools, ranging from 120x to 640x (Figure 3. 3). However, coverage at each single position along the gene, measured as Mean Individual per Base Coverage (MIBC, see Materials and Methods for details), is strongly conserved between pools, suggesting its sequence specificity.

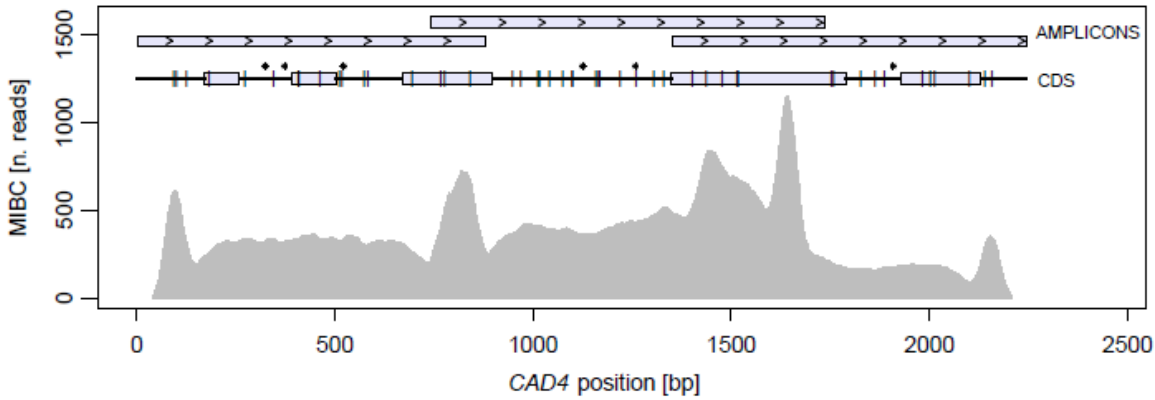

Figure 3. 2 MIBC along *CAD4* sequence. SNPs (vertical bars) and indels (asterisks) positions are indicated relative to the coding sequence (CDS, grey boxes) and introns (horizontal black lines).

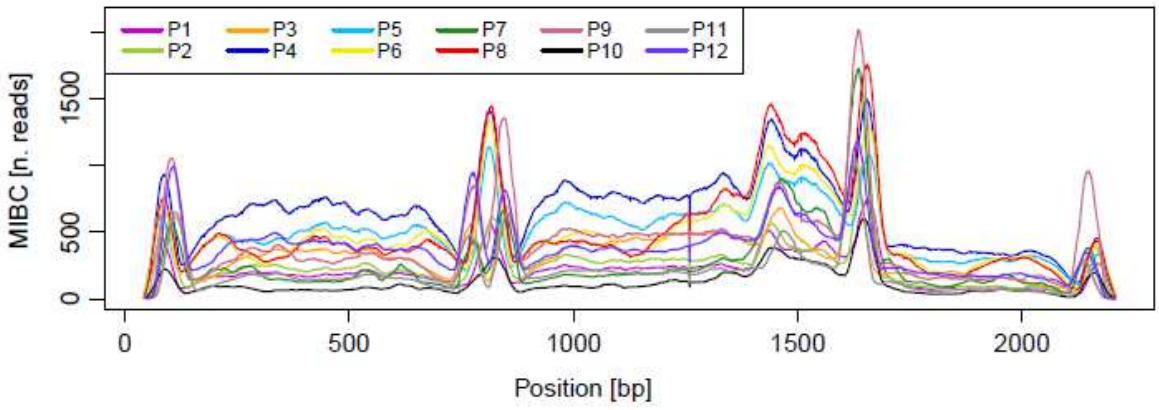

Figure 3. 3 MIBC along *CAD4* sequence in each pool. **P1**: MIBC of pool 1; **P2**: MIBC of pool 2; … ; **P12**: MIBC of pool 12.

Phase 2 (HCT1, C3H3, CCR7, 4CL3)

In phase 2 PCR products of the coding regions of *HCT1, C3H3, CCR7* and *4CL3* were obtained. PCR products of the four genes were pooled (see Materials and Methods for details) and sequenced in 768 accessions. A subset of the accessions and amplicons were also individually sequenced with Sanger technique, to estimate general performance of the method developed in phase 1; we will refer to them as the "test set". In phase 2 about 1.65 Gb of sequence data were generated, corresponding to an experiment-wide MIC of 181x (n=768, total length of consensus sequences 11500bp). After removing a) reads which could not be aligned to the reference (23%), b) reads which could not be assigned to an index (1%), and c) over represented reads at amplicon ends (5%), an experiment-wide MIC of 128x was obtained. We used Sanger sequencing on eight accessions to obtain a *P. nigra* consensus for the coding sequence of the genes; the length of each individual coding sequence (CDS) is reported in Table 3. 2. The consensus was used as a reference against which short reads were aligned. After removing reads which could not be aligned to the reference, reads which could not be assigned to an index and over represented reads, the MIC ranged from 108x in *CCR7* to 281x in *HCT1*. MIBC along each gene is shown in Figure 3. 4.

Table 3. 2 Summary statistics of SNPs identified in coding sequences of *CAD4*, *HCT1*, *C3H3*, *CCR7* and *4CL3*. CDS (bp): **Length of coding sequence in base pair. SNPs:** number of SNPs. **Missense:** number of missense SNPs. **Stop:** number of SNPs introducing a stop codon.

Gene	CDS	SNPs	Missense	Stop
CAD4	1074	19	8	0
HCT1	948	13	5	1
C3H3	1527	12	6	0
CCR7	1017	15	9	0
4CL3	1623	25	8	0

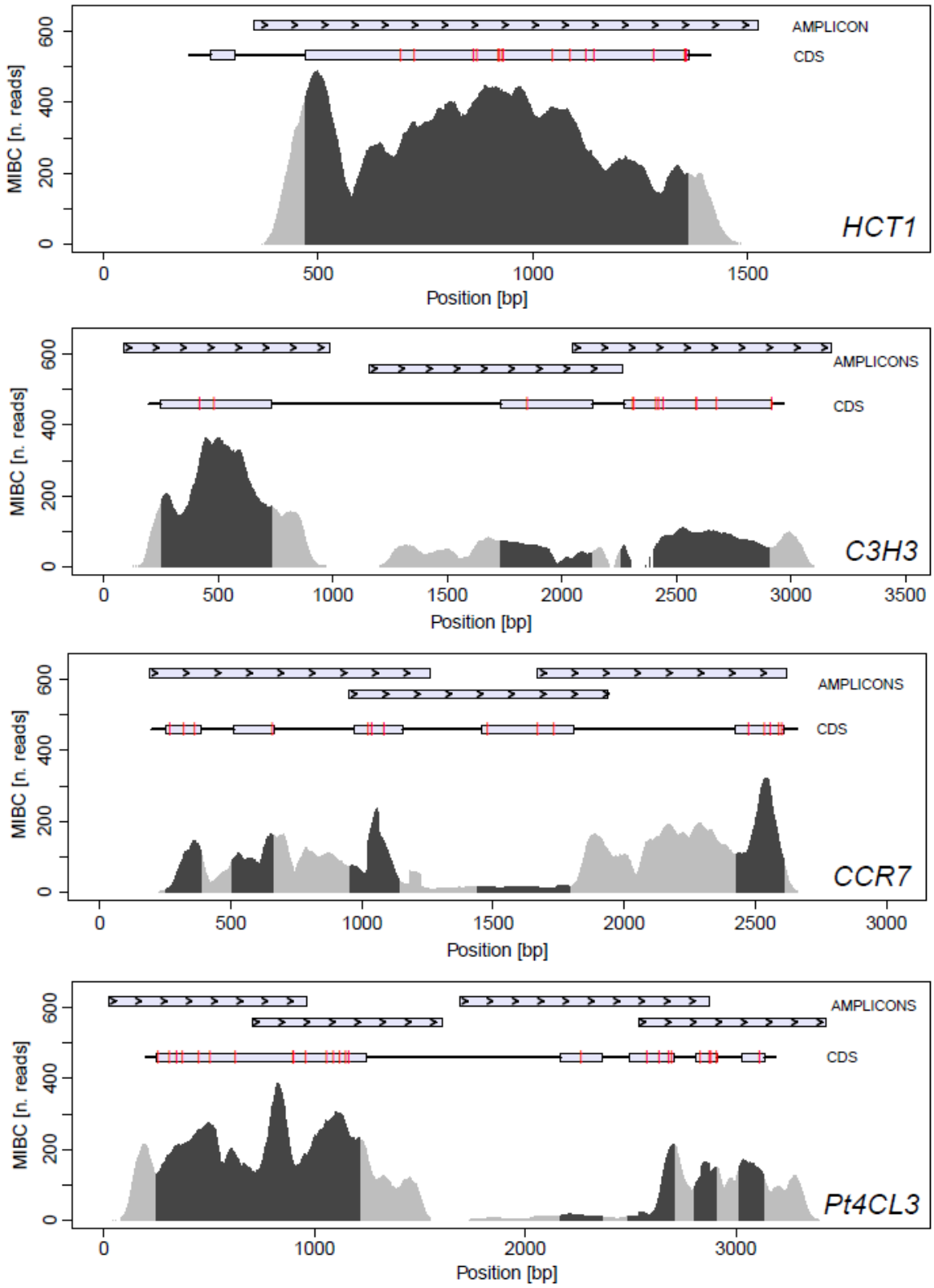

Figure 3. 4 MIBC along the sequences of the four additional genes sequenced in phase 2. SNPs (vertical red bars) positions are indicated relative to the coding sequence (CDS, grey boxes).

3.2.2 Variant detection

Phase 1 (CAD4)

To identify the more appropriate minor allele frequency (MAF) for SNP calling, we selected two pools (pool 5 and pool 9) as a training set. The training set was analyzed using both individual Sanger sequencing and pooled multiplexed NGS. Using individual Sanger sequencing, we identified a total of 42 SNPs, 19 in pool 5 and 23 in pool 9 (Table 3. 3, column Individual Sanger). Using multiplexed pooled NGS, we identified a total of 43 SNPs, 19 in pool 5 and 24 in pool 9 (Table 3. 3, column Pooled NGS); considering individual Sanger genotyping as the gold standard, 42 of the 43 SNPs identified by multiplexed pooled NGS were true positives and 1 was a false positive. No false negatives were identified. ROC analysis gave the best results (sensitivity 100%, specificity 99.9%) when we defined a SNP as any position in which more than 0.41% of the reads showed a base different from the consensus. Overall, pooled NGS was in agreement with individual Sanger sequencing and area under the ROC curve was 99.9%. The small difference obtained between the two techniques may be due to the joint effect of pooling and of the use of different sequencing technologies. Correlation of allele frequencies determined by Sanger individual sequencing and next generation pooled sequencing was high (Table 3. 3 and Figure 3. 5, Pearson's correlation coefficient r=0.96). Thus, the number of reads in a pooled sample is strongly correlated to allelic frequency in the origin population. As additional measure for assessing the ability of Illumina multiplexed pooled analysis to identify SNPs and indels, we mixed in each pool three controls for which the complete *CAD4* sequence was known from a previous study (Marroni *et al.*, 2011). In total, these 36 controls contributed 109 SNPs and 17 indels to the twelve pools. We were able to identify 105 of these SNPs and 15 indels, corresponding to sensitivity of 96% for SNP calling and of 88% to identify both SNPs and indels. Although rare, polymorphisms present in the control accessions might be present in additional accessions of each pool, thus the estimated sensitivity should be considered as an upper bound.

Using the identified MAF threshold, we performed SNP detection on the whole sample and identified 48 SNPs (1 every 47 bp), 19 of which in CDS (1 every 56 bp); 8 of them were non-synonymous (Table 3. 4). We identified 5 deletions and one insertion, all in non-coding regions (Table 3. 5 and Figure 3. 2). All the indels had already been

identified in a previous study (Marroni *et al.*, 2011). No indels were detected in the coding sequence of *CAD4*.

Table 3. 3 Minor allele frequency (MAF) of *CAD4* SNPs identified, in Pool 5 and Pool 9, by multiplexed pooled NGS and individual Sanger sequencing, respectively. [1]Position of the SNP on the reference sequence. [2]Minor allele frequency (MAF) using pooled multiplexed NGS. [3]Minor allele frequency (MAF) using individual Sanger sequencing. **ND**: No SNP detected.

		Pool 5		Pool 9	
Position[1]	**SNP**	**Pooled NGS[2]**	**Individual Sanger[3]**	**Pooled NGS[2]**	**Individual Sanger[3]**
948	T/A	0.0487	0.0735	0.0855	0.0758
969	C/G	0.1584	0.1471	0.1764	0.1667
1012	C/T	0.0090	0.0147	0.0167	0.0379
1016	T/G	ND	ND	0.0079	0.0076
1075	G/A	0.0122	0.0221	0.0478	0.0530
1098	C/T	0.2052	0.2206	0.1856	0.1970
1100	T/C	0.0082	0.0147	0.0098	0.0379
1159	A/G	0.1687	0.1439	0.1809	0.1719
1165	T/G	0.0100	0.0152	0.0054	0.0156
1168	T/A	0.0049	0.0076	ND	ND
1219	G/T	0.0048	0.0077	0.0370	0.0156
1260	A/G	ND	ND	0.0132	ND
1305	A/G	0.0108	0.0076	0.0193	0.0259
1329	A/G	ND	ND	0.0094	0.0172
1402	T/C	0.0111	0.0149	0.0066	0.0161
1437	A/G	0.0183	0.0147	0.0065	0.0077
1515	A/G	0.2141	0.2279	0.1457	0.1567
1518	G/A	0.0090	0.0075	0.0227	0.0373
1753	G/A	0.0046	0.0074	0.0359	0.0373
1758	A/G	0.0055	0.0074	0.0049	0.0075
1827	T/C	0.0338	0.0368	0.0183	0.0154
1886	T/A	0.2742	0.2426	0.1894	0.1875
2013	C/T	ND	ND	0.0154	0.0159
2101	C/T	ND	ND	0.0079	0.0079
2140	A/G	ND	ND	0.0105	0.0079

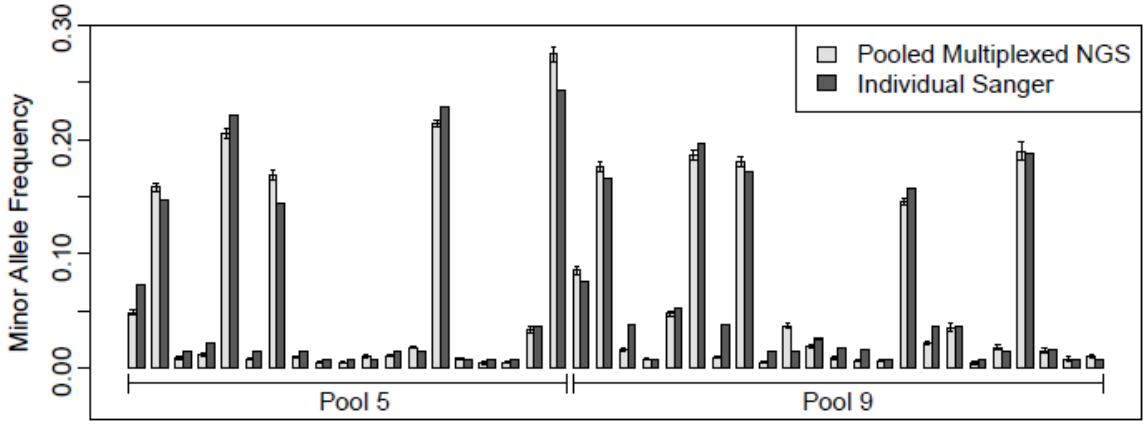

Figure 3. 5 Minor allele frequency of SNPs identified in the training set by pooled multiplexed NGS and individual Sanger sequencing. Error bars are calculated for pooled multiplexed NGS assuming a binomial distribution, with successes corresponding to the number of reads carrying the minor allele and attempts corresponding to the total number of reads.

Phase 2 (HCT1, C3H3, CCR7, 4CL3)

Using the SNP detection pipeline used in phase 1 we analyzed the four additional genes included in phase 2, to identify variants affecting amino acid composition of the corresponding gene products. We identified a total of 65 SNPs, 28 of which were non-synonymous (Table 3. 4). Five missense SNPs were identified in *HCT1*, nine in *CCR7*, five in *C3H3*, and eight in *4CL3*. In addition a SNP causing a premature stop codon was identified in *HCT1*. No indel was detected in the coding sequence of any of the four genes. To estimate general performance of the method developed in phase 1, a subset of accessions and amplicons included in phase 2 (the "test set") was selected for individual Sanger sequencing. The test set included all twelve pools for amplicon *HCT1*, pool 2 for amplicons *CCR7a* and *CCR7c*, and pool 12 for amplicon *4CL3b*. In total, 94 SNPs were called, 83 of which were identified by both approaches, six only by NGS and five by Sanger sequencing alone, with a sensitivity of 93%. Correlation of MAF between pooled multiplexed NGS and individual Sanger sequencing was 0.98, and correlation between the logarithms of the allele frequencies (sensitive to differences in small MAF) was 0.96. Figure 3. 6 shows logarithm of MAF of SNPs identified by individual Sanger sequencing as a function of logarithm of MAF of SNPs identified by NGS multiplexed pooled sequencing. Of the 83 SNPs identified by both approaches, 34 had a frequency lower than 5% and 10 a frequency lower than 1%. Each rare SNP is carried by one or a few accessions, and globally they appear in a small proportion of accessions.

Table 3. 4. List of non-synonymous SNPs of *CAD4*, *HCT1*, *C3H3*, *CCR7* and *4CL3*. [1]Relative to the coding sequence. [2]Common allele/rare allele. [3]Number of pools in which the SNP was identified. [4]Mean individual per base coverage of the SNP position. [5]Minor allele frequency in the whole sample. [6]Predicted number of chromosomes carrying the SNP.

Gene	Position[1]	SNP[2]	No. pools[3]	MIBC[4]	Frequency[5]	Carriers[6]	Aa change
CAD4	11	T/A	2	283	0.0011	2	L4H
CAD4	109	G/C	12	326	0.0114	18	V37L
CAD4	310	C/A	12	483	0.2015	310	N104H
CAD4	374	A/C	4	592	0.0029	4	Y125S
CAD4	597	A/G	12	657	0.1896	291	I199M
CAD4	835	G/A	8	233	0.0129	20	A279T
CAD4	925	A/G	1	159	0.0003	1	M309V
CAD4	956	C/T	4	286	0.0046	7	A319V
HCT1	278	C/T	11	280	0.0239	37	T93I
HCT1	508	C/T	1	822	0.0012	2	R170C
HCT1	517	C/T	2	493	0.0011	2	L173F
HCT1	632	T/C	1	501	0.0004	1	V211A
HCT1	710	G/C	6	263	0.0057	9	G237A
HCT1	729	C/A	12	227	0.0298	46	C243*
C3H3	598	C/G	12	54	0.4376	672	E200Q
C3H3	922	G/A	2	52	0.0009	1	I308V
C3H3	1033	T/C	8	75	0.0052	8	P345S
C3H3	1053	A/C	2	115	0.0014	2	Q351H
C3H3	1198	C/T	8	128	0.0226	35	P400S
CCR7	70	C/A	8	132	0.1967	302	L24I
CCR7	112	A/G	12	135	0.3034	466	T38A
CCR7	350	C/G	5	57	0.0069	11	A117G
CCR7	506	C/T	1	30	0.0303	47	A169V
CCR7	758	C/T	1	27	0.0359	55	S253F
CCR7	887	A/G	2	210	0.0007	1	K296R
CCR7	947	A/G	11	289	0.0191	29	K316R
CCR7	1003	C/G	8	170	0.2979	458	V335L
CCR7	1014	A/T	4	121	0.0059	9	Q338H
4CL3	7	G/A	11	127	0.0245	38	A3T
4CL3	61	T/G	4	231	0.0039	6	Y21D
4CL3	95	T/C	1	153	0.0004	1	V32A
4CL3	709	T/C	2	149	0.0008	1	F237L
4CL3	897	C/G	12	255	0.0887	136	D299E
4CL3	913	A/G	1	181	0.0008	1	M305V
4CL3	1477	A/T	1	109	0.0004	1	T493S
4CL3	1512	G/T	1	101	0.0012	2	Q504H

Table 3. 5 Insertions and deletions detected in *CAD4*. **Position**: Position in base pair relative to the length of *P. nigra* coding sequence. **Type**: Type of polymorphism (Ins = Insertion, Del = Deletion). **No. pools**: number of pools in which the polymorphism was identified. **MIBC**: Mean individual per base coverage of the considered position in the pools in which the polymorphism was identified. **Frequency pools**: Minor allele frequency in the pools carrying the polymorphism. **Frequency total**: Minor allele frequency in the whole sample.

Position	Type	Sequence	No. pools	MIBC	Frequency pools	Frequency total
325	Ins	TGTGTA	8	264.67	0.0082	0.0055
374	Del	CTT	9	257.27	0.0048	0.0036
522	Del	A	12	342.98	0.0365	0.0365
1126	Del	C	9	402.33	0.0205	0.0154
1259	Del	AA	12	444.43	0.2964	0.2964
1909	Del	T	11	191.13	0.0089	0.0082

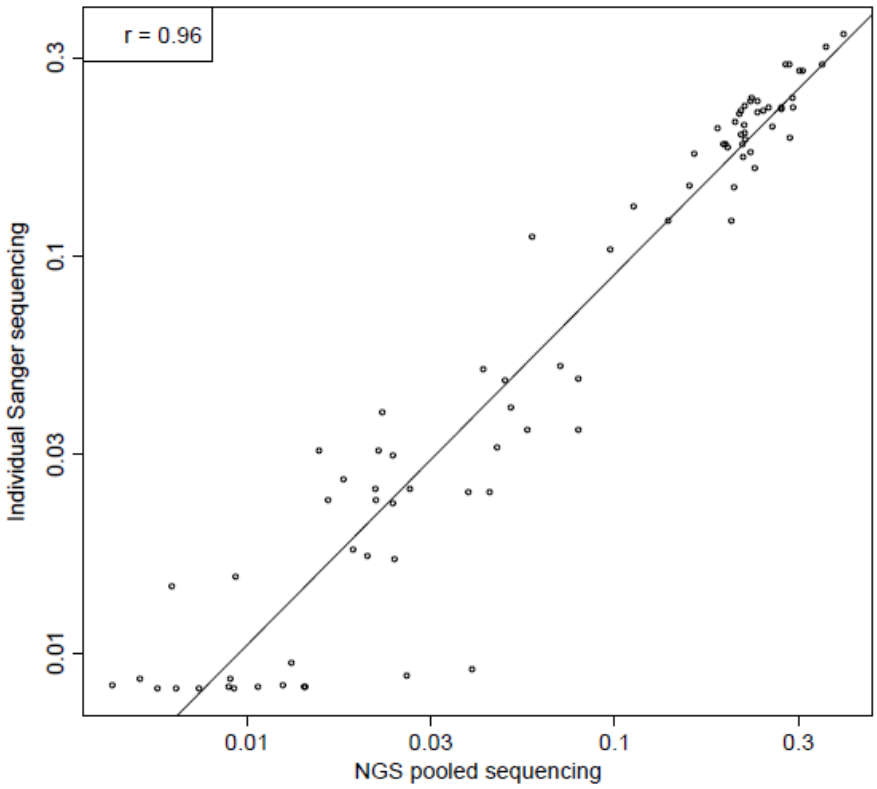

Figure 3. 6 Minor allele frequency of SNPs identified in the test set by pooled multiplexed NGS and individual Sanger sequencing.

Among the large proportion of variants with a frequency lower than 5%, we identified in *HCT1* a variant causing a premature stop codon (C243*, Table 3. 4); the resulting gene product is substantially shorter than the expected 315 amino acids. We confirmed

the variant and identified 41 heterozygous and one homozygous mutation carriers by individual Sanger sequencing in the twelve pools.

3.2.3 Removing sequencing and alignment errors

False positive SNPs can arise at the 5' and 3' ends of Illumina reads due to the higher error rate of the sequencing process or to the presence of small insertions/deletions near the read ends. To adjust for this we 1) analyzed forward and reverse strand separately and required that each SNP was identified in both strands; and 2) partitioned each read in three segments of equal length, and required that each SNP was identified in each of the segments of the read (see Materials and Methods for details). Analysis performed on the training set (phase 1) without these additional quality controls identified a total of 50 SNPs, 8 of which were false positives using individual Sanger sequencing as a gold standard. The positive predictive value was thus 84%. Applying the above mentioned quality controls we identified 43 SNPs, one of which was false (PPV=97.7%). In both analyses we identified no false negative SNPs.

3.2.4 Effect of using a high fidelity DNA polymerase on SNP detection

Given the sample size of 64 diploid individuals for each pool, the method was required to detect variants with a theoretical minimum frequency of 1 in 128 (0.78%). False positive SNPs can arise as a consequence of either wrong alignments or sequencing errors or errors introduced in the sequencing templates during the PCR amplification reaction due to mis-incorporation of dNTPs by DNA polymerase. *Taq* polymerase is known to be a particularly error-prone polymerase, with an estimated error rate between 1.1 errors per 10^4 bp and 2 errors per 10^5 bp according to manufacturer, and this is known to create problems when sequencing cloned PCR products. To investigate the role of DNA polymerase error rate we amplified one candidate gene (*HCT1*) using a high fidelity polymerase with an error rate of 1 per 10^7 bp. We varied the MAF threshold required to call a SNP from 0 to 1%, recorded the number of identified SNPs as a function of MAF threshold and compared results obtained using the two different enzymes. When the MAF threshold was close to zero, the fraction of bases carrying a

putative SNP was between 0.9 and 1.0 (Figure 3. 7). When the MAF threshold for SNP calling increased, the proportion of bases identified as polymorphic decreased. In Figure 5, a dot displays the frequency at which the number of bases identified as SNPs is lowered to 50% of the initial value. The corresponding frequency was 0.1% for *HCT1* (the only one amplified using a high fidelity DNA polymerase), and more than 0.2% for all the genes for which amplification was performed using Amplitaq Gold. When the MAF threshold increased to 0.4%, performances of the two different polymerases were comparable. Overall, our data suggest that the use of an accurate polymerase decreases the process error rate and facilitates the detection of extremely rare variants. However, variants with frequencies lower than 1% can still be accurately detected even without the use of a high fidelity polymerase.

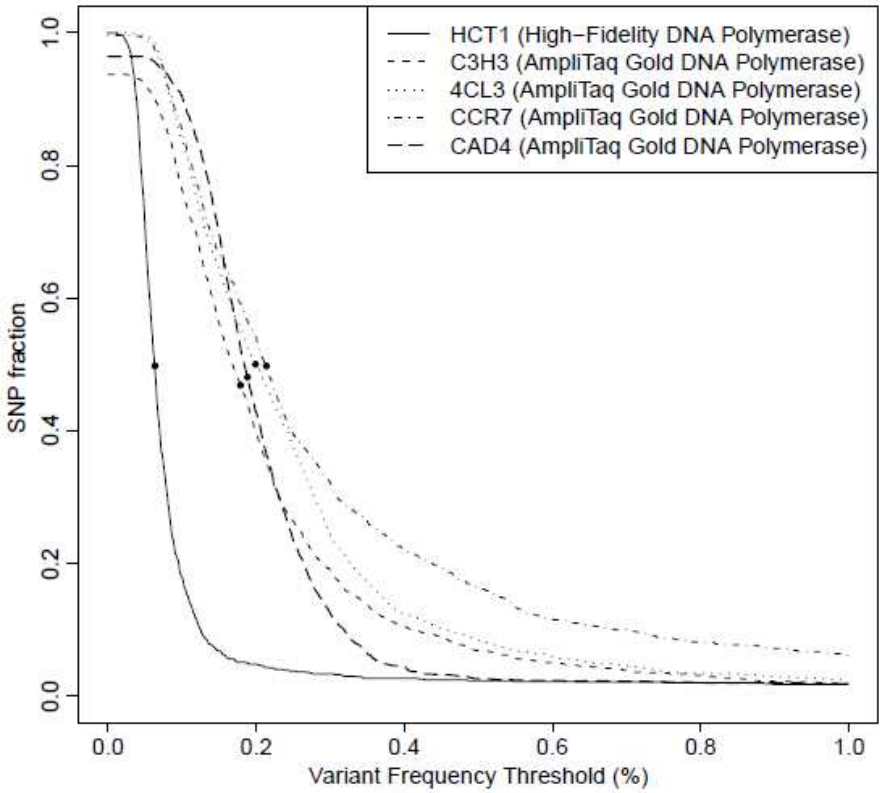

Figure 3. 7 Number of called SNP per nucleotide as a function of the MAF set as threshold in the five genes studied in the experiment. The dots represent the frequency for which number of SNPs is lowered to 50% of the initial value. Continuous line: *HCT1*, sequenced using a high fidelity polymerase. Thick dashed line: *CAD4*, sequenced with Taq polymerase. Thin dashed line: *C3H3*, sequenced with Taq polymerase. Dotted line: *4CL3*, sequenced with Taq polymerase. Dashed-dotted line: *CCR7*, sequenced with Taq polymerase.

3.2.5 Effect of decreasing Mean Individual Coverage (MIC) on SNP detection

To investigate the effect of decreasing MIC on SNP detection and to identify the optimal coverage for variant detection, we performed simulations on subsets of the data generated in phase 1. Figure 3. 8 shows the number of SNPs as a function of MIC (continuous line). The graph also shows the corresponding number of SNPs in common with those identified in the analysis on the whole dataset (dashed line), which can be considered a conservative estimate of true positive SNPs. When MIC is above 150x, the results are not distinguishable from those obtained with the whole data set. Performance is worse for MIC lower than 100x, where almost 50% of the identified SNPs were not identified in the whole data set (i.e. likely to be false positives).

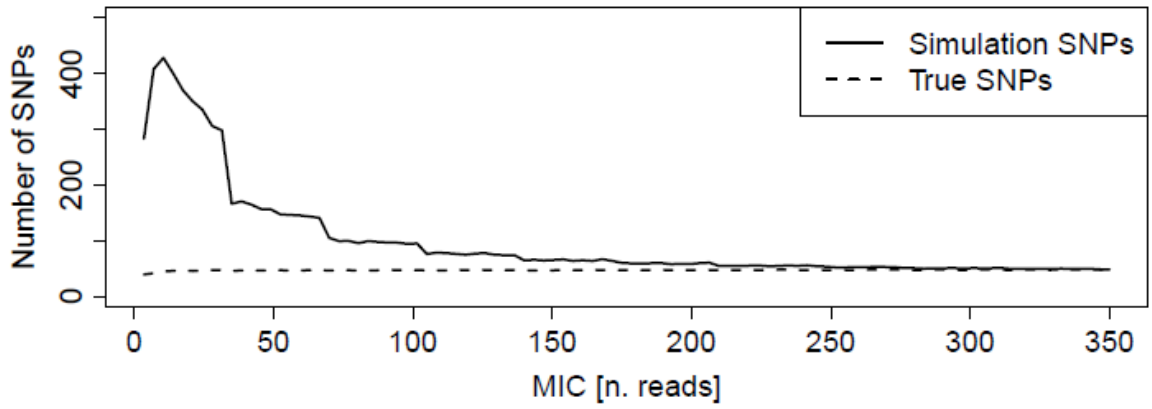

Figure 3. 8 Number of SNPs identified as a function of MIC. Results are plotted as the average of results from ten independent simulations (continuous line). The average number of SNPs included in the intersection between SNPs identified in the simulation and in the whole set of reads (dashed lines) are used as an estimate of true positives.

3.2.6 Population genetics parameters

Accuracy of nucleotide diversity estimation by pooled multiplexed NGS was evaluated by comparing nucleotide diversity in training and test set. Estimates of nucleotide diversity based on multiplexed pooled NGS and individual Sanger sequencing were highly correlated (r=0.99, Figure 3. 9). Nucleotide diversity and statistical tests for neutrality (Tajima's D test) were computed in the whole sample. Results are shown in Table 4. No Tajima's D test showed significant deviation from neutrality. However,

most of Tajima's D tests showed negative values. Overall nucleotide diversity ranged from $0.65*10^{-3}$ to $1.86*10^{-3}$. Non-synonymous to synonymous nucleotide diversity ratio ranged from 0.03 in *HCT1* and *4CL3* to 0.47 in *CCR7*.

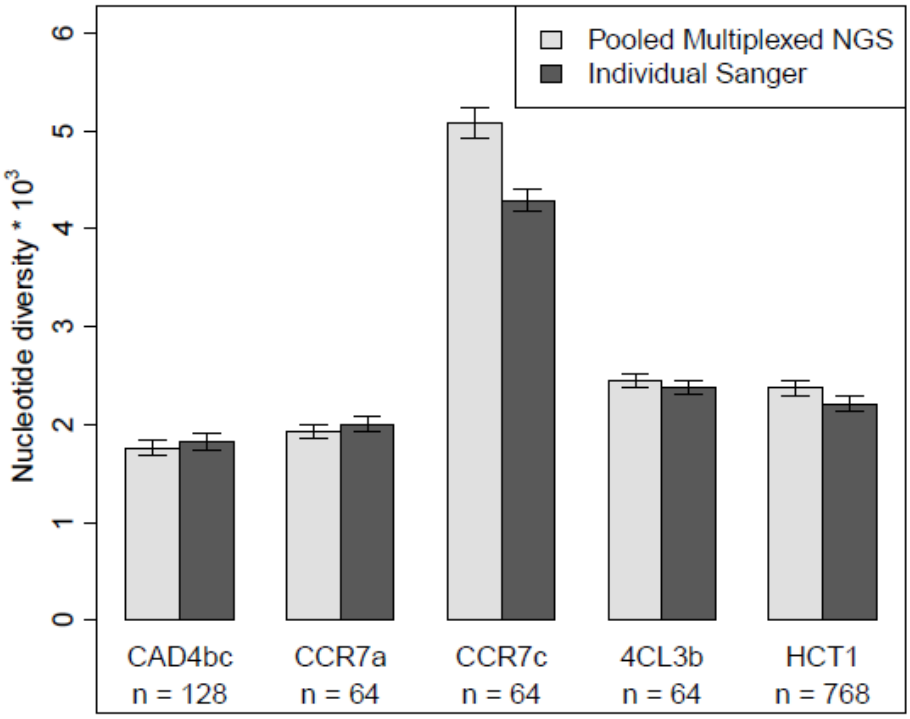

Figure 3. 9 Nucleotide diversity calculated using allele frequency estimated by pooled multiplexed NGS (light bars) and by individual Sanger sequencing (dark bars).

3.3 Discussion

Next generation sequencing of selected genomic regions represents a powerful approach to identify the complete spectrum of DNA sequence variants. Accurate detection and genotyping of SNPs is crucial for using population sequencing to detect rare, as well as common, functional variants affecting any given trait. For this reason, a cheap and fast method for the identification of polymorphisms is likely to be of great importance for determining the spectrum of variation and for identifying carriers of

functional variants. We report on the use of multiplexed pooled next generation sequencing of PCR products to identify SNPs in five candidate genes involved in lignin biosynthesis.

Our aim was to detect rare, as well as common, polymorphisms in a sample of 768 poplar accessions arranged in 12 pools consisting of 64 accessions each. For this reason, we developed a custom analysis workflow with strong discrimination ability between real SNPs and sequencing or alignment errors. Given the small number of genes that we sequenced, PCR was the method of choice. However, errors due to DNA polymerase might affect the detection of rare variants. We performed a subset of amplifications using a high fidelity polymerase, and showed that the use of an accurate DNA polymerase increase the ability to discriminate between sequencing errors and true polymorphisms (Figure 3. 7).

Each of the 12 pools was composed by a relatively high number of poplar accessions (n=64), and the number of individuals sequenced in a single reaction was very high (n=768). Therefore, a high Mean Individual Coverage was required to avoid that SNPs in under-represented accessions were missed. In phase 1 we obtained a MIC of 350x. Simulations showed that lower MIC (around 150x) still allowed to obtain reliable results (Figure 3. 8).

False positive SNPs can arise at the 5' and 3' ends of Illumina reads due to the higher error rate of the sequencing process or to the presence of small insertions/deletions near the read ends. The workflow that we developed was effective in removing SNPs in proximity of small insertions/deletions, and substantially reduced false positive findings.

Applying our workflow to the whole data set, we identified 37 non-synonymous SNPs in five genes involved in lignin biosynthesis (Table 3. 4), one of which (C729A) caused a premature stop codon (C243*) in *HCT1*. We performed individual Sanger sequencing to identify carriers of the C243* mutation. Carriers of the stop codon have been selected for extensive phenotypic evaluation, and will be used in conventional breeding program to obtain offspring with improved lignin composition. Among SNPs confirmed by individual Sanger sequencing, we were able to identify a SNP occurring only once in 1536 chromosomes (expected frequency 0.065%). This gives an idea of the potential that pooled multiplexed NGS has to identify rare variants. The ability to confidently identify rare variants is crucial. Mutations affecting the phenotype are likely to be

negatively selected. Their frequency f will depend on the mutation rate μ and on the strength of the negative selection s. At the equilibrium, the predicted frequency of a dominant mutation is $f = \frac{\mu}{s}$, and that of a recessive mutation is $f = \sqrt{\frac{\mu}{s}}$. Assuming a gene mutation rate in the range 10^{-8} to 10^{-5} and a decrease in fitness of 1%, the expected frequency of a dominant allele in the population will be lower than 0.1% and that of a recessive allele lower than 5%. Not surprisingly, more than 40% of the SNPs identified in the present study had a frequency lower than 5%, and eight SNPs are predicted to appear in only one chromosome (Table 3. 4). Knockout mutations, such as those that can be obtained by gene silencing through transformation, are likely to be fully recessive and have a selection coefficient equal to 1. This would translate into an equilibrium frequency range of 0.0001-0.0032 for the same range of mutation rate. This would require screening a number of 475 to 15000 individuals to have a 95% chance of identifying the desired mutation. These numbers, though large, are clearly approachable using the method here described that can therefore be adopted to look for rare mutations that could be utilized in breeding programs in place of transgenic events.

We detected one such mutations that causes a premature stop codon (C243*) in *HCT1* and that was found at a rather high frequency (3%), including in a homozygous individual. The reason for such a high frequency and for the vitality of the homozygote could either be that the mutation is not causing a gene knockout due to its location towards the COOH-terminus of the protein that would therefore retain at least a partial activity, or that the gene is partially or completely functionally redundant due to the presence of additional family members (Shi *et al.*, 2010).

Our method accurately identified rare variants, with low false-positive and low false-negative rates, and allowed to correctly estimate minor allele frequency (Figure 3. 5). As a consequence, all population genetics parameters that can be obtained from allele frequency, such as nucleotide diversity, are also accurately estimated. Additional population genetic parameters such as Tajima's D can also be calculated. The workflow that we developed can be used to identify common and rare SNPs in any organism. Given its ability to discriminate true positive SNPs from bias, it is particularly suited for the screening of large populations in search of rare variants that could be immediately used in breeding programs. In addition, studies aimed at the genetic characterization of different populations of a given organism may take advantage of our workflow.

Individuals belonging to each population will be pooled together, and population genetics parameters can be accurately estimated for each population. Finally, researchers investigating qualitative phenotypes may compose pools based on the phenotypic category, accurately estimate allele frequency of SNPs in the two phenotypic classes, and perform pooled association studies following statistical approaches that have already been developed (Sham *et al.*, 2002).

In conclusion, we showed that our workflow based on pooled multiplexed NGS is an efficient and accurate method to screen a large number of individuals for mutations providing the basis for a next generation Ecotilling method (Comai *et al.*, 2004). Sensitivity and specificity of the method are extremely high, and the identification of polymorphisms is highly quantitative, allowing accurate estimation of allele frequencies and population genetic parameters in large samples.

4

Structural Variation in Poplar

4.1 Materials and Methods

4.1.1 Plant material

The experimental sample consisted of 4 *Populus nigra* genotypes (BDG, 71077-308, POLI and BEN3), 2 *Populus deltoides* genotypes (L150-089 and L155-079) and 12 *P. nigra* x *P. deltoides* F1 hybrids, obtained by crossing two of the four *P. nigra* and the two *P. deltoides* genotypes with a partial factorial design. Pedigree information of the 12 hybrids is reported in Figure 4. 1.

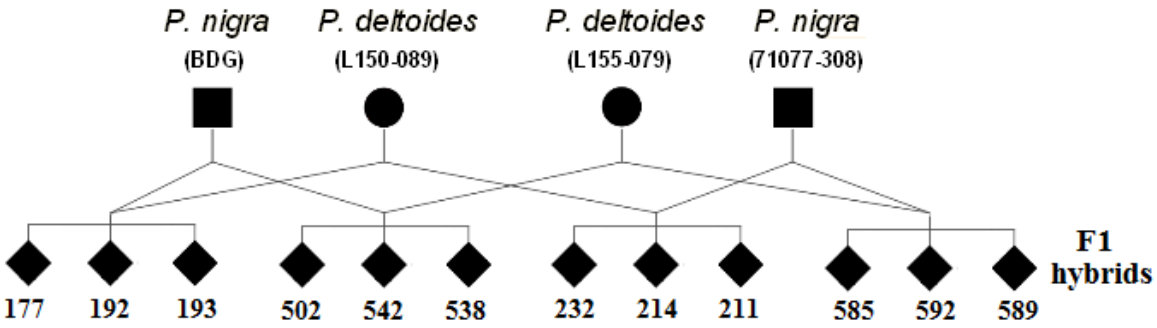

Figure 4. 1 Representation of the studied interspecific poplar pedigree. Two *P. nigra* males were crossed with 2 *P. deltoides* females and three F1 hybrids per cross were selected.

4.1.2 DNA extraction, library preparation, and next-generation sequencing

Leaf tissues from greenhouse-grown plants were ground in liquid nitrogen and high-molecular-weight genomic DNA was extracted from nuclei using a modification of Zhang protocol (Zhang *et al.*, 1995). To prepare NGS libraries, 5 µg of nuclear DNA was randomly fragmented by Fragmentase treatment (NEBNext™ dsDNA Fragmentase™, New England Biolabs) at 37°C for 1 hour. Libraries were prepared using Illumina reagents, according to manufacturer's specifications (Illumina, San Diego, CA). End repair of fragmented DNA was performed using T4 DNA polymerase and Klenow polymerase with T4 polynucleotide kinase. Subsequently, an "A" base was added at the 3' end using a 3'–5' exonuclease-deficient Klenow fragment. The paired end adaptor (Illumina) with a single T base overhang at the 3′ end was ligated to the above products. The PE adaptor ligated products were separated on a 2% agarose and excised at approximately 600 bp. Fragments were enriched by 16-cycle PCR reaction using PE primers 1.1 and 2.1 (Illumina). A Genome Analyzer flowcell was prepared on the supplied cluster station and libraries were sequenced on the Illumina GA2x platform according to the manufacturer's instructions. The library of sample POLI was sequenced on the newer Illumina HiSeq platform. Images from the instrument were processed using the manufacturer's pipeline software to generate FASTQ sequence files.

4.1.3 Short read alignment and phylogeny reconstruction

CLC Genomics Workbench (CLC bio, Cambridge, MA) was used to remove low quality 3' ends of each read. After trimming, only pairs where both reads were longer than 50 bp were retained. Reads were aligned to the *P. trichocarpa* reference sequence using the short read alignment program BWA (Li and Durbin, 2009) with default parameters. Mean individual coverage for each sample was calculated by summing the coverage at each position of the reference genome and dividing the result by the number of positions of the genome covered by at least one read. Mean physical coverage was calculated with the same criteria but taking into account also positions comprised between the two sequenced reads. To reconstruct phylogeny we compared the reference *P. trichocarpa* sequence with the consensus sequence of the four parental accessions. The genome-wide number of nucleotide differences was calculated for all pairs of

individuals and was used to build a distance matrix. A phylogenetic tree based on the distance matrix was reconstructed using an Unweighted Pair Group Method with Arithmetic Mean (UPGMA) approach using phylip (Felsenstein, 1989).

4.1.4 Detection of deletions

BreakDancerMax (Chen *et al.*, 2009) was employed to detect deletions relative to the *P. trichocarpa* reference sequence. BreakDancerMax uses span size information of each paired-end read to identify paired-end reads with an anomalously long span size. Based on simulation results, deletions were called for the 6 *P. nigra*/*P. deltoides* individuals requiring for at least one individual a minimum number of anomalous read pairs to establish a connection of 5 (option *r*) and a minimum MAQ mapping quality of 60 (option *q*). In addition, a maximum structural variant size of 50000 (option *m*) was required. For sample POLI, which had a mean coverage about three times the coverage present in the other 5 samples, option *r* was set to 15. BreakDancerMax was also employed to detect deletions in the 12 hybrids. Due to the lower mean coverage obtained in hybrids, in this analysis BreakDancerMax was run with default parameters ($r = 2$, $q = 35$). Results for each hybrid were compared with those obtained in highly covered individuals to identify which variants present in parents were also identified in the F1 progeny. The deleted sequences were annotated in order to identify 1) their homology with transposable elements and 2) their gene content. The homology with transposable elements was analyzed by a blastn (Altschul *et al.*, 1990) analysis of the deleted sequences against a database of repetitive elements. The database was composed by all the plant sequences present in RepBase16.02 (Jurka *et al.*, 2005), all the sequences from TREP Release 10 (Keller *et al.*, 2002), all the sequences from the Plant Repeats Database at MSU (Ouyang and Buell, 2004), and a list of transposable elements annotated from *Vitis vinifera*, *Prunus persica* and *P. trichocarpa*. In addition, the database contained a list of 6273 *P. trichocarpa* specific repetitive sequences identified using RepeatScout (Price *et al.*, 2005).

4.1.5 Detection of insertions

For the detection of insertions with respect to the *P. trichocarpa* reference sequence, a custom pipeline was developed. The pipeline aims at the detection of insertions

resulting from known DNA elements, such as transposable elements; it is composed by three main steps:

1- Putative insertions are recognized by the presence of singletons (i.e. reads aligned to the reference having the mates unaligned or aligned in multiple positions of the genome) flanking the insertion site. In the occurrence of an insertion, singletons should fall into two groups with opposite orientation pointing toward the putative site of insertion (Figure 4. 2 and Figure 4. 3, Step 1) and their mates are expected to be unmapped because they derive from the inserted sequence, which, by definition, is not present in the reference genome. To identify the putative insertion sites, for each of the 19 chromosomes, all the forward and reverse oriented singletons were extracted from the alignment file and then separately *de novo* assembled using the CAP3 Sequence Assembly Program (Huang and Madan, 1999). CAP3 was run by setting an overlap length cutoff of 16 (option *o*), a clipping range of 6 (option *y*), an overlap similarity score cutoff of 251 (option *s*), a maximum overhang percent length of 100 (option *h*), a match score factor of 40 (option *m*), a segment pair score cutoff of 21 (option *i*) and a chain score cutoff of 31 (option *j*). The obtained "forward" and "reverse" contigs were aligned with *blastn* against the corresponding chromosome of the *P. trichocarpa* reference genome. Putative points of insertions were selected as regions of the chromosome flanked on the left by a "forward" contig and on the right by a "reverse" one, with a maximum distance between the two contigs lower than the mean insert size.

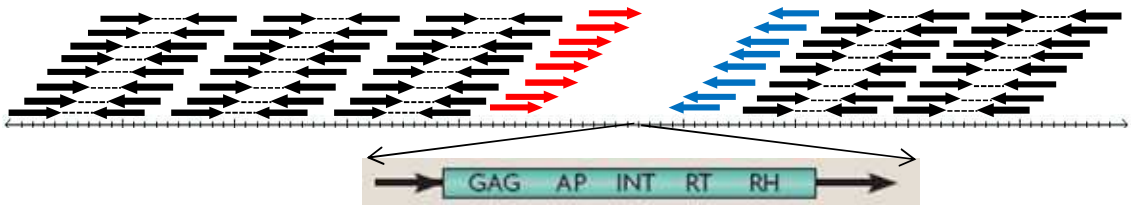

Figure 4. 2 Schematic representation of the insertion signature. Red and blue arrows represent the two groups of singletons with opposite orientation pointing toward the putative site of insertion.

2- To reconstruct the two ends of the putatively inserted sequence, the unaligned mates of the singletons used to assemble the "forward" and "reverse" contigs were selected and *de novo* assembled using the tool CAP3 (Figure 4. 3, Step 2).

3- To characterize the whole inserted sequence, contigs obtained in step 2 were aligned using *blastn* against a database of known plant transposable elements consisting of the

whole set of databases used for the annotation of deleted sequences, with the addition of the sequence regions that were identified as deletions. Insertions were detected when the two contigs aligned at the two extremities of the same sequence within this set (Figure 4. 3, Step 3).

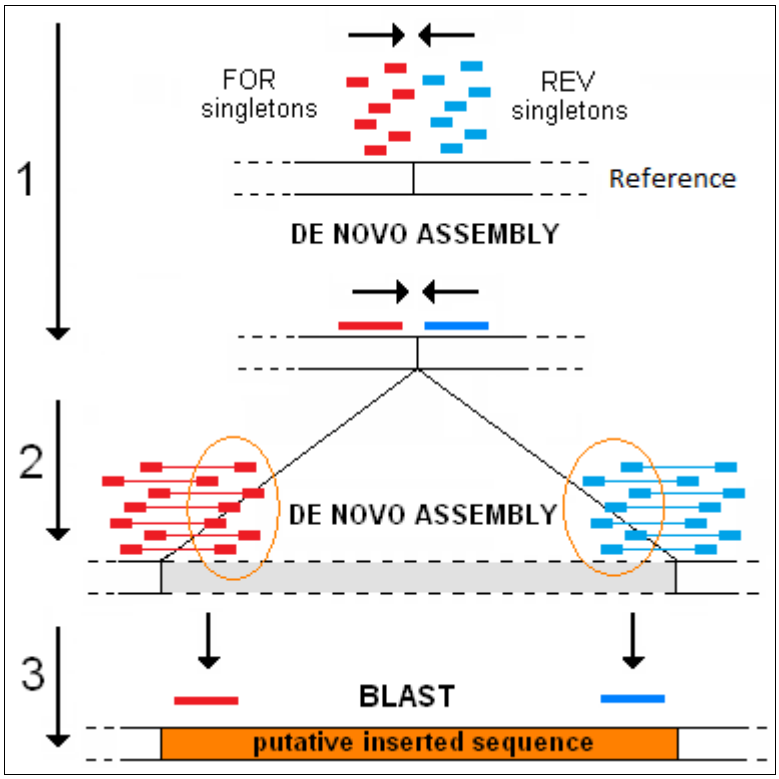

Figure 4. 3 Graphical representation of the pipeline developed for the detection of insertions.

4.1.6 Simulations

To investigate the sensitivity in identifying structural variants and to choose the best parameters for the analysis, one thousand insertions and deletions were simulated for the sample L155-079, randomly chosen from the six high coverage sequenced individuals. Variants were simulated by randomly selecting one thousand 1 to 30 Kb DNA sequences in the original *P. trichocarpa* reference sequence and moving them to a new randomly chosen position, forming a modified reference, *SV.reference* (Figure 4. 4). Simulated insertions were expected where the 1000 sequences were removed from the original reference, while deletions were expected where the sequences have been

inserted. To ensure sufficient coverage on both sides of the simulated variants, sequences were moved from and to positions of the genome having a mean sequence coverage of at least 5x in the surrounding 500 bp in the chosen genotype. To perform the detection of the simulated structural variants, L155-079 reads were aligned against the *SV.reference* using BWA as described before.

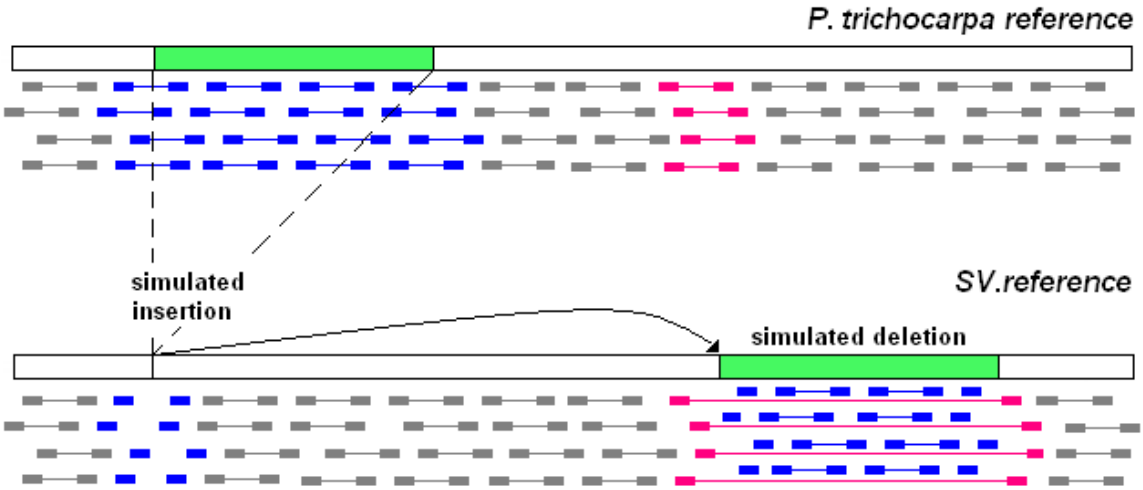

Figure 4. 4 Representation of the strategy employed to simulate 1000 insertions and deletions in the *P. trichocarpa* reference genome. It assumes no structural variation between *P. trichocarpa* and *P. nigra* in the regions involved.

Identification of simulated deletions

To identify simulated deletions, BreakDancerMax was used to analyze the sample L155-079 aligned against the modified *SV.reference.* This algorithm detects deletions using read pairs that are mapped at a distance > 3 standard deviation of the insert size. BreakDancerMax was run requiring a maximum structural variant size of 50000 (option *m*), a minimum number of read pairs to establish a connection of 2 (option *r*) and a minimum MAQ mapping quality of 35 (option *q*). True positives were defined as deletions detected by BrekDancerMax overlapping 50% reciprocally with a simulated variant. To quantify BreakDancerMax's performance with respect to different parameter settings, results were filtered by progressively increasing values of *r* and *q* and analyzing the effect on results. Performance was quantified in terms of the number of true positives (TP) and the number of total positives (P). The number of false positives (FP) is unknown and can only be estimated on the basis of the number of total positives. In fact, in addition to the 1000 simulated deletions, other true deletions that

were originally present in sample L155-079 with respect to *P. trichocarpa* can be identified. To identify the optimal confidence score threshold and the optimal minimum number of anomalously mapped pair reads required to call a deletion, we analyzed the percentage of TP and P as a function of the applied thresholds. This analysis aimed at the selection of those parameters at which the number of P considerably decreased compared to TP, in order to maximize true positives, while minimizing false positives. In addition, to analyze the possible factors affecting sensitivity, a comparison of the sequence coverage in the 500 bp surrounding the simulated variants between true positives and false negatives was performed. Boxplots and coverage statistics in the two datasets were computed excluding from the analysis the 2.5% extreme values of the coverage.

Identification of simulated insertions

To evaluate the power to detect insertions, the alignment of sample L155-079 against the modified *SV.reference* was analyzed with a custom pipeline (see section 4.1.5). True positives were defined as insertions detected by our pipeline less than 500bp apart from the simulated insertion site. To evaluate the effect of sequence coverage on sensitivity, a comparison of the sequence coverage between true positives and false negatives in the 500 bp surrounding the simulated insertions was performed.

4.1.7 Gene content analysis

The *P. trichocarpa* v2.2 gene annotation (Tuskan *et al.*, 2006) was used to study the gene content of the identified deletions and the gene fraction interrupted by the identified insertions. Sequences of these two subsets of genes were used as query for a blastx analysis against the Viridiplantae (taxid: 33090) non redundant protein (nr) database. Blastx results were imported into the Blast2GO tool (Conesa *et al.*, 2005) for the functional annotation. Blast2GO extracts the GO terms associated to each of the obtained blastx hit and returns an evaluated GO annotation for the query sequences. Blast2GO functional annotation was performed taking into account only those functional terms which were covered by at least 10% of the dataset. Over- or under-representation of GO terms in the two subsets, as compared with the rest of the genome, was tested using a Fisher's Exact Test implemented in the Gossip (Blüthgen *et al.*,

2005) package integrated in Blast2GO. To reduce the number of false positives, a false discovery rate correction for multiple testing (Benjamini and Hochberg, 2007) was applied and only differences with a corrected p-value <0.05 were selected.

4.1.8 PCR validation

To experimentally validate a set of identified insertions and deletions we used a PCR-based assay. We performed PCR amplifications of the ends of 36 deletions and 36 insertions in order to obtain differential amplifications in the presence or absence of the putatively detected variants. We aimed at obtaining at least 20 informative amplifications for each kind of variant. We designed 4 primers for each variant (Figure 4. 5) that were combined in 3 primer pairs: one pair (1-2) amplifying the 5' junction between the deleted/inserted sequence and the reference sequence, one pair (3-4) amplifying 3' junction, and a third pair (1-4) connecting the two genomic regions flanking the variant. Deletions are confirmed by the amplification of the two external primers (1-4), while insertions are confirmed by the amplification of the two junctions (1-2 and 3-4). Primer design was performed using BatchPrimer3 (You *et al.*, 2008). DNA amplifications were performed in 15 µl PCR reactions, using KAPA2G Fast Hot Start Ready Mix (Kapa Biosystems). The reactions were performed in the Geneamp 9700 PCR system (Applied Biosystems, Foster City, CA), under the following conditions: 95 °C for 2 minutes, 35 cycles of 15 seconds at 95 °C, 15 seconds at 56 °C and 15 seconds at 72 °C, followed by a final extension of 1 minute at 72 °C. Amplification results were run on a 1% agarose gel.

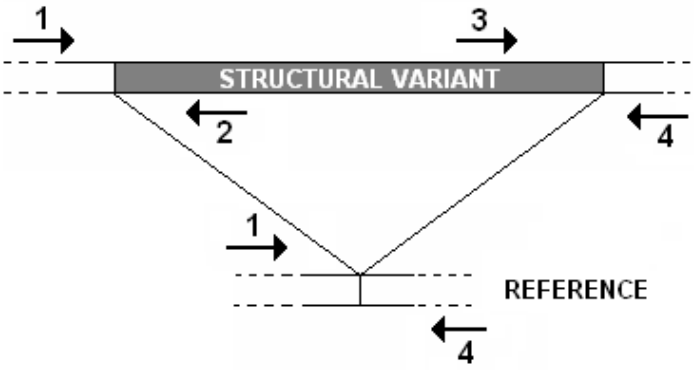

	Primer pairs		
Variant	**1-2**	**3-4**	**1-4**
DEL	-	-	+
INS	+	+	-

Figure 4. 5 Representation of the PCR assay performed to validate detected insertions and deletions with the expected amplification patterns for the two kinds of structural variation.

4.2 Results

4.2.1 Sequencing

We performed whole-genome next-generation sequencing of 18 poplar accessions: 4 *Populus nigra* accessions, 2 *Populus deltoides* accessions and 12 *P. nigra* x *P. deltoides* F1 hybrids, obtained by crossing two out the four re-sequenced *P. nigra* and the two re-sequenced *P. deltoides* with a partial factorial design. Short reads were trimmed on the basis of the FASTQ quality scores. After trimming, the mean read length ranged from 82.6 to 105.3 (Table 4. 1).

Table 4. 1 List of all the *P. nigra* (N), *P. deltoides* (D) and *P. nigra* x *P. deltoides* (N x D) resequenced accession with the corresponding library and coverage statistics obtained after the alignment to the *P. trichocarpa* reference genome.

Sample	Species	Mean read length	Mean insert size	Sequence coverage	Physical coverage	% reference covered
BDG	N	96.3	554.4	16.9	48.6	61.7
71077-308	N	82.8	441.9	17.4	46.4	74.0
L150-089	D	104.7	227.9	20.7	22.6	64.2
L155-079	D	92.5	439.3	19.1	45.3	70.5
POLI	N	96.7	390.2	69.7	140.7	76.6
BEN3	N	82.6	194.1	17.4	20.5	71.1
661200177	N x D	105.3	413.6	10.5	20.6	69.8
661200192	N x D	104.2	345.0	8.8	14.5	63.4
661200193	N x D	101.7	410.7	6.0	12.0	62.0
661200232	N x D	91.2	412.7	6.8	15.4	62.9
661200214	N x D	96.3	358.8	10.2	19.1	67.6
661200211	N x D	97.9	415.2	9.1	19.3	65.8
661200502	N x D	96.8	317.8	8.3	13.6	62.1
661200542	N x D	96.94	593.27	10.6	32.3	62.3
661200538	N x D	97.48	369.87	10.2	19.3	64.3
661200585	N x D	92.07	555.96	13.1	39.5	61.3
661200592	N x D	93.86	513.85	6.9	18.8	67.8
661200589	N x D	91.01	396.09	11.5	24.9	69.2

Populus trichocarpa v2 (Tuskan *et al.*, 2006) was used as a reference against which short reads were aligned. After removing reads aligned to the reference in multiple

positions, we obtained a mean individual coverage ranging from 6x to ~70x (Table 4. 1). The original study design aimed at sequencing *2 P. nigra* and 2 *P. deltoides* accessions at 20x and the F1 hybrids at 10x. The two additional *P. nigra* accessions (BEN3 and POLI) were sequenced in the framework of a collaborative effort, with a coverage of 17x and 70x respectively. The percentage of the *P. trichocarpa* reference sequence covered by at least one read was at least 60% in all the resequenced individuals. The mean insert size was ~400 bp or more in all individuals, generating a mean physical coverage of at least twice the sequence coverage. This was not true for L155-079 and BEN3 in which insert size was ~200 bp and physical coverage was only slightly greater than sequence coverage.

4.2.2 Simulations

To quantify the performance of structural variants detection as a function of parameters settings, we simulated in the *P. trichocarpa* reference sequence one thousand deletions and insertions ranging from 1 kb to 30 kb in size. We aligned reads obtained from sample L155-079 against the simulated reference sequence and we analyzed the performance in the identification of the simulated variants. To identify deletions we used BreakDancerMax (Chen *et al.*, 2009), an algorithm for high-resolution mapping of genomic structural variation from next generation paired-end sequencing reads. BreakDancerMax detects different kinds of structural variants, using read pairs that are mapped with unexpected separation distances or orientation. We considered a deletion as true positive if at least 50% of the detected variant overlapped with at least 50% of a simulated variant. BreakDancerMax associates with each prediction a confidence score that can be used to discriminate between true positives (TP) and false positives (FP). In this experiment FP can only be estimated using the total number of positives (P) as a proxy because the modified reference, in addition to the 1000 simulated deletions, includes deletions originally present in sample L155-079. To identify the optimal confidence score threshold for the detection of deletions, we analyzed the number of TP (blue line) and P (red line) as a function of the applied score threshold (Figure 4. 6). If all the identified deletions were true (simulated or not) the two curves would have the same trend. However, increasing the confidence score threshold the number of positives decreased faster than the number of true positives, suggesting the presence of a large proportion of false positives when using low confidence score thresholds. At higher

thresholds, the two curves decayed at a similar pace. This suggests that applying higher thresholds the majority of the detected deletions are true. In order to maximize true positives, while minimizing false positives we decided to select 60 as confidence score threshold. Applying this threshold we excluded ~10% of the true positives and ~30% of the total positives.

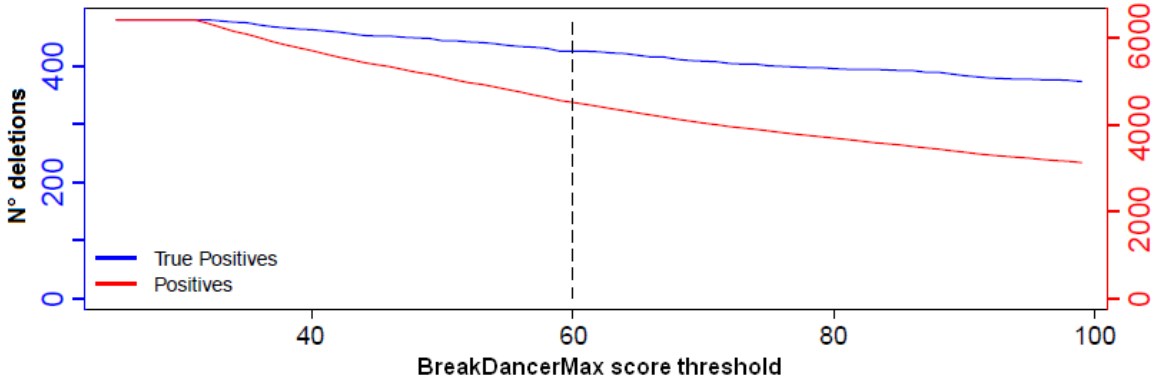

Figure 4. 6 Number of true positives (blue) and total positives (red) deletions as a function of the BreakDancerMax score threshold. A dashed line highlights the score threshold chosen for the analysis.

We performed a similar analysis to identify the optimal threshold for the number of anomalously mapped pair reads required to call a deletion. We plotted the number of TP (blue line) and the number of P (red line) as a function of the required number of supporting pair reads (Figure 4. 7).

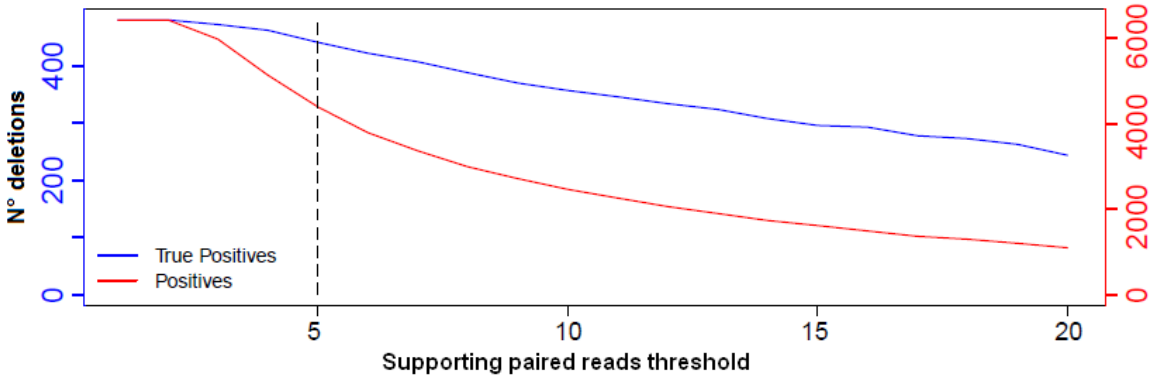

Figure 4. 7 Number of true positives (blue) and total positives (red) deletions as a function of the number of supporting paired reads required to call a variant. A dashed line highlights the number of supporting reads required for the analysis.

At very low thresholds, the number of positives decreased faster than the number of true positives, thus suggesting the presence of a high false discovery rate when applying very low thresholds. When requiring at least 5 supporting paired reads, the two curves showed a similar trend, suggesting a balance between the maximization of true positives and minimization of false positives. In fact, by requiring at least 5 supporting reads we excluded less than 10% of true positives and more than 30% of all positives.
Selecting all the deletions identified by BreakDancerMax with a confidence score ≥ 60 and supported by at least 5 read pairs, we were able to detect 408 out of the 1000 simulated variants. Simulated deletions not detected in this analysis are likely to occur in regions of the genome were it is difficult to map short reads, such as repetitive regions. We compared the mean coverage in the flanking regions of the simulated deletions between true positives and false negatives (Figure 4. 8). In TP the median coverage was 26.7x while in FN it was sensibly lower (13.9x), while the mean coverage for the individual was 19.1x. This analysis suggests that a large extent of the undetected variants did not contain enough anomalously mapped reads in their flanking regions to be detectable by BreakDancerMax. These estimates have to be considered upper bounds for the sensitivity because in addition to coverage, hetero- vs. homo-zygous state of the variant may significantly affect the ability to detect them (in the simulations all variants were by definition homozygous).

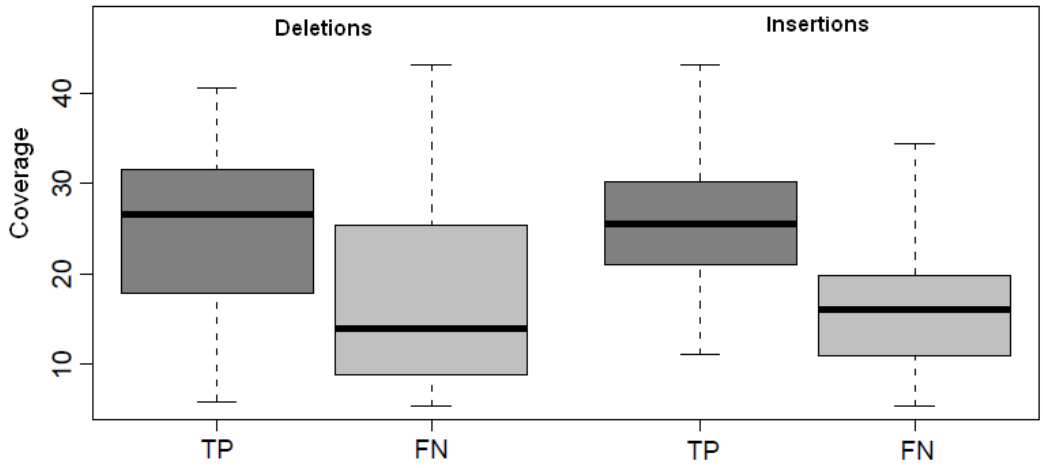

Figure 4. 8 Coverage distributions in the flanking regions of true positives (gray) and false positives (light gray) for simulated deletions (left boxes) and insertions (right boxes). The whiskers extend out to the datasets extreme values.

To analyze the accuracy of the detected deletion boundaries, we calculated the correlation between the predicted and the actual size of the simulated deletions (Figure 4. 9). The correlation was high (Pearson's correlation coefficient r = 0.99) and only in few cases the predicted length was larger than the simulated one.

To identify simulated insertions we employed a custom pipeline (see section 4.1.5). We considered an insertion a true positive if the distance between the predicted and the simulated point of insertion was less than 500 bp. We identified 435 out of the 1000 simulated insertions. The comparison in terms of mean coverage in the regions flanking the simulated insertion site between true positives and false negatives highlights also in this case a significant difference between the two subgroups (Figure 4. 8). In TP the median coverage was 26.6x, while in FN it was 17x.

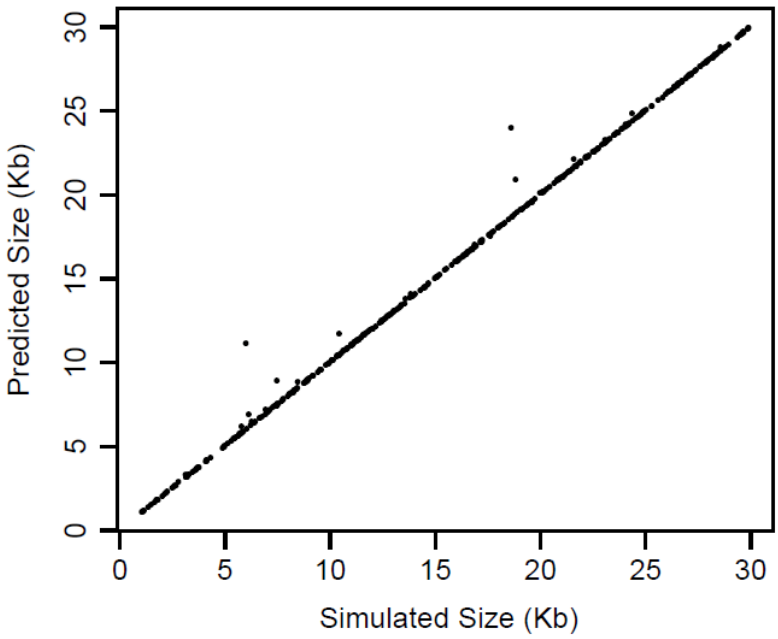

Figure 4. 9 Correlation between the original lengths of the simulated deletions and those predicted by BreakDancerMax.

The selection of BreakDancerMax thresholds was also supported by a similar analysis performed in *Vitis vinifera*. In this case, we simulated 1000 insertions and deletions by modifying the *V. vinifera* reference genome (Jaillon *et al.*, 2007) and by aligning to the modified reference short reads obtained from the same accession used to build the

reference. This analysis allowed the estimation of both true positives and false positives. To analyze BreakDancerMax performance in detecting deletions, we analyzed the percentage of TP (blue line), FP (green line) and P (red line) as a function of the applied score threshold and number of required supporting reads (Figure 4. 10). In both graphs, the percentage of false positives decreased faster than the percentage of true positives when increasing the thresholds. This analysis confirmed that requiring a score ≥ 60 and at least 5 supporting reads, we retained the majority of true positives (~76 and ~98% respectively) and discarded a great portion of the false positives (~53% and ~48% respectively). Using these thresholds we were able to identify deletions with a positive predictive value (PPV) of 77% and a false discovery rate (FDR) of 23%. On the other hand, using our pipeline for the detection of the simulated insertions, we obtained a PPV of 92% and a FDR of 8%.

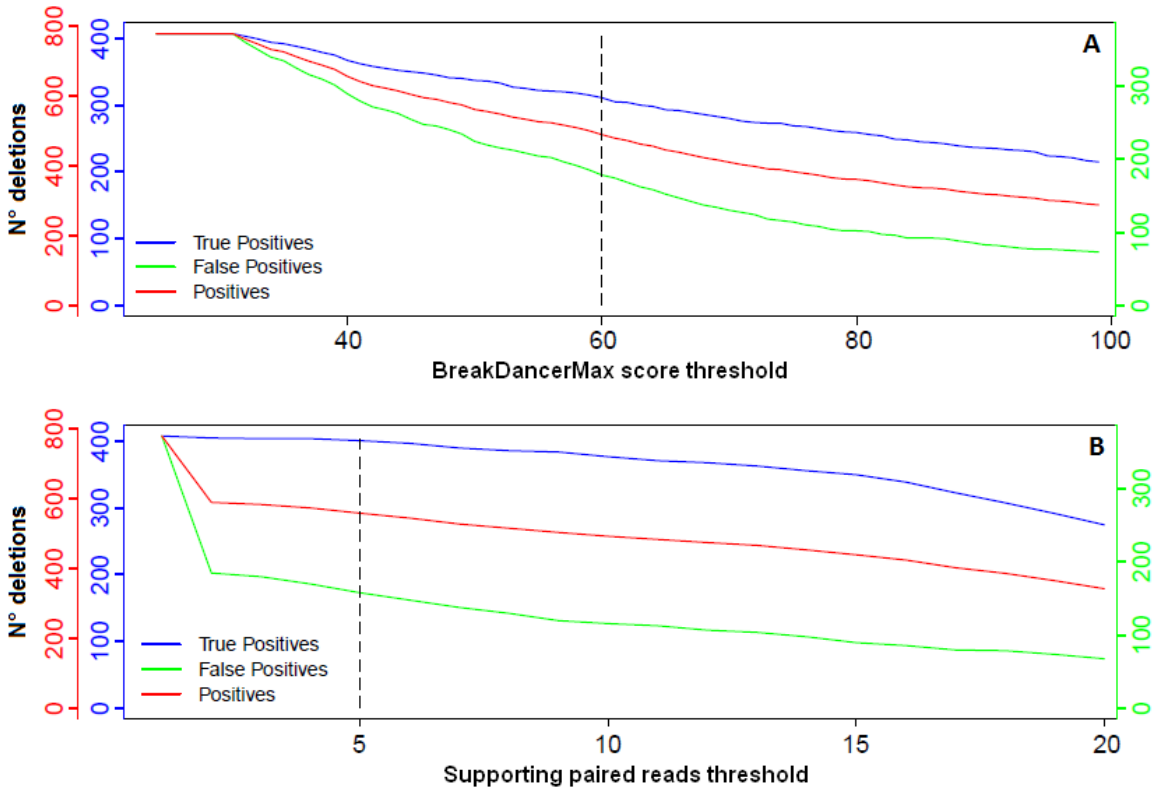

Figure 4. 10 Simulation results in *V. vinifera*. Number of true positives (blue), false positives (green) and total positives (red) deletions as a function of the BreakDancerMax score threshold (**A**) and of the number of required supporting reads (**B**). A dashed line highlights the thresholds chosen for the analysis.

4.2.3 Structural variants detection and classification

We detected deletions in *P. nigra* and *P. deltoides* individuals with respect to the *P. trichocarpa* reference sequence using the software BreakDancerMax, applying the thresholds *q*=60 and *r*=5, selected according to simulation results. We identified a total of 3380 deletions ranging from 240 bp to 47009 bp in size (Figure 4. 11).

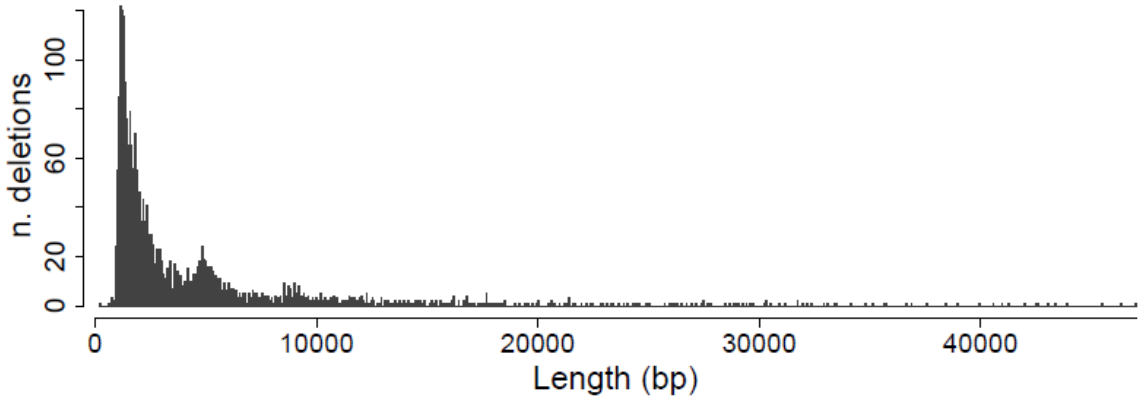

Figure 4. 11 Length distribution of the 3380 deletions identified with BreakDancerMax

The number of variants identified in each of the 6 samples is reported in Table 4. 2. In samples L150-089 and BEN3 the number of identified deletions was significantly lower than in the other samples. This was probably due to the very short size of sequenced inserts in these two samples and, as a consequence, to the lower physical coverage.

Table 4. 2 Summary of the identified deletions and insertions in the 6 resequenced *P. nigra* and *P. deltoides* individuals and the corresponding total number of Mb involved.

	BDG (*P. nigra*)	**71077-308** (*P. nigra*)	**L150-089** (*P. deltoides*)	**L155-079** (*P. deltoides*)	**POLI** (*P. nigra*)	**BEN3** (*P. nigra*)	**Total**	**Mb**
DEL	1489	1997	420	1612	2039	390	3380	14.7
INS	687	1788	280	1533	3059	197	5877	23.3

0.01% of the identified deletions corresponded to stretches of "N" bases in the *P. trichocarpa* reference sequence, inserted in the reference assembly to connect two subsequent contigs. 77% of the deletions identified in at least one of the four parents of

the pedigree were identified also in at least one of the F1 hybrids. A blastn analysis of the deleted sequences against a database of plant repetitive elements showed that 76% of the identified deletions were homologous with a repetitive element present in the database. Of these, the majority showed homology with class I LTR retrotransposons; a more detailed classification is reported in Table 4. 3.

Table 4. 3 Classification of the variants on the basis of their homology with Class I (Retrotransposons) or Class II (DNA transposons). **DEL**: deletions; **INS**: insertions; **LTR**: long terminal repeats; **SINE**: small interspersed nuclear elements; **LINE**: long interspersed nuclear elements; **TIR**: terminal inverted repeats.

	Class I			**Class II**			**Unknown**
DEL	77.12%			13.89%			8.99%
INS	88.53%			8.22%			3.25%
	LTR	**SINE**	**LINE**	**TIR**	**Helitron**	**Unknown**	
DEL	74.79%	1.63%	0.70%	8.02%	3.04%	2.84%	
INS	84.69%	2.62%	1.23%	3.08%	1.00%	4.13%	

For the detection of insertions resulting from the transposable elements activity, we developed a custom pipeline. We identified a total of 5877 insertions in *P. nigra* and/or *P. deltoides* individuals with respect to the *P. trichocarpa* reference sequence (Table 4. 2). The number of identified insertions is consistent with the number of identified deletions for each individual. In sample POLI, sequenced at a higher coverage, we identified a significantly higher number of insertions. 37% of the insertions identified in at least one of the four parents of the pedigree were identified also in at least one of the F1 hybrids. As observed for deletions, the majority of insertions resulted from the activity of class I LTR retroelements (Table 4. 3). According to our estimated phylogenetic tree, *P. deltoides* and P. *trichocarpa* resulted more closely related with each other than to *P. nigra*, but the overall distance between the three species was quite similar (Figure 4. 12).

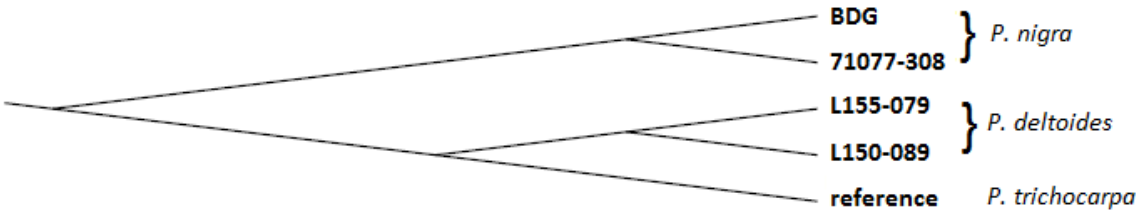

Figure 4. 12 Topology of the phylogenetic relationship between *P. nigra*, *P. deltoides* and *P. trichocarpa*.

To study the agreement of our results with the predicted phylogenesis, we stratified the identified variants by species (Table 4. 4). When analyzing the whole dataset, a great part of the variants (51% of deletions and 71% of insertions) resulted to be *P. nigra* specific. For deletions, the remaining variants were equally distributed between *P. deltoides* specific and *P. nigra*/*P. deltoides* shared variants. For insertions, the number of variants shared by the two species was considerably lower (2%). To eliminate any bias introduced by having different *P. nigra* and *P. deltoides* sample sizes, we performed the same classification by comparing only one *P. nigra* accession (71077-308) with one *P. deltoides* (L155-079), comparable in terms of coverage and insert size. In this case, the difference between *P. nigra* and *P. deltoides* specific variants was lower, but the percentage of shared deletions was still considerably higher than the percentage of shared insertions.

Table 4. 4 Percentage of variants identified only in *P. nigra* accessions (**N**), only in *P. deltoides* accessions (**D**) or in both species, compared to the *P. trichocarpa* reference genome (**T**). The classification is reported when comparing all the resequenced individuals and when comparing only 2 accessions (71077-308 and L155-079). +: sequence presence (insertion); -: sequence absence (deletion).

	all	**71077-308 / L155-079**	**T**	**N**	**D**
DEL	26%	31%	+	-	-
	51%	44%	+	-	+
	23%	25%	+	+	-
INS	2%	3%	-	+	+
	71%	52%	-	+	-
	27%	45%	-	-	+

To study the intraspecific distribution of the identified variants, we focused on *P. nigra* variants, for which we had resequenced 4 different genotypes. We selected all the deletions satisfying the BreakDancerMax imposed thresholds in at least one *P. nigra* individual and all the insertions identified in at least one *P. nigra* individual and, for each variant, we counted the number of *P. nigra* individuals in which that variant was detected (Figure 4. 13). 76% of the deletions and 27% of the insertions were identified in at least two samples.

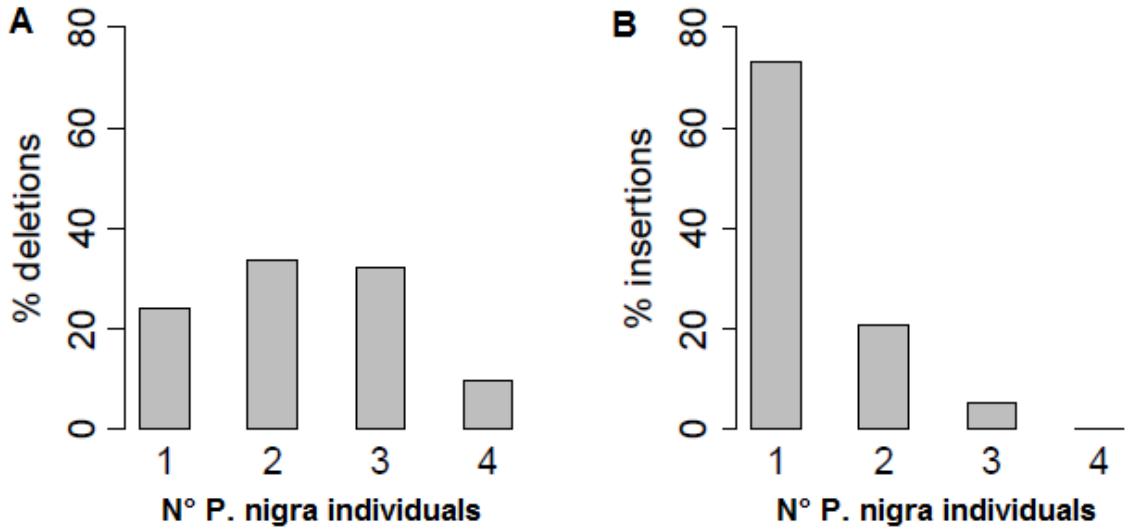

Figure 4. 13. Number of *P. nigra* individuals in which deletions (**A**) and insertions (**B**) were identified.

4.2.4 Gene content analysis

The deleted sequences contained 1350 predicted genes according to the *P. trichocarpa* v2.2 gene annotation. A blastx analysis of the gene sequences against the *Viridiplantae* nr database showed a strong prevalence of genes encoding for retrotransposons proteins, like the Gag-Pol polyprotein. A Gene Ontology (GO) classification of blastx results on the basis of their molecular function was performed using Blast2GO. 521 (~39%) sequences were associated to a GO term. The functional annotation showed a prevalence of genes with GO molecular function (transferase activity, nucleotide binding and hydrolase activity) that can be related to TE proteins, like the Gag-Pol

polyprotein (Figure 4. 14). Among these genes, we looked for enrichment in GO terms involved in biological processes, cellular components, and molecular function. None of the GO terms resulted over- or under-represented in the deleted genes, compared to the remaining *P. trichocarpa* genes.

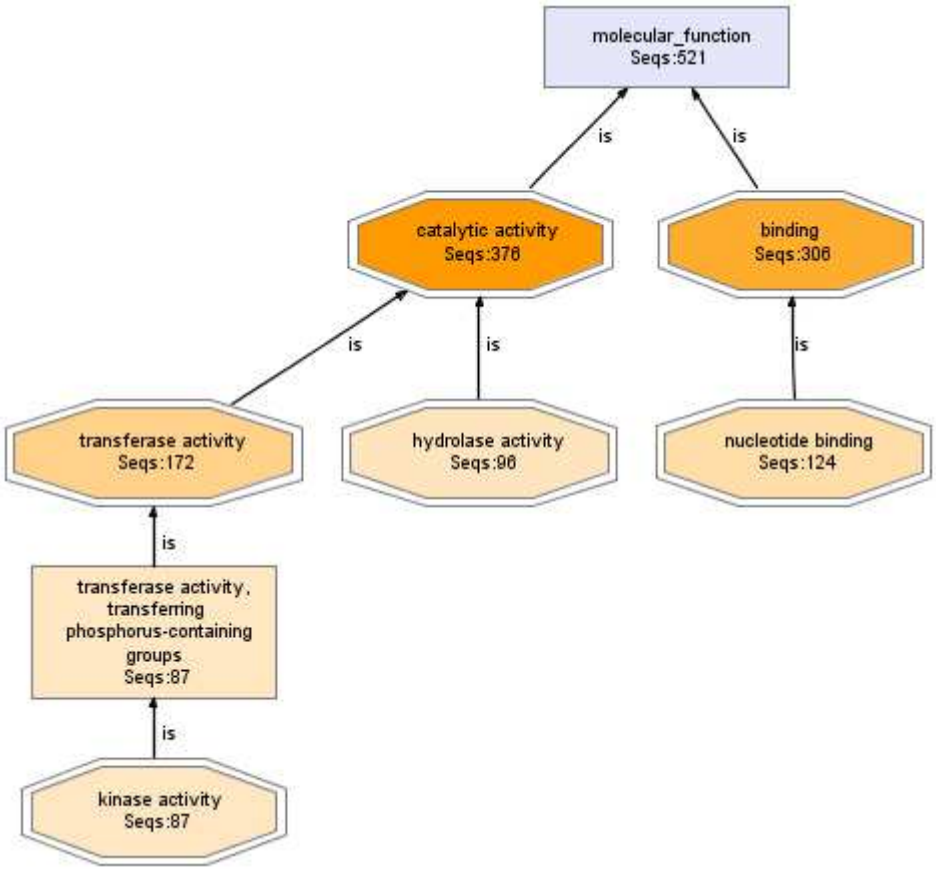

Figure 4. 14 Molecular function annotation graph. The combined annotation of the genes identified in the deleted sequences is visualized together. Only functional terms covered by at least the 10% of the dataset are displayed.

According to the *P. trichocarpa* v2.2 gene annotation, we found 1315 genes interrupted by one of the identified insertions. The sequences of these genes were used as query for a blastx analysis against the *Viridiplantae* nr database and blastx results were used for the functional classification with blast2GO. 571 (~43%) sequences were associated to a GO term. The resulting functional annotation was similar to the one obtained for deletions, showing also in this case a prevalence of genes with GO molecular function that can be related to TE proteins (Figure 4. 15). We detected over-representation of

genes related to catalytic activity (GO: 0003824, Fisher's exact test P = 1.42E-5).

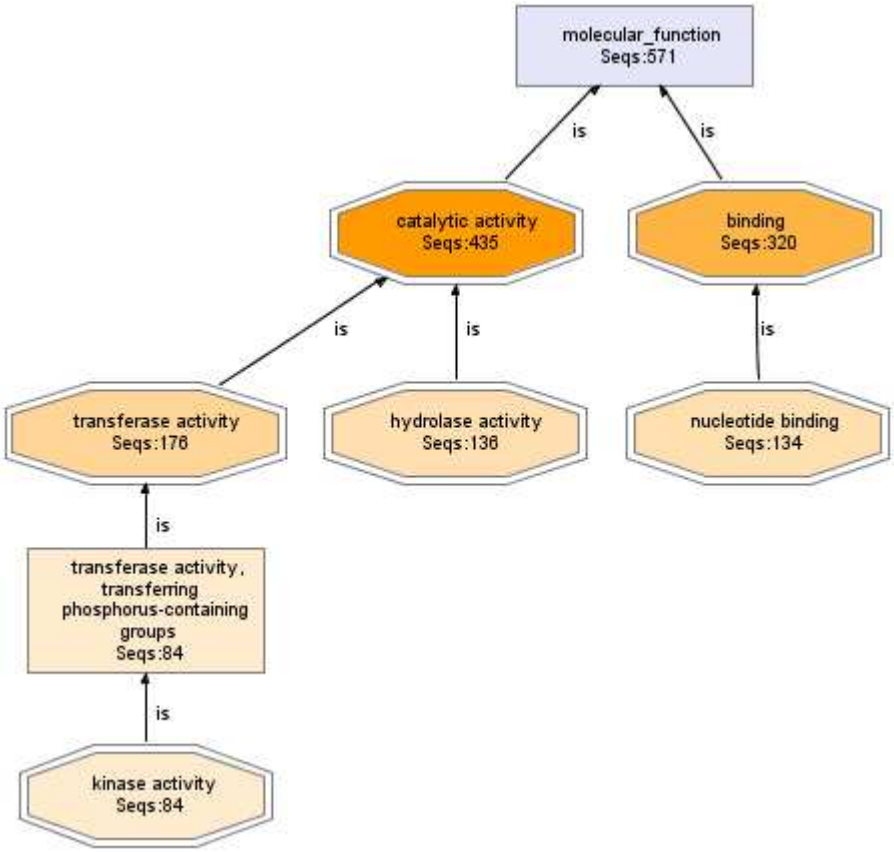

Figure 4. 15 Molecular function annotation graph of the genes interrupted by insertions.

Among all blastx results, we focused on variations related to genes involved in the lignin biosynthesis pathway. We identified 3 insertions occurred across genes involved in the lignin biosynthesis pathway (Table 4. 5).

Table 4. 5 List of the 3 insertions affecting genes of the lignin biosynthesis pathway. For each gene, the description, the locus name and any aliases.

Insertion coordinates	*P. trichocarpa* v2.0 annotation	v1.1 annotation
Chr 1: 11740891-11740892	cinnamoyl-CoA reductase (POPTR_0001s14910)	n.a.
Chr 2: 746313-746164	4-coumarate-CoA ligase (POPTR_0002s01420)	eugene3.00020113
Chr 9: 6083466-6083762	similar to putative cinnamoyl-CoA reductase (POPTR_0009s06280)	eugene3.00091073

To obtain a genome-wide view of the distribution of deletions and insertions in the poplar genome, we plotted the number of identified variants every 250 kb for each of the 19 chromosomes (Figure 4. 16). Deletions and insertions were evenly distributed across the whole genome. Peaks of variation were located in repetitive regions of the genome in which the gene density is low.

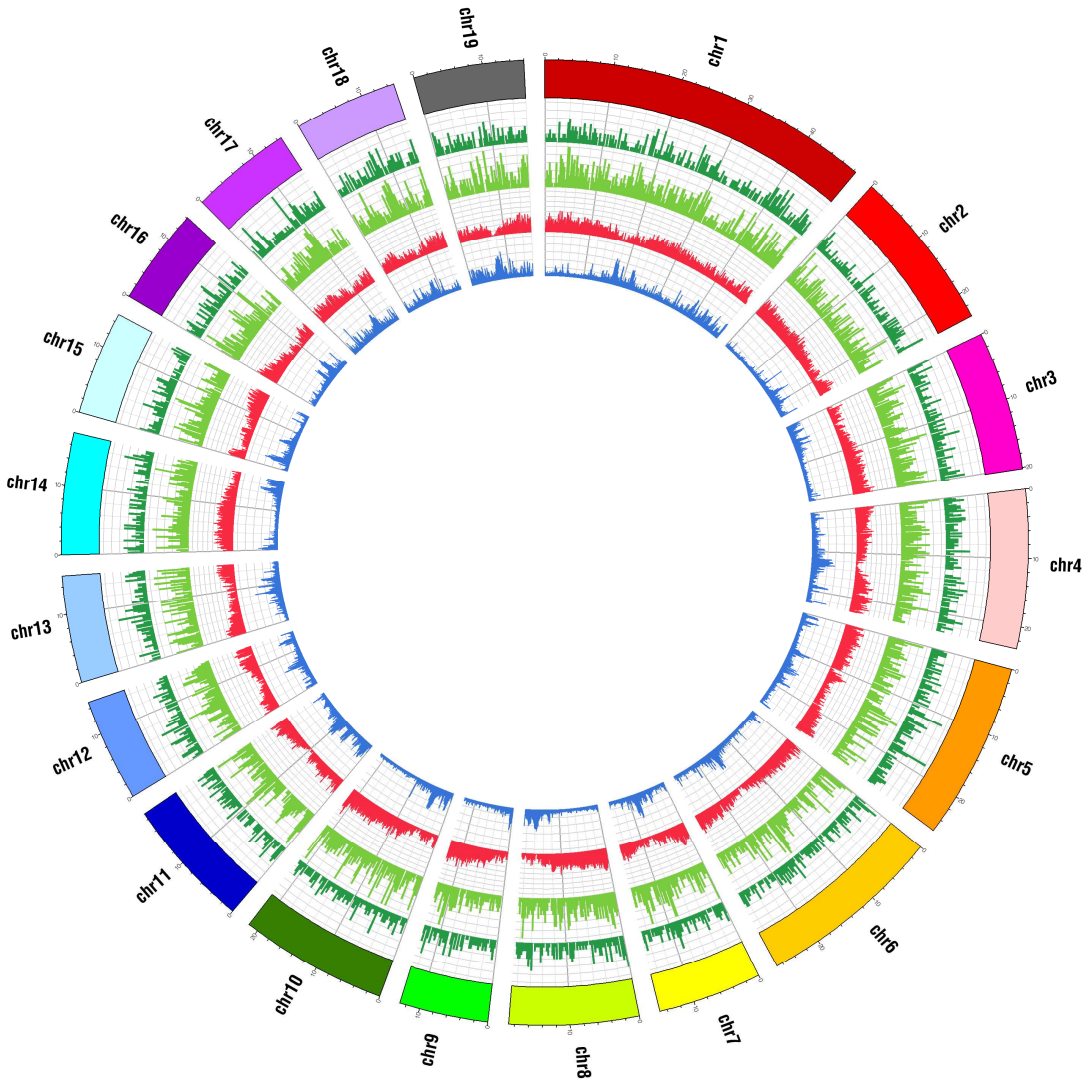

Figure 4. 16. SV distribution across the 19 poplar chromosomes. **Dark green bars**: deletions. **Light green bars**: insertions. **Red bars**: gene density distribution calculated as the number of genes every 100 kb. **Blue bars**: repetitiveness of the genome calculated with a k-mer analysis using the tool Tallymer (Kurtz *et al.*, 2008).

4.2.5 Experimental validation

To experimentally validate a randomly selected set of deletions and insertions, we performed a PCR assay in order to obtain differential amplifications in the presence or absence of the structural variant. We tested 72 variants (36 deletions and 36 insertions), with the aim to obtain a clear pattern of amplification for at least 10 deletions and 10 insertions in one selected *P. nigra* accession and 10 deletions and 10 insertions identified in a selected *P. deltoides* accession. The 40 selected variants are reported in Table 4.6 and Table 4. 7 and the corresponding amplification results are reported in Figure 4. 17 and Figure 4. 18. We validated 20 out of 20 deletions and 18 out of 20 insertions, with a sensitivity of 100% and 90% respectively. For the remaining 18 deletions and insertions the interpretation of results was more difficult since we didn't obtain an informative amplification pattern. Of the validated deletions, only one (d06) resulted to be heterozygous, while heterozygous and homozygous insertions were evenly distributed.

Table 4. 6 List of the 20 deletions experimentally validated. For each deletion the pattern of amplification of primer pairs 1-2, 3-4 and 1-4 is reported.

Code	Position	Sample	1-2	3-4	1-4
d01	scaffold_10: 8397408-8402308	BDG	-	-	+
d02	scaffold_14: 11019337-11037238	BDG	-	-	+
d03	scaffold_18: 7680748-7692364	BDG	-	-	+
d04	scaffold_15: 1319103-1320399	BDG	-	-	+
d05	scaffold_16: 8781111-8801836	BDG	-	-	+
d06	scaffold_5: 6753207-6757329	BDG	+	+	+
d07	scaffold_6: 18462886-18464273	BDG	-	-	+
d08	scaffold_6: 25864965-25866186	BDG	-	-	+
d09	scaffold_7:7490958-7497631	BDG	-	-	+
d10	scaffold_3:194124-210301	BDG	-	-	+
d11	scaffold_1:12546068-12547330	L155-079	-	-	+
d12	scaffold_1:18128918-18151283	L155-079	-	-	+
d13	scaffold_1:42647880-42651248	L155-079	-	-	+
d14	scaffold_10:9945390-9946547	L155-079	-	-	+
d15	scaffold_15:8818337-8820973	L155-079	-	-	+
d16	scaffold_19:15738619-15740339	L155-079	-	-	+
d17	scaffold_2:20543660-20544840	L155-079	-	-	+
d18	scaffold_2:22774250-22783226	L155-079	-	-	+
d19	scaffold_3:12293382-12295220	L155-079	-	-	+
d20	scaffold_4:2714918-2716137	L155-079	-	-	+

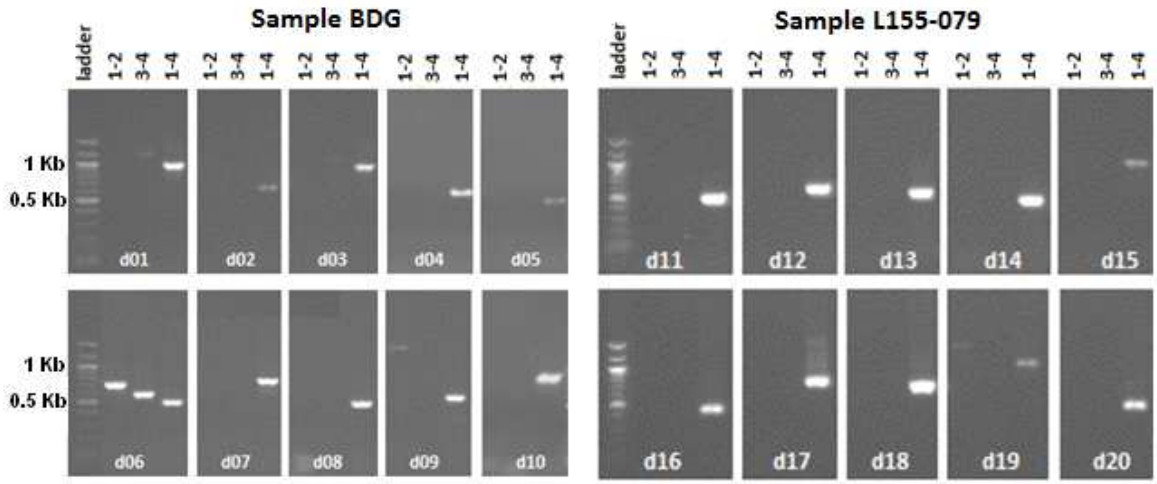

Figure 4. 17 Patterns of PCR amplifications obtained for the tested deletions. Primer pairs 1-2 and 3-4 amplify when the sequence is not deleted, while an amplification of the pair 1-4 confirms the deletion.

Table 4. 7 List of the 20 insertions experimentally validated with the corresponding patterns of amplification.

Code	Position	Sample	1-2	3-4	1-4
i01	scaffold_1: 11626170-11626310	BDG	+	+	-
i02	scaffold_1: 38987758-38988092	BDG	+	+	+
i03	scaffold_10: 42612-42858	BDG	+	+	-
i04	scaffold_10: 1930787-1930958	BDG	+	+	+
i05	scaffold_10: 4173204-4173232	BDG	+	+	-
i06	scaffold_10: 7963636-7963740	BDG	+	+	-
i07	scaffold_11: 11005150-11005241	BDG	+	+	+
i08	scaffold_15: 461383-461438	BDG	+	+	-
i09	scaffold_19: 14470729-14470994	BDG	-	-	+
i10	scaffold_2: 4315180-4315284	BDG	-	-	+
i11	scaffold_11: 4752432-4752562	L155-079	+	+	+
i12	scaffold_12: 12802485-12802527	L155-079	+	+	+
i13	scaffold_13: 345826-345781	L155-079	+	+	-
i14	scaffold_18: 2810221-2810495	L155-079	+	+	+
i15	scaffold_19: 10489904-10490254	L155-079	+	+	-
i16	scaffold_2: 14700347-14700475	L155-079	+	+	+
i17	scaffold_4: 16589093-16589379	L155-079	+	+	-
i18	scaffold_6: 13623627-13623688	L155-079	+	+	-
i19	scaffold_6: 26870616-26870688	L155-079	+	+	-
i20	scaffold_7: 3007814-3007727	L155-079	+	+	+

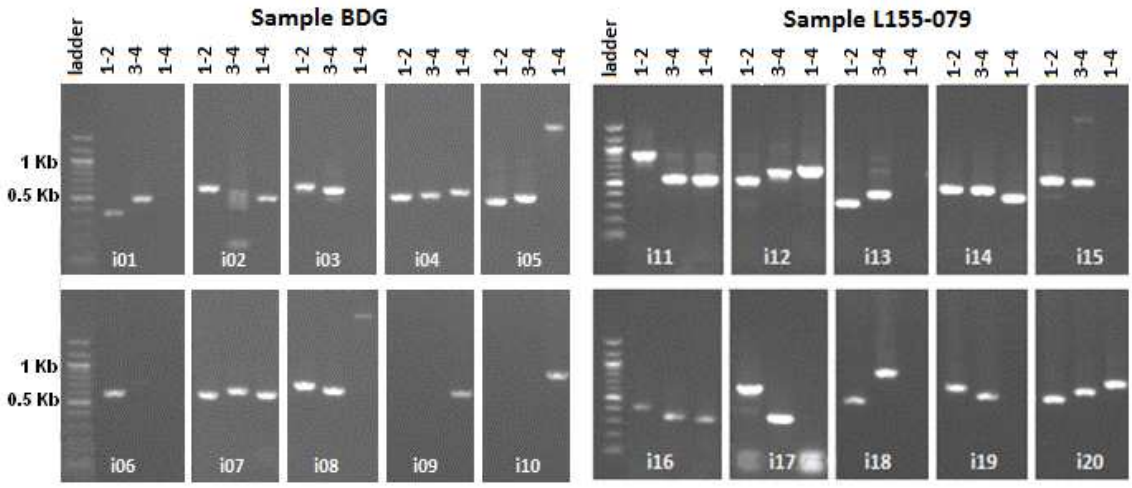

Figure 4. 18 Patterns of PCR amplifications obtained for the tested insertions. Amplification of primer pairs 1-2 and 3-4 confirms the insertions while the pair 1-4 amplifies when there is no insertion.

4.3 Discussion

In the present study we performed a genome-wide analysis of structural variation (SV) between *Populus nigra* and *Populus deltoides*. Although the global impact of structural variation is unknown, it might have dramatic consequences on phenotypic diversity (Weigel and Mott, 2009). In humans, it has been recently demonstrated that SVs are quite common and may have considerable effects on human phenotypic variation by altering gene dosage, disrupting coding sequences, or perturbing regulation (Hurles *et al.*, 2008). A recent work in maize (Springer *et al.*, 2009) reported the presence of several thousands of DNA segments, including genic sequences, that are present in one inbred line but absent from another. Little is known about the prevalence of structural variation in poplar and its relationship with the origin of intra-specific diversity. We focused on the detection of deletions and insertions of 1-50 Kb by means of Illumina paired-end sequencing of 4 *P. nigra* accessions, 2 *P. deltoides* accessions and 12 *P. nigra* x *P. deltoides* F1 hybrids. Most of these variants are probably due to the recent movement of transposable elements (TEs), that are very active in many plants.

The analysis was performed using as reference the genome of a different *Populus* species (*P. trichocarpa*). On average we were able to cover ~70% of the *P. trichocarpa* reference genome with reads obtained from both *P. nigra* and *P. deltoides* accessions.

Thus, the alignment to the *P. trichocarpa* reference genome constitutes a powerful resource for detecting a large portion of structural changes in these two species.

For the detection of structural variants we exploited the paired-end mapping information generated from next-generation sequencing data. Using this signature, deletions can be easily detected and there are different available tools that can be employed for this aim (Medvedev *et al.*, 2009). On the other hand, the detection of novel insertions is more complicated and available tools can only detect very short insertions that are enclosed by two sequenced reads of the same insert. For this reason we performed the detection of structural variants employing two different approaches for the two different types of variation: we used the software BreakDancerMax (Chen *et al.*, 2009) for the detection of deletions and we developed a custom pipeline, specifically aimed at the detection of insertions resulting from the movement of transposable elements. To quantify the performance in the detection of these variants with the two approaches, we simulated one thousand deletions and insertions and we measured our ability to identify them. We detected 40.8% of the simulated deletions and 43.5% of the simulated insertions. The two approaches gave very similar results in terms of true positive rate, suggesting the presence of a common factor that affects the performance of both methods. One possible factor is the presence in the SVs flanking regions of sequences that are difficult to map, such as repetitive sequences. This problem was already reported by BreakDancer developers. They found that, at 100 fold physical coverage, out of the 844 structural variants identified on chromosome 17 of J. Craig Venter's genome (Levy *et al.*, 2007), only about 365 (43.2%) contained two or more anomalously mapped reads in their flanking regions and were detectable by BreakDancerMax. Thus, working on different species does not have significant effects on the performance of the tool. Moreover, Chen and colleagues showed that BreakDancer's performance is strongly dependent on the physical coverage of the dataset. This evidence was confirmed by our results in which, for both simulated deletions and insertions, the median coverage in the flanking regions of true positives was higher than the median coverage of false positives. In addition, simulation results confirmed the high accuracy of BreakDancerMax in the prediction of deletion sizes. In our simulation, false positive rate (FPR) could not be estimated because, in addition to the 1000 simulated deletions, the modified reference also contained true deletions. For this reason, we performed a PCR-based validation of a random set of identified variants. The experimental validation is the gold standard method to verify the

reliability of our results. Even if we tested only a limited number of variants, results were valuable to predict the false discovery rate. In fact, we obtained a FDR of 5% for the two methods combined. In addition, simulation results obtained in *V. vinifera* confirmed that the imposed thresholds for the detection of deletions ensured the exclusion of a substantial proportion of false positives. In *V. vinifera* we estimated PPV and FDR of the two approaches for the detection of structural variants. Deletions were detected with PPV=77% and FDR=23% and insertions with a PPV=92% and FDR=8%. These results suggest that BreakDancerMax performance in detecting deletions is still amenable to improvements.

The most significant source of false positives from BreakDancer arises from alignment artifacts in short-read data (Koboldt *et al.*, 2010). Thus, a large fraction of false positives is probably located in regions that are difficult to map, such as repetitive regions. The false discovery rate may also be affected by the insert size of the sequenced library. In this study, we used relatively small insert sizes (200-500 bp); using larger insert sizes has the advantage of greater genomic coverage per sequenced fragment but increases the difficulty of breakpoint annotation. It is likely that complete characterization of all variants will require paired-end sequencing of several libraries of different insert sizes, allowing reads to fall outside any repetitive sequence present near the breakpoints.

Overall, we identified 3380 deletions and 5887 insertions in the studied accessions with respect to the *P. trichocarpa* reference genome, corresponding to 14.7 Mb and 23.3 Mb respectively. The number of identified variants per sample was quite variable. This was mostly due to the variability of the sequenced libraries insert size. In fact, in the two samples (L150-089 and BEN3) having a mean insert size considerably lower than the other ones, also the number of identified variants was considerably lower. On the other hand, in sample POLI, having a mean coverage almost 4 times the coverage of the other samples, we identified a greater number of both deletions and insertions. These considerations highlight the importance of insert size and physical coverage in the detection of structural variants using the paired-end mapping signature.

In plants, transposable elements are a major source of genetic variation (Kidwell and Lisch, 1997). As expected, the majority of the identified variants were related with the activity of transposable elements, with a clear predominance of class I LTR retrotransposons. These elements vary in size from several hundred bases to over 10 kb (J L Bennetzen, 2000). Plotting the size distribution of the identified deletions, we

observed two signature peaks at ~5Kb and at 1 Kb that could be respectively related to entire retrotransposons and to retroelements undergone to subsequent rearrangements. LTR retrotransposons transpose with the so called copy-and-paste mechanisms, thus leaving a copy of themselves in the original site. For this reason, we expected that the majority of the identified SVs, both insertions and deletions, originated from the insertion of a new TE copy in a different position. Only ~10% of the variants showed homology with class II DNA transposons. These elements transpose with the cut-and-paste mechanisms, thus creating both a deletion (in the original site) and an insertion (in the new site). Therefore, only a small proportion of the variants are expected to originate from the excision of a TE from its original site.

When stratifying the identified deletions and insertions by species, we observed that a great part of the variants was *P. nigra* specific. This result was probably due to the different size of the two compared sets. In addition, a great part of the *P. nigra* variants was composed by events detected in only one sample (POLI), for which we had a 4-fold coverage with respect to all the other accessions. In fact, when comparing variants identified in only one individual per species, the number of *P. nigra* and *P. deltoides* variants was more comparable. Focusing on deletions, 31% of the identified variants were shared between the two species. These events are likely insertions of LTR retrotransposons occurred in *P. trichocarpa* rather than deletions occurred in both *P. nigra* and *P. deltoides* individuals. 44% of the deletions were identified only in the *P. nigra* individual. These variants may be due to a) *P. trichocarpa* exclusive insertions (false negative deletions in *P. deltoides*), b) real *P. nigra* deletions generated by the excision of a DNA transposon, or c) insertions occurred in the *P. trichocarpa*/*P. deltoides* ancestor. Deletions due to DNA trasposons (case b) are expected to be a small proportion. Simulations showed that the algorithm for the detection of deletions resulted in a high number of false negatives. So, a substantial proportion of the deletions that we classify as *P. nigra* specific might be present also in *P. deltoides* but were not detected (case a). 25% of the deletions were detected only in the *P. deltoides* sample. In this case, variants can be explained as a) *P. trichocarpa* exclusive insertions (implying a missed detection in *P. nigra*) or b) real *P. deltoides* deletions. The difference between the proportion of species-specific deletions observed in *P. nigra* (44%) and in *P. deltoides* (25%) might be due to insertions that occurred in the *P. trichocarpa*/*P. deltoides* ancestor (case c).

Only ~3% of the insertions were shared between *P. nigra* and *P. deltoides*. These variants are likely deletions occurred in *P. trichocarpa*, resulting from the activity of class II transposable elements. Therefore, the percentage of shared deletions between the two species was considerably higher than the percentage of shared insertions and this is consistent with the observation that most of the SVs are originated by retrotransposon activity. 52% and 45% of insertions were identified only in the *P. nigra* or in the *P. deltoides* individual, respectively. The higher rate of *P. nigra* specific insertions is in agreement with the estimated phylogeny.

Focusing on the intraspecific distribution of the identified variants, we found a higher proportion of deletions (76%) detected in at least two *P. nigra* individuals with respect to insertions (27%). Therefore, many insertions are intraspecific polymorphisms, while most of deletions are interspecific polymorphisms. This was confirmed by PCR validation experiments in which we obtained that the majority of the deletions are homozygous, while heterozygous and homozygous insertions were evenly distributed. All these evidences are consistent with the hypothesis that a large part of the variants detected as deletions in *P. nigra* and/or *P. deltoides* are actually retrotransposons insertions in *P. trichocarpa*.

The gene content analysis of the deleted sequenced confirmed that a great part of the deletions resulted from the activity of transposable elements and suggested that insertions have preferentially occurred in regions rich in transposable elements. According to Fisher test, we didn't notice any particular enrichment in GO terms for the selected genes. This suggests that genes encoding for TE proteins are largely distributed across the whole genome.

Focusing only on variants detected in the four parentals of the pedigree, we observed that 77% of the deletions and 37% of the insertions identified in at least one of the four parents, were identified also in at least one of the F1 hybrids. One reason explaining the missed variations in hybrids may be the lower physical coverage obtained with respect to the parental accessions. In addition, a substantial proportion of these variants is expected to be heterozygous in hybrids, and for this reason the paired-end mapping signature is expected to be found only in half of the sequenced reads. The difference between the proportion of deletions and insertions identified in hybrids may have two main causes: 1) Compared to 20-30% of deletions, only 2-3% of insertions are shared between the two species, and inherited (most likely in homozygous state) by F1 hybrids. 2) The majority of the parental deletions are homozygous, while heterozygous

and homozygous insertions were evenly distributed. As a consequence a greater proportion of deletions are inherited by F1 compared to insertions.

Focusing on genes involved in the lignin biosynthesis pathway, we identified 3 insertions that are occurred in one of these genes, with a possible effect on their transcription. In particular, two of them encoded for a cinnamoyl-CoA reductase and one encoded for a 4-coumarate-CoA ligase. However, there is no experimentally proof of active involvement of these genes in the biosynthesis of lignin. In a recent study aimed at quantifying the expression and the regulation of all the genes involved in the monolignol biosynthesis (Shi *et al.*, 2010), two of them (POPTR_0001s14910 and POPTR_0009s06280) were not even considered, while for the other (POPTR_0002s01420) no proof of transcription in differentiating xylem was reported.

In summary, we performed a genome-wide comparative analysis of two closely related *Populus* species and we provided a detailed catalogue of structural variants across the whole genome. We confirmed that structural variants contribute to a substantial amount of the overall genetic variation in poplar. The detected deletions and insertions cover the 10% of the whole poplar reference genome. We found that a great proportion of this variability was driven by the activity of class I LTR retroelements. Our results are in agreement with a previous analysis of sequence variation among the three species in Sanger sequences of three BAC clones (G. Zaina and M. Morgante, unpublished). Both analyses showed limited levels of variation in transcribed regions, while intergenic regions harbor much more variation. In addition, in both cases most of the structural variation was explained by TEs not shared by the species. Future functional studies of the detected variants could be of help in understanding the mechanisms of speciation in poplar as well as the role of artificial and natural selection in these genomes. Understanding the role of inter- and intraspecific structural variants in poplar may have important implications for yield improvement and plant breeding.

5

Copy Number Variation in Poplar

5.1 Materials and Methods

The experimental samples are the same used in Chapter 3 (section 4.1.1). DNA extraction, library preparation, and next-generation sequencing procedures are described in section 4.1.2 while short read alignment is described in section 4.1.3.

5.1.1 Depth of coverage analysis

Depth of coverage analysis was performed using only paired reads that mapped uniquely in the genome with correct orientation and spacing of the two ends. For each sample, duplicated sequences were removed with the samtools *rmdup* utility (Li *et al.*, 2009) to eliminate local peaks of coverage that could alter the analysis. Ideally, the depth of coverage analysis would involve a comparison in terms of coverage across the whole genome between a resequenced and a reference individual in order to identify regions that are more or less represented in the resequenced individual compared to the reference. Such a design provides the greatest power to describe deletions and duplications in any individual in comparison to the reference individual that was used to construct the reference sequence. Different resequenced individuals can then be a posteriori compared to one another once their structure in relation to the reference has been established. In the present work, the lack of a *P. trichocarpa* resequenced individual obliged us to perform the comparison between all the possible pairs of the *P. nigra* and *P. deltoides* resequenced individuals. To identify regions of copy number variation between the resequenced individuals it was necessary to compare the coverage present in these individuals across the whole genome. The comparison was performed

after dividing the whole genome into non-overlapping windows of unequal length, containing a constant number of mapped reads in one of the two resequenced individuals. The partition into windows is affected by the sample used to count the number of mapped reads. Preliminary analysis showed that regions deleted (or showing low coverage) in one individual are better detected if the partition is performed counting the number of mapped reads of the other individual. For this reason, for each pair of samples (e.g. sample *a* and sample *b*), the coverage comparison was performed twice, once defining windows using mapped reads of sample *a* and once using those of sample *b*. With the aim of identifying regions of variation at least 50 Kb long, windows with a mean size of ~5 Kb were obtained by requiring a specific number of mapped reads for each accession that varied depending on the read coverage obtained in each individual. For each window, the ratio in log2-scale between the number of mapped reads in sample *a* and the number of mapped reads in sample *b* was calculated. Log2 ratios were normalized on the basis of the total number of paired reads mapped in each sequenced sample. Log2 ratios formed the raw input to the binary circular segmentation algorithm implemented in R as the DNAcopy library of the Bioconductor project. This algorithm identifies change-points in copy number between the two samples under consideration by an iterative binary segmentation (Olshen *et al.*, 2004). Regions of the genome larger than 50 kb having a log2ratio between sample *a* and sample *b* higher than a threshold *t* were selected as candidate CNVs.

To determine the optimal log2ratio threshold *t*, uniquely mapped paired reads from sample BEN were randomly divided in two equal-size subsets. Both subsets were used to divide the genome into windows having a mean size of 5 kb, by requiring 350 mapped reads per window. For each window of both partitions, coverage log2 ratios between the two subsamples were calculated. To minimize the false discovery rate, the log2 ratio threshold *t* was selected so that *t* was substantially higher than the log2 ratio obtained between the two subsamples in ~99% of the windows.

The threshold *t* was used to select from DNAcopy segmentation results all the regions larger than 50 Kb having a log2ratio >*t* between the two individuals under evaluation. For each comparison *a/b* and *b/a*, where the subject at the numerator was used to define windows, only positive values were used and the combination of positive results from the two reciprocal comparisons provided the whole set of CNVs among that pair of genotypes.

5.1.2 Gene content analysis

The *P. trichocarpa* v2.2 gene annotation (Tuskan *et al.*, 2006) was used to analyze the gene content of the identified CNVs and to select disease resistance genes. For a more detailed annotation, the sequences of the genes included in these regions were used as a query for a blastx analysis against the *Viridiplantae* nr database. Blastx results were imported into the Blast2GO tool for the functional annotation. Over- or under-representation of GO terms of the selected regions, as compared with the rest of the genome, were searched using a Fisher's Exact Test implemented in the Gossip (Blüthgen *et al.*, 2005) package integrated in Blast2GO. To reduce the number of false positives, a false discovery rate correction for multiple testing (Benjamini and Hochberg, 2007) was applied and only differences with a corrected p-value <0.05 were selected.

5.2 Results

5.2.1 Depth of coverage analysis

We assessed whether copy number changes between the *P. nigra* and *P. deltoides* individuals could be identified from the depth of coverage signature resulting from next-generation sequencing data. The number of paired reads retained after removal of duplicated reads for each sample is reported in Table 5.1, together with the number of mapped pairs of reads required to obtain windows of approximately 5000bp.

Coverage log2 ratios were used as the input for a circular binary segmentation algorithm, developed for SNP array data, to generate statistical predictions of copy number changes between the two individuals under comparison. To study the intrinsic variability of this analysis and to choose the log2 ratio threshold for the selection of copy number changes, we calculated the log2 ratios between two subsamples of the same individual. The distribution of log2 ratios in each window between the two subsamples had a mean of 0.015 and a standard deviation of 0.29 (Figure 5. 1). To minimize the false discovery rate we selected a log2 ratio threshold *t* of 0.9. Only 0.16% of the individual windows obtained in the two subsamples had a log2 ratio > *t*. Since a minimum of 2 windows are requested by DNAcopy to define a CNV, this has to be considered as an upper threshold for the false discovery rate in our process. The

requirement we set of for at least 50 kb (i.e. on average 10 windows) large segments to be above the threshold makes this even more true.

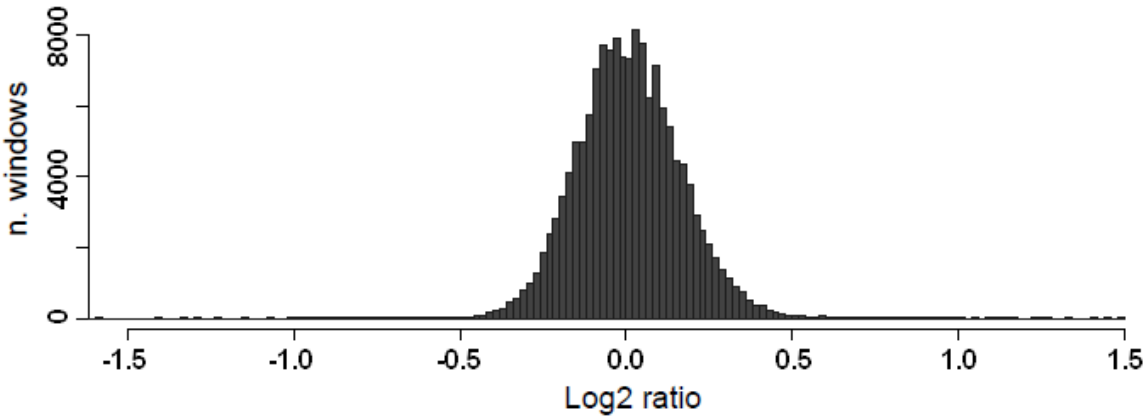

Figure 5. 1 Coverage log2 ratio distribution of each window obtained by comparing two subsamples of the accession BEN3.

Table 5. 1 Summary of the genome fragmentation in windows obtained for each of the six *P. nigra* (N) or *P. deltoides* (D) individuals and number of the identified CNVs per individual with the corresponding total number of Megabases.

Sample	Species	N° paired reads	Reads per window	N° windows	Mean window length (bp)
POLI	N	201246501	2500	82002	4915
BEN3	N	51374873	700	74829	5386
BDG	N	15835588	200	80298	5019
71077-308	N	52288417	700	76217	5288
L150-089	D	51816841	700	75551	5334
L155-079	D	57674034	700	83954	4800

We defined a CNV as a genomic region in which the log2 ratio between two individuals was $\geq t$. The number of CNVs and the corresponding total number of Megabases identified in each comparison is reported in Table 5. 2. We stratified CNVs by species (Figure 5. 2 A). 232 CNVs, corresponding to ~34 Mb, had a coverage log2 ratio significantly higher in at least one *P. nigra* individual with respect to at least one *P. deltoides* individual (red) and 177 CNVs (~28 Mb) had the opposite signal (blue); 3 CNVs showed a contrasting evidence and occurred in both directions. 176 CNVs (~22 Mb) were detected by comparing individuals of the same species (yellow); as expected, the majority of these CNVs were observed in *P. nigra* comparisons, for which we had more individuals to compare. The coverage log2 ratio distribution obtained for the CNVs detected comparing individuals of different species in the two directions (*P.*

nigra/*P. deltoides* and *P. deltoides*/*P. nigra*) was very similar, ranging from 1 to 6 and with a mean of ~2. In CNVs detected comparing individuals of the same species, the distribution of log2 ratios was quite different: the mean was 1.4 and the majority of log2 ratio values were lower than 2 (Figure 5. 2 B).

Table 5. 2 Number and Megabases of CNVs identified in all comparisons.

		Total number of Mb					
		POLI (*P. nigra*)	**BEN3** (*P. nigra*)	**BDG** (*P. nigra*)	**71077-308** (*P. nigra*)	**L150-089** (P. deltoides)	**L155-079** (*P. deltoides*)
N° identified CNVs	**POLI** (*P. nigra*)		5.88	3.70	2.09	10.67	10.09
	BEN3 (*P. nigra*)	49		4.65	5.61	13.46	15.04
	BDG (*P. nigra*)	29	35		3.22	15.35	14.32
	71077-308 (*P. nigra*)	20	38	29		11.05	11.03
	L150-089 (P. deltoides)	71	87	93	69		3.14
	L155-079 (*P. deltoides*)	77	94	94	77	29	

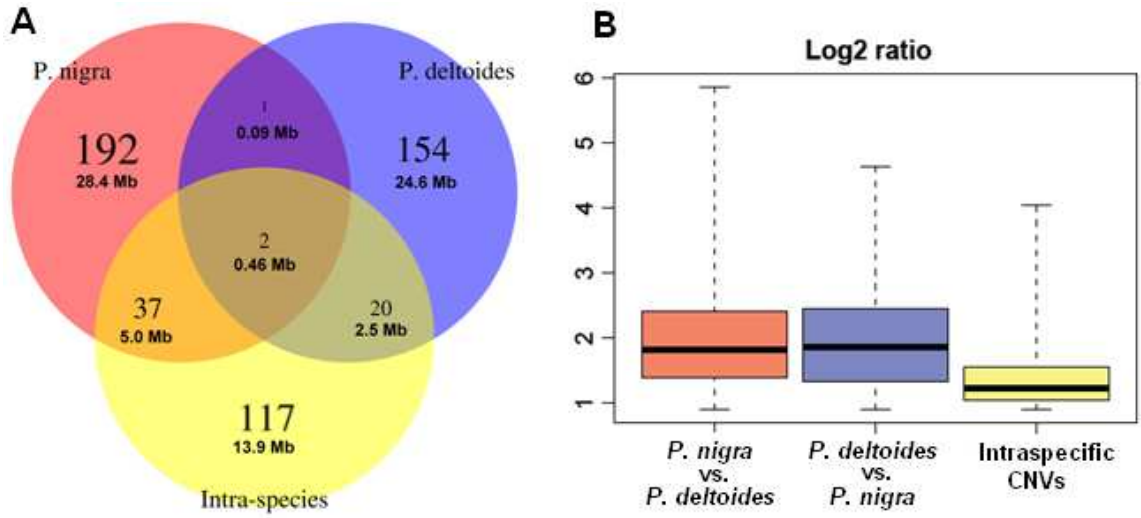

Figure 5. 2 Summary statistics of the identified copy number variants stratified by species. **Red**: CNV detected by comparing the coverage of *P. nigra* individuals over the coverage of *P. deltoides* ones. **Blue**: CNV detected by comparing the coverage of *P. deltoides* individuals over the coverage of *P. nigra* ones. **Yellow**: CNV detected by comparing the coverage of individuals of the same species. (**A**) Venn diagram summarizing the number of CNVs with the total number of Megabases involved. (**B**) Boxplot representing the distribution of the coverage log2 ratios.

For each region of copy number variation detected by comparing two parents of the pedigree, we calculated the coverage log2 ratios between each of the three corresponding F1 hybrids and the parental with the lower number of copies. The distribution of the log2 ratio obtained in parents and in the three hybrids is reported in Figure 5. 1. In all families the mean log2 ratio obtained for hybrids was about half of that obtained by comparing the two parentals.

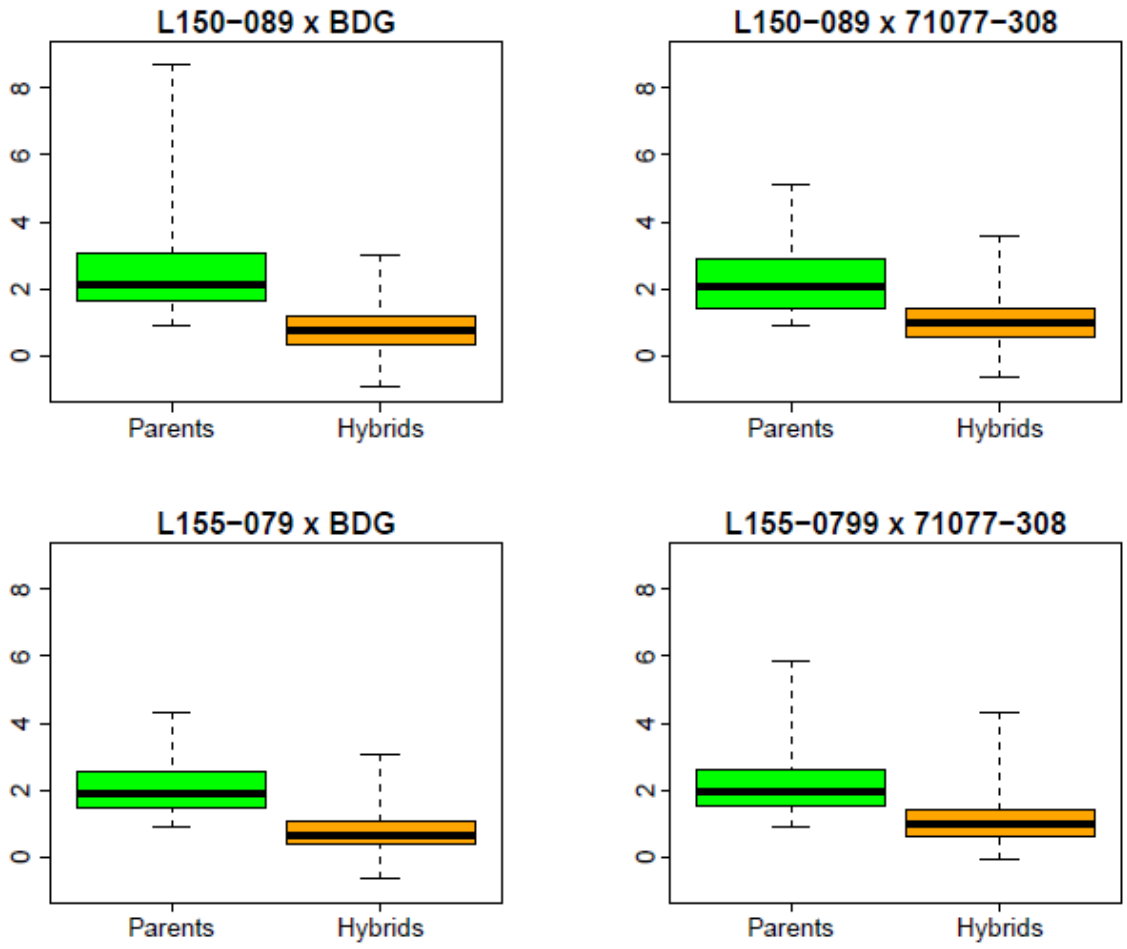

Figure 5. 3 Distribution of the Log2 ratios obtained in parents and in the corresponding three hybrids for the four studied crosses.

To obtain an overall view of the copy number variation identified between *P. nigra* and *P. deltoides* individuals, we plotted the log2 ratios obtained in each window for a selected *P. nigra*/*P. deltoides* (POLI and L155-079) pairwise comparison along the *P. trichocarpa* 19 chromosomes (Figure 5. 4) and we highlighted all the identified inter-specific CNVs. This genomic view revealed that the copy number variation between the two species is not evenly distributed throughout the poplar genome. There are a number

of highly conserved genomic regions showing very little or no copy number variation between *P. nigra* and *P. deltoides* individuals.

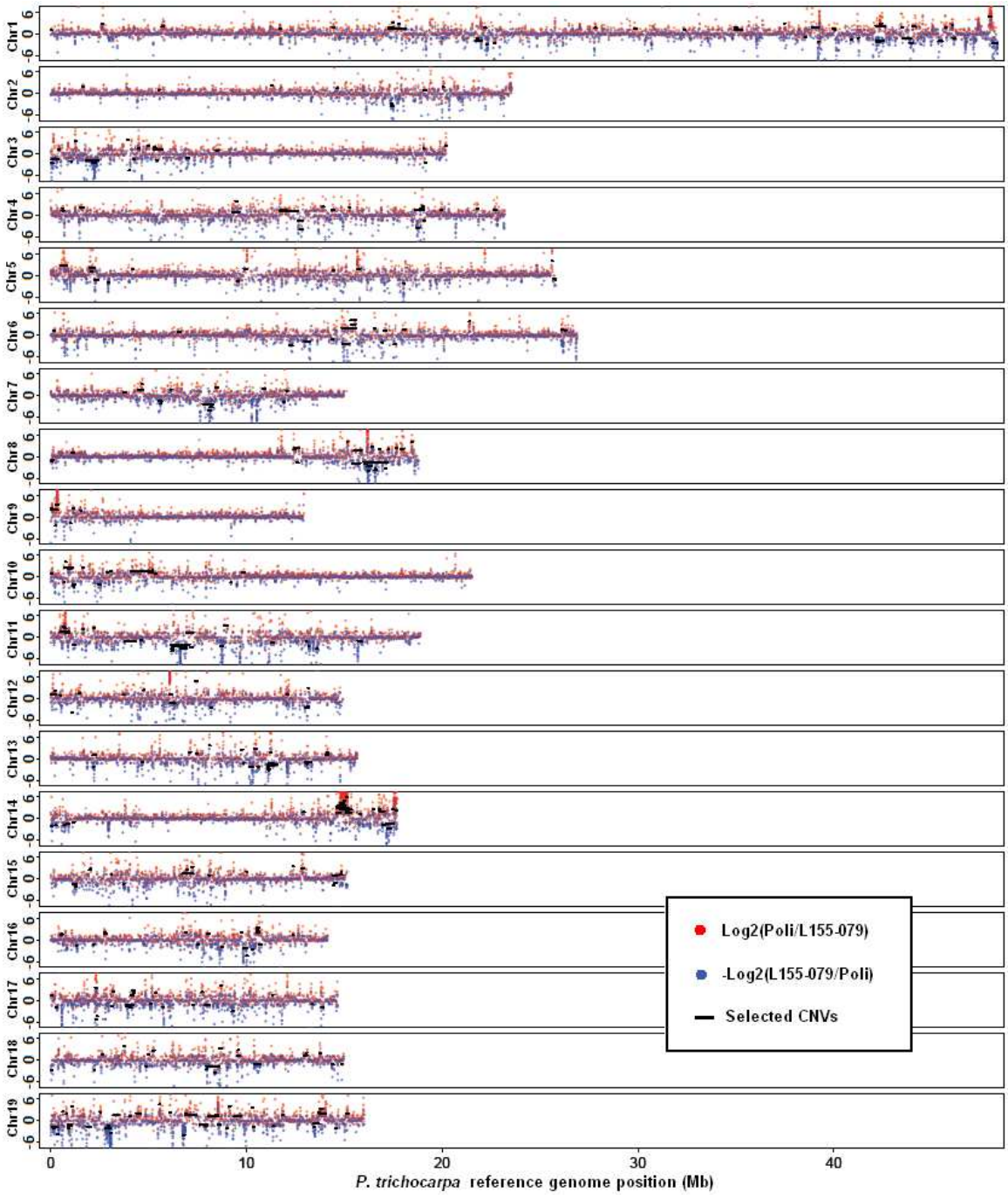

Figure 5. 4 Genomic distribution of log2 POLI/L155-079 signals (red) and -log2 L155-079/POLI signals (blue) for each chromosome. Black lines highlight all the identified inter-specific CNVs.

In the whole chromosome 2 we identified only few small regions of copy number variation. In chromosome 9, with the exception of the first 1.5 Mbs, there was no evidence of copy number variation between the two species. In addition, the proximal half of chromosome 8 and the distal half of chromosome 10 resulted conserved in terms of copy number between the *P. nigra* and *P. deltoides* individuals.

We identified a ~0.8 Mb CNV on chromosome 14 (positions 14585845-15349532). In this region there is a strong positive signal of the coverage log2 ratio between all the *P. nigra* over the two *P. deltoides* individuals. A closer inspection of this genomic region with a Genome Browser (Figure 5. 5) confirmed a strong difference in terms of sequence coverage between *P. nigra* and *P. deltoides* individuals, more marked in the central 0.5 Mb region. This region contains 34 annotated genes, 18 of them coding for a O-Glycosyl hydrolases family 17 protein.

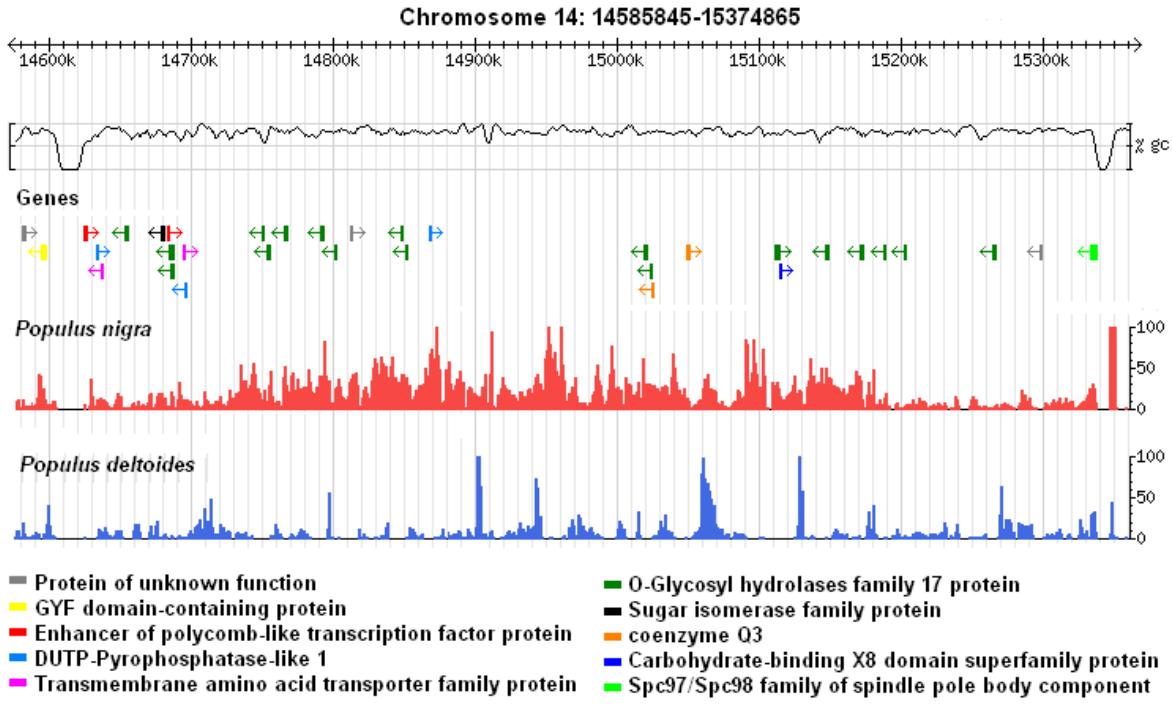

Figure 5. 5 Genome browser visualization of a 800 kb region on chromosome 14 that is present with more copies in *P. nigra* with respect to *P. deltoides*. The sequence coverage of a *P. nigra* (red) and a *P. deltoides* individual (blue) and the gene distribution along this region are reported.

Another interesting region with an opposite signal was identified on chromosome 3 (positions 1789806-2391690). In this case *P. deltoides* individuals had a significantly

higher coverage with respect to *P. nigra* individuals (Figure 5. 6). Also in this region there are many genes and a large part of them encodes for a Leucine-Rich Repeat (LLR) protein belonging to the NBS-LRR disease resistance protein family.

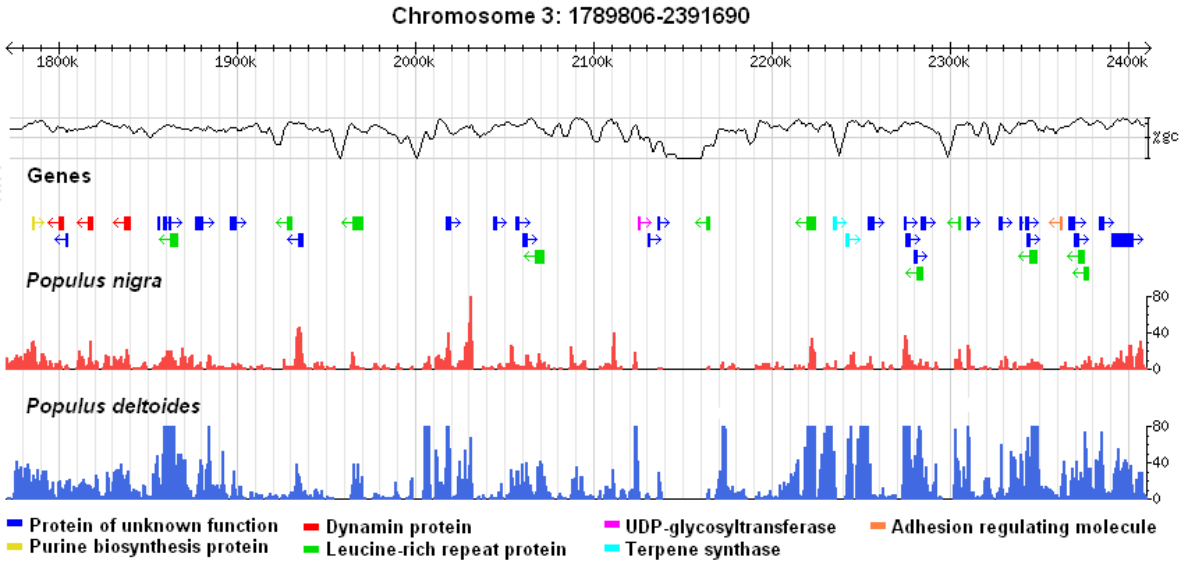

Figure 5. 6 Genome browser visualization of a 600 kb region on chromosome 3 that is present with more copies in *P. deltoides* with respect to *P. nigra* individuals.

5.2.2 Gene content analysis

The regions of copy number variation contained a total of 2661 predicted genes, with a density of about one gene every 20 kb. Considering that the gene density estimated for the whole *P. trichocarpa* reference genome is of about one gene every 10 kb, genomic regions involved in CNVs are depleted of genes compared to the rest of genome. This was visually confirmed by comparing the CNV and gene density distribution in the whole genome (Figure 5. 7). Regions with low gene density are rich in CNVs, while in regions with high gene density the number of identified CNV is limited. For example, in chromosome 8, 9 10 and 14 there are extended regions with a high gene density and a low rate of repetitiveness in which only very few or no CNVs were detected. On the other hand, CNVs seemed to be preferentially located in repetitive regions of the genome in which the gene density is low (Figure 5. 7).

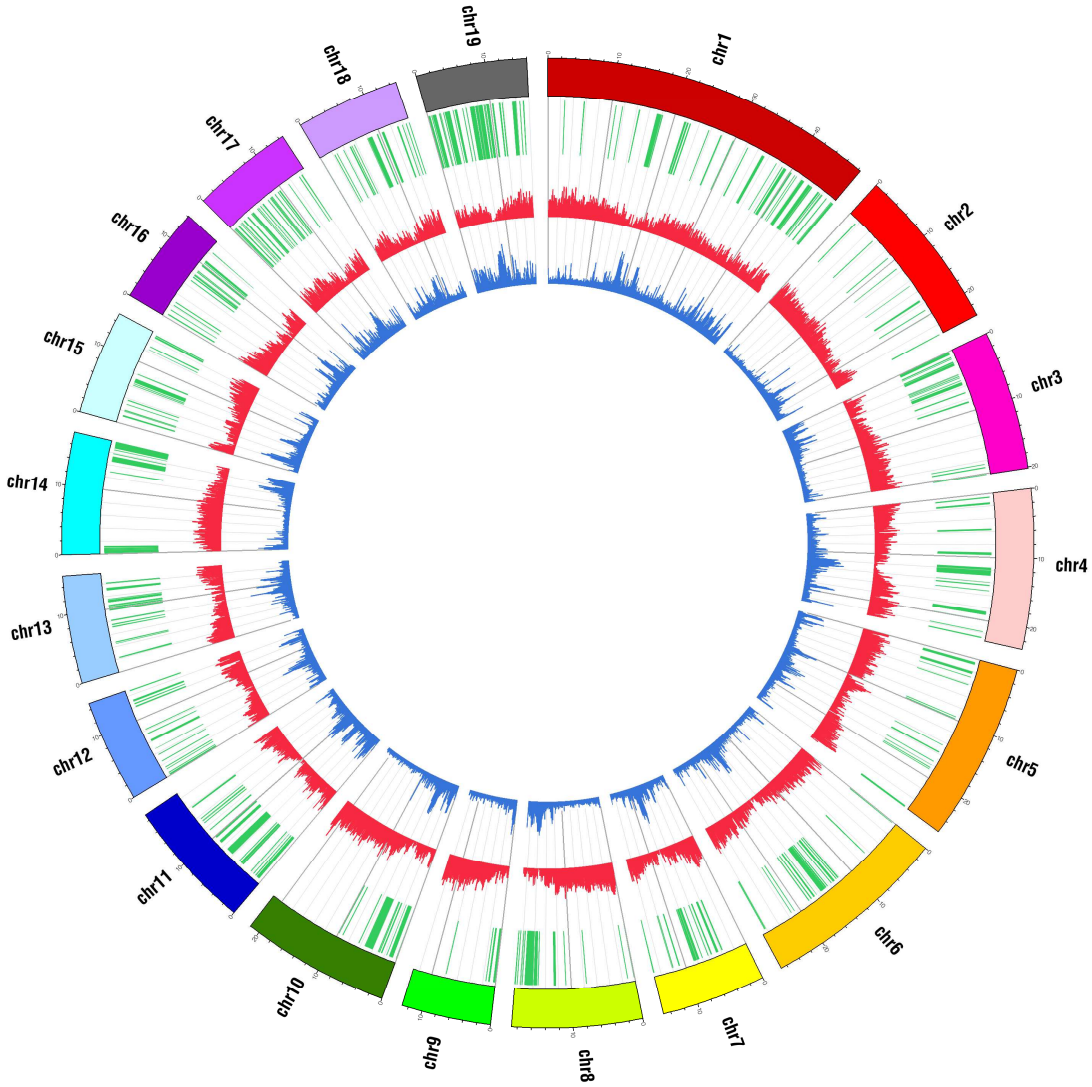

Figure 5. 7 CNV distribution across the 19 poplar chromosomes. **Green segments**: all the regions of copy number variation identified by comparing all the 6 resequenced individuals. **Red bars**: gene density distribution calculated as the number of genes every 100 kb. **Blue bars**: repetitiveness of the genome calculated with a k-mer analysis using the tool Tallymer (Kurtz *et al.*, 2008).

The predicted genes included in the selected CNVs were often organized in clusters in which a single gene was present in more copies. This type of organization was observed for different gene families: disease resistance genes, receptor-like protein kinases, zinc ion binding proteins, terpene synthases, glucosidases, N-acyltransferases and ankyrin repeat family proteins. Disease resistance genes were the most represented and deserved particular attention. Among the 2661 genes included in the regions of copy number variation, 392 encoded for a disease resistance family protein (Table 5.3), accounting for ~25% of the 1528 disease resistance genes present in the whole *P. trichocarpa*

genome. The proportion of disease resistance genes in regions of copy number variation was significantly higher compared to the rest of the genome (Odds Ratio 5.6, Fisher's exact test $p<2^{-16}$).

Table 5. 3 Contingency table that displays the frequency distribution of the disease resistance (**DR**) and not disease resistance (**Not DR**) genes in the regions showing (**CNVs**) and not showing (**Not CNVs**) copy number variation.

	DR genes	Not DR genes	Total genes
CNVs	392	2269	2661
Not CNVs	1136	36872	38008
Whole genome	1528	39141	40669

Given our interest in lignin composition, we looked for the presence of genes of the lignin biosynthesis pathway. We identified two copies of the gene cinnamoyl CoA reductase 1 (POPTR_0001s14890 and POPTR_0001s14910) and one copy of the gene 4-coumarate-CoA ligase 2 (POPTR_0006s18490) in which the predicted copy number resulted different between *P. nigra* and *P. deltoides* individuals (Table 5. 4).

Table 5. 4 List of the 3 genes of the lignin biosynthesis pathway with a copy number difference between *P. nigra* and *P. deltoides*.

Region of variation	Comparison	Log2 ratio	Gene ID	*P. trichocarpa* v2.0 annotation
Chr 1: 11703969-11706534	BEN3/ L150-089	1.33	POPTR_0001s14890	cinnamoyl coa reductase 1 (CCR1)
Chr 1: 11738342-11740892	BEN3/L150-089	1.33	POPTR_0001s14910	cinnamoyl coa reductase 1 (CCR1)
Chr 6: 16950343-16958604	L150-089/BDG	1.89	POPTR_0006s18490	4-coumarate CoA ligase 2 (4CL2)

The sequences of genes included in CNVs were used as query for a blastx analysis against the *Viridiplantae* nr database and blastx results were used for the functional classification with blast2GO. We tested for enrichment in gene ontology terms involved in biological processes, cellular components and molecular function using a Fisher's test with the Benjamini and Hochberg correction. We identified a number of GO terms

that were over-represented (P<0.05) in the regions of copy number variation, as compared with the complete genome (Table 5. 5).

Table 5. 5 Over-represented gene ontology (GO) categories for genes in the regions of copy number variation compared with the complete *P. trichocarpa* genome. GO terms belonging to the same process (P) or function (F) are marked with the same color.

GO-ID	GO term	GO Category	P-Value	#Test	#Ref
GO:0006952	defense response	P	3.25E-016	46	122
GO:0012501	programmed cell death	P	5.75E-012	28	55
GO:0045087	innate immune response	P	5.75E-012	23	32
GO:0002376	immune system process	P	5.75E-012	23	33
GO:0006955	immune response	P	5.75E-012	23	33
GO:0004872	receptor activity	F	5.75E-012	74	419
GO:0006915	apoptosis	P	6.64E-012	27	53
GO:0008219	cell death	P	6.64E-012	28	59
GO:0016265	death	P	6.64E-012	28	59
GO:0004888	transmembrane receptor activity	F	8.24E-011	32	92
GO:0003824	catalytic activity	F	4.17E-009	674	9518
GO:0016301	kinase activity	F	1.50E-008	186	1893
GO:0004672	protein kinase activity	F	3.73E-008	153	1480
GO:0042973	glucan endo-1,3-beta-D-glucosidase activity	F	3.73E-008	21	49
GO:0016772	transferase activity, transferring phosphorus-containing groups	F	1.25E-007	194	2062
GO:0060089	molecular transducer activity	F	1.41E-007	85	668
GO:0004871	signal transducer activity	F	1.41E-007	85	668
GO:0016773	phosphotransferase activity, alcohol group as acceptor	F	1.90E-007	160	1616
GO:0008422	beta-glucosidase activity	F	4.11E-006	21	69
GO:0006950	response to stress	P	4.59E-006	61	450
GO:0000989	transcription factor binding transcription factor activity	F	1.09E-005	11	15
GO:0003712	transcription cofactor activity	F	1.09E-005	11	15
GO:0015926	glucosidase activity	F	1.80E-005	22	85
GO:0000988	protein binding transcription factor activity	F	1.73E-004	11	22
GO:0004097	catechol oxidase activity	F	1.67 E-003	5	2
GO:0016740	transferase activity	F	2.48 E-003	289	3849
GO:0009986	cell surface	C	3.10 E-003	6	6

Over-represented genes under the biological processes category were mostly related to response to stimulus and were primarily involved in stress and defense (GO:0006952, GO:0045087, GO:0002376). GO terms related to cell death were also largely over-represented in the regions of copy number variation (GO:0012501, GO:0006915,

GO:0008219, GO:0016265). In addition, we found statistically significant over-representation of GO terms related to the catalytic activity molecular function, and in particular GO terms related to transferase activity of phosphorus-containing groups. Other over-represented molecular functions were molecular transducer activity (GO:0004888, GO:0060089 and GO:0004871), glucosidase activity (GO:0042973, GO:0008422 and GO:0015926) and protein binding transcription factor activity (GO:0000989, GO:0003712 and GO:0000988).

5.3 Discussion

Several studies in model systems have proven effective in elucidating both the size and the spectrum of genomic structural variation within one species, or between multiple species (Tuzun *et al.*, 2005; Nicholas *et al.*, 2009; Springer *et al.*, 2009; Hurwitz *et al.*, 2010; Ventura *et al.*, 2011). In humans, these studies have offered insights into human health, and helped elucidating the role of copy number variants in complex diseases (Hannes and Vermeesch, 2008; Helbig *et al.*, 2009). Studies on structural variation in plant species are difficult because of the size and complexity of many plant genomes, but they could have tremendous utility in identifying genomic regions associated with complex traits, domestication and adaptation. In 2009, Springer and colleagues reported the employment of comparative genome hybridization (CGH) technology to investigate structural variation in maize, while in 2010 Hurwitz and coauthors published a work in which BAC end sequences and physical maps where employed to analyze the genome-wide structural variation among three closely related *Oryza* species.

The present study is the first to use next-generation sequencing technologies to identify CNVs in any plant species. In addition, it is the first attempt of performing genome-wide analysis of copy number variation between the two species *Populus nigra* and *Populus deltoides*. To date, studies on interspecific genetic variation of the genus *Populus*, have focused on a limited number of markers, like AFLPs and microsatellites, distributed along the genome (Cervera *et al.*, 2005; Cervera *et al.*, 2001). We used next-generation sequencing data to perform a genome-wide analysis of CNVs between the two species *Populus nigra* and *Populus deltoides*. Overall, we identified 192 regions (~28.4 Mb) present with a higher copy number in *P. nigra* and 154 CNVs (~24.6 Mb)

with the opposite signature. In addition, 117 regions, corresponding to a total of 13.9 Mb, exhibit an intraspecific pattern of copy number variation. On average, we identified ~80 regions of copy number variation, corresponding to ~13 Mb when comparing two individuals of a different species and ~30 CNV (4 Mb) when comparing individuals of the same species (Table 5. 2). As expected, CNVs were more frequent between the two species than within species. In addition, intraspecific CNVs showed a mean log2 ratio of ~2 (Figure 5. 2), that was sensibly higher than that observed comparing individuals of the same species. This may suggest that CNVs identified between different species are more likely to be homozygous than those detected comparing individuals of the same species. We also identified many extended regions of the genome that showed little or no variation between the two species. In general, these conserved regions are rich in genes and poor in repetitive sequences. On the other hand, in CNVs we found a high level of repetitiveness and diminished gene content, as compared with the rest of the genome. Transposable elements make up a high proportion of repetitive DNA, indicating a possible contribution of these elements to the gain and loss of sequence in the poplar genome. In poplar, the LTR retrotransposons represent the most active class or transposable elements (see Chapter 4). LTR retroelements have been previously shown to be major contributors to genome size evolution in rice (Ma and Bennetzen, 2004). Transposable elements may also be important in new gene formation and genome evolution. For example *Helitron*-related transposable elements have been shown to carry pseudogenes in maize and to contribute to the expansion and evolution of the maize genome (Yang and Bennetzen, 2009).

Our analysis showed that the regions of copy number variation had a lower-than-average gene content. However, some categories of GO terms, such as those related to defense against stresses, cell death, transferase activity of phosphorus-containing groups, molecular transducer activity, glucosidase activity and protein binding transcription factor activity, were overrepresented compared to the rest of the genome.

Overall, in the regions of copy number variation we identified 2661 predicted genes. Three of them are genes involved in the lignin biosynthesis pathway: two encoded for a Cinnamoyl CoA Reductase 1 (CCR1) and the other encoded for a 4-Coumarate CoA Ligase 2 (4CL2). To date, there is no proof of transcription in differentiating xylem for these genes (Shi *et al.*, 2010); however an analysis of differential expression between individuals carrying a different number of copies of these genes will be of help to investigate a possible effect on lignin biosynthesis.

A large fraction of the genes included in CNVs encodes for disease resistance proteins, such as the Nucleotide Binding Site-Leucine Rich Repeat (NBS_LRR) gene family. Fisher's exact test showed that the regions of copy number variation are significantly enriched in disease resistance genes with respect to the rest of the genome. In maize, evidences that disease resistance genes exhibit copy number variation for different haplotypes have already been reported (Smith *et al.*, 2004). In addition, the over-representation of disease resistance genes in regions of structural variation between different species has already been reported for rice (Hurwitz *et al.*, 2010). Evidences of the high variability of disease resistance genes have been also reported for *Arabidopsis thaliana* (Clark *et al.*, 2007). In *A. thaliana*, tandem duplications and losses have been found to play the dominant role in affecting copy number of disease resistance genes (Cannon *et al.*, 2004). We observed that in the regions of copy number variation genes were often organized in clusters. Tandem duplication processes are considered to be a major cause for the generation of cluster of duplicated genes and for the expansion of some genes families. For example, the extant distribution and diversity in *Arabidopsis* genome of the NBS-LRR sequences has been generated by extensive duplication and ectopic rearrangements that involved segmental duplications (Meyers *et al.*, 2003). Unequal recombination occurring when interspersed repetitive elements promote non-homologue crossing-over is thought to be the primary mechanism driving the expansion of gene clusters (Leister, 2004). After the duplication, each paralogue gene may retain the same function as the ancestral copy or may lose the original function and/or obtain a new function. Genes that confer a selective advantage are thus maintained by natural selection. Therefore, the genes that we have found to be over-represented in the CNVs may reflect recent gene acquisition events occurred in one of the two poplar species and are candidate markers of interspecific divergence. In plants, interspecific CNVs may contribute to heterosis (Springer *et al.*, 2009). In this study we identified hundreds genomic regions showing a different copy number between *P. nigra* and *P. deltoides* accessions. In hybrids these regions will be inherited with a large number of different combinations, providing the opportunity for novel gene complements and trans-interactions with respect to the parents.

In summary, with this study we obtained a catalogue of CNVs across the poplar genome. These regions may be useful tools to explore the mechanisms of speciation in poplar and understand the molecular basis of heterosis in poplar hybrids.

List of References

Abecasis, G.R., Noguchi, E., Heinzmann, A., *et al.*, (2001) Extent and distribution of linkage disequilibrium in three genomic regions. *American journal of human genetics*, 68(1), 191-197.

Achaz, G., Coissac, E., Viari, A. and Netter, P., (2000) Analysis of intrachromosomal duplications in yeast Saccharomyces cerevisiae: a possible model for their origin. *Molecular biology and evolution*, 17(8), 1268-75.

Alkan, C., Coe, B.P. and Eichler, E.E., (2011) Genome structural variation discovery and genotyping. *Nature reviews. Genetics*.

Altschul, S.F., Gish, W., Miller, W., Myers, E.W. and Lipman, D.J., (1990) Basic local alignment search tool. *Journal of molecular biology*, 215(3), 403-10.

Barakat, A., Bagniewska-Zadworna, A., Choi, A., Plakkat, U., DiLoreto, D.S., Yellanki, P. and Carlson, J.E., (2009) The cinnamyl alcohol dehydrogenase gene family in Populus: phylogeny, organization, and expression. *BMC plant biology*, 9, 26.

Baucher, M., Chabbert, B., Pilate, G., *et al.*, (1996) Red Xylem and Higher Lignin Extractability by Down-Regulating a Cinnamyl Alcohol Dehydrogenase in Poplar. *Plant physiology*, 112(4), 1479-1490.

Benjamini, Y. and Hochberg, Y., (2007) Controlling the False Discovery Rate: A Practical and Powerful Approach to Multiple Testing.

Bennetzen, J L, (2000) Transposable element contributions to plant gene and genome evolution. *Plant molecular biology*, 42(1), 251-69.

Bentley, D.R., Balasubramanian, S., Swerdlow, H.P., *et al.*, (2008) Accurate whole human genome sequencing using reversible terminator chemistry. *Nature*, 456(7218), 53-9.

Blüthgen, N., Brand, K., Cajavec, B., Swat, M., Herzel, H. and Beule, D., (2005) Biological profiling of gene groups utilizing Gene Ontology. *Genome informatics. International Conference on Genome Informatics*, 16(1), 106-15.

Brunner, S., Fengler, K., Morgante, M., Tingey, S. and Rafalski, A., (2005) Evolution of DNA sequence nonhomologies among maize inbreds. *The Plant cell*, 17(2), 343-60.

Campbell, P.J., Stephens, P.J., Pleasance, E.D., *et al.* (2008) Identification of somatically acquired rearrangements in cancer using genome-wide massively parallel paired-end sequencing. *Nature genetics*, 40(6), 722-9.

Cannon, S.B., Mitra, A., Baumgarten, A., Young, N.D. and May, G. (2004) The roles of segmental and tandem gene duplication in the evolution of large gene families in Arabidopsis thaliana. *BMC plant biology*, 4, 10.

Cervera, M.T., Storme, V, Soto, A., Ivens, B, Montagu, M Van, Rajora, O.P. and Boerjan, W (2005) Intraspecific and interspecific genetic and phylogenetic relationships in the genus Populus based on AFLP markers. *TAG. Theoretical and applied genetics. Theoretische und angewandte Genetik*, 111(7), 1440-56.

Cervera, M.T., Storme, Veronique, Ivens, Bart, Gusmao, J., Liu, B.H., Hostyn, V., Slycken, J. Van, Montagu, Marc Van and Boerjan, Wout (2001) Dense Genetic Linkage Maps of Three Populus Species (Populus deltoides, P. nigra and P. trichocarpa) Based on AFLP and Microsatellite Markers. *Genetics*, 158(2), 787-809.

Chen, F. and Dixon, R.A. (2007) Lignin modification improves fermentable sugar yields for biofuel production. *Nature biotechnology*, 25(7), 759-61.

Chen, K., Wallis, J.W., McLellan, M.D., *et al.* (2009) BreakDancer: an algorithm for high-resolution mapping of genomic structural variation. *Nature methods*, 6(9), 677-81.

Chou, H.H. and Holmes, M.H. (2001) DNA sequence quality trimming and vector removal. *Bioinformatics (Oxford, England)*, 17(12), 1093-104.

Clark, R.M., Schweikert, G., Toomajian, C., *et al.* (2007) Common sequence polymorphisms shaping genetic diversity in Arabidopsis thaliana. *Science (New York, N.Y.)*, 317(5836), 338-42.

Comai, L., Young, K., Till, B.J., *et al.* (2004) Efficient discovery of DNA polymorphisms in natural populations by Ecotilling. *Plant J*, 37(5), 778-786.

Conesa, A., Götz, S., García-Gómez, J.M., Terol, J., Talón, M. and Robles, M. (2005) Blast2GO: a universal tool for annotation, visualization and analysis in functional genomics research. *Bioinformatics (Oxford, England)*, 21(18), 3674-6.

Cooper, G.M., Zerr, T., Kidd, J.M., Eichler, E.E. and Nickerson, D.A. (2008) Systematic assessment of copy number variant detection via genome-wide SNP genotyping. *Nature genetics*, 40(10), 1199-203.

Dixon, R.A., Chen, F., Guo, D. and Parvathi, K. (2001) The biosynthesis of monolignols: a "metabolic grid", or independent pathways to guaiacyl and syringyl units? *Phytochemistry*, 57(7), 1069-1084.

Doorsselaere, J. Van, Baucher, M., Feuillet, C., Boudet, A. M., Montagu, M. Van and Inze, D. (1995) Isolation of cinnamyl alcohol dehydrogenase cDNAs from

two important economic species: alfalfa and poplar. Demonstration of a high homology of the gene within angiosperms. *Plant physiology and biochemistry*, 33(1), 105-109.

Douglas, C., (2011) Genomics of adaptation and wood properties in Populus trichocarpa. *BMC Proceedings*, 5(Suppl 7), O2.

Druley, T.E., Vallania, F.L.M., Wegner, D.J., *et al.*, (2009) Quantification of rare allelic variants from pooled genomic DNA. *Nature Methods*, 6(April 2009), 263-265.

EREC, (2008) Renewable Energy Technology Roadmap 20% by 2020. *European Renewable Energy Council*.

Eichler, E.E. and Sankoff, D., (2003) Structural dynamics of eukaryotic chromosome evolution. *Science (New York, N.Y.)*, 301(5634), 793-7.

Ewing, B. and Green, P., (1998) Base-calling of automated sequencer traces using phred. II. Error probabilities. *Genome research*, 8(3), 186-194.

Ewing, B., Hillier, L., Wendl, M C and Green, P., (1998) Base-calling of automated sequencer traces using phred. I. Accuracy assessment. *Genome research*, 8(3), 175-185.

Eyre-Walker, A., (2010) Evolution in health and medicine Sackler colloquium: Genetic architecture of a complex trait and its implications for fitness and genome-wide association studies. *Proceedings of the National Academy of Sciences of the United States of America*, 107 Suppl (suppl_1), 1752-6.

Fay, J.C. and Wu, C.I., (2000) Hitchhiking under positive Darwinian selection. *Genetics*, 155(3), 1405-13.

Felsenstein, J., (1989) PHYLIP -- Phylogeny Inference Package (Version 3.2). *Cladistics*, 0(5), 164-166.

Feuk, L., Carson, A.R. and Scherer, S.W., (2006) Structural variation in the human genome. *Nature reviews. Genetics*, 7(2), 85-97.

Fransz, P.F., Armstrong, S., Jong, J.H. de, Parnell, L.D., Drunen, C. van, Dean, C., Zabel, P., Bisseling, T and Jones, G.H., (2000) Integrated cytogenetic map of chromosome arm 4S of A. thaliana: structural organization of heterochromatic knob and centromere region. *Cell*, 100(3), 367-76.

Frascaroli, E., Canè, M.A., Landi, P., Pea, G., Gianfranceschi, L., Villa, M., Morgante, M. and Pè, M.E., (2007) Classical genetic and quantitative trait loci analyses of heterosis in a maize hybrid between two elite inbred lines. *Genetics*, 176(1), 625-44.

Futschik, A. and Schlötterer, C., (2010) Massively Parallel Sequencing of Pooled DNA Samples--The Next Generation of Molecular Markers. *Genetics*, 186(1), 207-218.

Gilchrist, E.J., Haughn, G.W., Ying, C.C., *et al.*, (2006) Use of Ecotilling as an efficient SNP discovery tool to survey genetic variation in wild populations of Populus trichocarpa. *Molecular ecology*, 15(5), 1367-78.

Gordon, D., Abajian, C. and Green, P., (1998) Consed: a graphical tool for sequence finishing. *Genome research*, 8(3), 195-202.

Greenman, C., Stephens, P., Smith, R., *et al.*, (2007) Patterns of somatic mutation in human cancer genomes. *Nature*, 446(7132), 153-8.

Guex, N. and Peitsch, M.C., (1997) SWISS-MODEL and the Swiss-PdbViewer: an environment for comparative protein modeling. *Electrophoresis*, 18(15), 2714-23.

Halpin, C., Holt, K., Chojecki, J., Oliver, D., Chabbert, B., Monties, B., Edwards, K., Barakate, A. and Foxon, G.A., (1998) Brown-midrib maize (bm1)--a mutation affecting the cinnamyl alcohol dehydrogenase gene. *The Plant journal : for cell and molecular biology*, 14(5), 545-53.

Hamberger, B., Ellis, M., Friedmann, M., Azevedo Souza, C. de, Barbazuk, B. and Douglas, C.J., (2007) Genome-wide analyses of phenylpropanoid-related genes in Populus trichocarpa, Arabidopsis thaliana, and Oryza sativa: the Populus lignin toolbox and conservation and diversification of angiosperm gene families. *Can J Bot*, 85(12), 1182-1201.

Hannes, F. and Vermeesch, J.R., (2008) Benign and pathogenic copy number variation on the short arm of chromosome 4. *Cytogenetic and genome research*, 123(1-4), 88-93.

Havlík, P., Schneider, U.A., Schmid, E., *et al.*, (2010) Global land-use implications of first and second generation biofuel targets. *Energy Policy*, In press.

Hedrick, P. and Kumar, S., (2001) Mutation and linkage disequilibrium in human mtDNA. *European journal of human genetics : EJHG*, 9(12), 969-72.

Helbig, I., Mefford, H.C., Sharp, A.J., *et al.*, (2009) 15q13.3 microdeletions increase risk of idiopathic generalized epilepsy. *Nature genetics*, 41(2), 160-2.

Heuertz, M., Paoli, E. De, Källman, T., Larsson, H., Jurman, I., Morgante, M., Lascoux, M. and Gyllenstrand, N., (2006) Multilocus patterns of nucleotide diversity, linkage disequilibrium and demographic history of Norway spruce [Picea abies (L.) Karst]. *Genetics*, 174(4), 2095-105.

Hill, W. and Weir, B.S., (1988) Variances and covariances of squared linkage disequilibria in finite populations. *Theoretical population biology*, 33(1), 54-78.

Hisano, H., Nandakumar, R. and Wang, Z.-Y., (2009) Genetic modification of lignin biosynthesis for improved biofuel production. *In Vitro Cellular & Developmental Biology - Plant*, 45(3), 306-313.

Hormozdiari, F., Hajirasouliha, I., Dao, P., Hach, F., Yorukoglu, D., Alkan, C., Eichler, E.E. and Sahinalp, S.C., (2010) Next-generation VariationHunter: combinatorial algorithms for transposon insertion discovery. *Bioinformatics (Oxford, England)*, 26(12), i350-7.

Huang, X. and Madan, A., (1999) CAP3: A DNA sequence assembly program. *Genome research*, 9(9), 868-77.

Hughes, A.L., Friedman, R., Ekollu, V. and Rose, J.R., (2003) Non-random association of transposable elements with duplicated genomic blocks in Arabidopsis thaliana. *Molecular phylogenetics and evolution*, 29(3), 410-6.

Hurles, M.E., Dermitzakis, E.T. and Tyler-Smith, C., (2008) The functional impact of structural variation in humans. *Trends in genetics : TIG*, 24(5), 238-45.

Hurwitz, B.L., Kudrna, D., Yu, Y., Sebastian, A., Zuccolo, A., Jackson, S.A., Ware, D., Wing, R.A. and Stein, L., (2010) Rice structural variation: a comparative analysis of structural variation between rice and three of its closest relatives in the genus Oryza. *The Plant journal : for cell and molecular biology*, 63(6), 990-1003.

Ingman, M. and Gyllensten, U., (2009) SNP frequency estimation using massively parallel sequencing of pooled DNA. *Eur J Hum Genet*, 17(3), 383-386.

Ingvarsson, P.K., (2008) Multilocus patterns of nucleotide polymorphism and the demographic history of Populus tremula. *Genetics*, 180(1), 329-40.

Jaillon, O., Aury, J.-M., Noel, B., *et al.*, (2007) The grapevine genome sequence suggests ancestral hexaploidization in major angiosperm phyla. *Nature*, 449(7161), 463-7.

Jiang, R., Tavaré, S. and Marjoram, P., (2009) Population genetic inference from resequencing data. *Genetics*, 181(1), 187-97.

Jung, H.J. and Ni, W., (1998) Lignification of plant cell walls: impact of genetic manipulation. *Proceedings of the National Academy of Sciences of the United States of America*, 95(22), 12742-12743.

Jurka, J., Kapitonov, V.V., Pavlicek, A., Klonowski, P., Kohany, O. and Walichiewicz, J., (2005) Repbase Update, a database of eukaryotic repetitive elements. *Cytogenetic and genome research*, 110(1-4), 462-7.

Keller, B., Wicker, T. and Matthews, D.E., (2002) TREP: a database for Triticeae repetitive elements. *Trends in plant science*, 7(12), 561-562.

Kidwell, M.G. and Lisch, D., (1997) Transposable elements as sources of variation in animals and plants. *Proceedings of the National Academy of Sciences of the United States of America*, 94(15), 7704-11.

Kircher, M., Stenzel, U. and Kelso, J., (2009) Improved base calling for the Illumina Genome Analyzer using machine learning strategies. *Genome biology*, 10(8), R83.

Koboldt, D.C., Chen, K., Wylie, T., Larson, D.E., McLellan, M.D., Mardis, E.R., Weinstock, G.M., Wilson, R.K. and Ding, L., (2009) VarScan: variant detection in massively parallel sequencing of individual and pooled samples. *Bioinformatics (Oxford, England)*, 25(17), 2283-2285.

Koboldt, D.C., Ding, L., Mardis, E.R. and Wilson, R.K., (2010) Challenges of sequencing human genomes. *Briefings in bioinformatics*, 11(5), 484-98.

Korbel, J.O., Abyzov, A., Mu, X.J., Carriero, N., Cayting, P., Zhang, Z., Snyder, M. and Gerstein, M.B., (2009) PEMer: a computational framework with simulation-based error models for inferring genomic structural variants from massive paired-end sequencing data. *Genome biology*, 10(2), R23.

Korbel, J.O., Urban, A.E., Affourtit, J.P., *et al.*, (2007) Paired-end mapping reveals extensive structural variation in the human genome. *Science (New York, N.Y.)*, 318(5849), 420-6.

Kurtz, S., Narechania, A., Stein, J.C. and Ware, D., (2008) A new method to compute K-mer frequencies and its application to annotate large repetitive plant genomes. *BMC genomics*, 9, 517.

Lapierre, C., Pollet, B., Petit-Conil, M., *et al.*, (1999) Structural alterations of lignins in transgenic poplars with depressed cinnamyl alcohol dehydrogenase or caffeic acid O-methyltransferase activity have an opposite impact on the efficiency of industrial kraft pulping. *Plant physiology*, 119(1), 153-64.

Lee, S., Hormozdiari, F., Alkan, C. and Brudno, M., (2009) MoDIL: detecting small indels from clone-end sequencing with mixtures of distributions. *Nature methods*, 6(7), 473-4.

Leister, D., (2004) Tandem and segmental gene duplication and recombination in the evolution of plant disease resistance gene. *Trends in genetics : TIG*, 20(3), 116-22.

Levy, S., Sutton, G., Ng, P.C., *et al.*, (2007) The diploid genome sequence of an individual human. *PLoS biology*, 5(10), e254.

Li, H. and Durbin, R., (2009) Fast and accurate short read alignment with Burrows-Wheeler transform. *Bioinformatics (Oxford, England)*, 25(14), 1754-60.

Li, H., Handsaker, B., Wysoker, A., Fennell, T., Ruan, J., Homer, N., Marth, G., Abecasis, G. and Durbin, R., (2009) The Sequence Alignment/Map format and SAMtools. *Bioinformatics (Oxford, England)*, 25(16), 2078-9.

Li, L., Zhou, Y., Cheng, X., Sun, J., Marita, J.M., Ralph, J. and Chiang, V.L., (2003) Combinatorial modification of multiple lignin traits in trees through multigene cotransformation. *Proceedings of the National Academy of Sciences of the United States of America*, 100(8), 4939-44.

Li, X., Weng, J.-K. and Chapple, C., (2008) Improvement of biomass through lignin modification. *Plant J*, 54(4), 569-581.

Librado, P. and Rozas, J., (2009) DnaSP v5: a software for comprehensive analysis of DNA polymorphism data. *Bioinformatics (Oxford, England)*, 25(11), 1451-2.

Lohse, K. and Kelleher, J., (2009) Measuring the degree of starshape in genealogies--summary statistics and demographic inference. *Genetics research*, 91(4), 281-92.

Lomsadze, A., Ter-Hovhannisyan, V., Chernoff, Y.O. and Borodovsky, M., (2005) Gene identification in novel eukaryotic genomes by self-training algorithm. *Nucleic acids research*, 33(20), 6494-506.

Lynch, M. and Conery, J.S., (2003) The evolutionary demography of duplicate genes. *Journal of structural and functional genomics*, 3(1-4), 35-44.

Ma, J. and Bennetzen, Jeffrey L, (2004) Rapid recent growth and divergence of rice nuclear genomes. *Proceedings of the National Academy of Sciences of the United States of America*, 101(34), 12404-10.

MacKay, J.J., O'Malley, D.M., Presnell, T., Booker, F.L., Campbell, M M, Whetten, R.W. and Sederoff, R.R., (1997) Inheritance, gene expression, and lignin characterization in a mutant pine deficient in cinnamyl alcohol dehydrogenase. *Proceedings of the National Academy of Sciences of the United States of America*, 94(15), 8255-60.

Manolio, T.A., Collins, F.S., Cox, N.J., *et al.*, (2009) Finding the missing heritability of complex diseases. *Nature*, 461(7265), 747-53.

Mardis, E.R., (2008) Next-generation DNA sequencing methods. *Annual review of genomics and human genetics*, 9, 387-402.

Marroni, F., Pinosio, S., Zaina, G., Fogolari, F., Felice, N., Cattonaro, F. and Morgante, M., (2011) Nucleotide diversity and linkage disequilibrium in Populus nigra cinnamyl alcohol dehydrogenase (CAD4) gene. *Tree Genetics & Genomes*, 7(5), 1011-1023.

Marroni, F., Toni, C., Pennato, B., Tsai, Y.-Y., Duggal, P., Bailey-Wilson, J.E. and Presciuttini, S., (2005) Haplotypic structure of the X chromosome in the COGA population sample and the quality of its reconstruction by extant software packages. *BMC genetics*, 6 Suppl 1, S77.

McDonald, J.H. and Kreitman, M., (1991) Adaptive protein evolution at the Adh locus in Drosophila. *Nature*, 351(6328), 652-4.

Medvedev, P., Stanciu, M. and Brudno, M., (2009) Computational methods for discovering structural variation with next-generation sequencing. *Nature methods*, 6(11 Suppl), S13-20.

Meyers, B.C., Kozik, A., Griego, A., Kuang, H. and Michelmore, R.W., (2003) Genome-wide analysis of NBS-LRR-encoding genes in Arabidopsis. *The Plant cell*, 15(4), 809-34.

Mueller, J.C., (2004) Linkage disequilibrium for different scales and applications. *Briefings in bioinformatics*, 5(4), 355-64.

Nachman, M.W., Boyer, S.N. and Aquadro, C.F., (1994) Nonneutral evolution at the mitochondrial NADH dehydrogenase subunit 3 gene in mice. *Proceedings of the National Academy of Sciences of the United States of America*, 91(14), 6364-8.

Nei, M. and Li, W.H., (1979) Mathematical model for studying genetic variation in terms of restriction endonucleases. *Proceedings of the National Academy of Sciences of the United States of America*, 76(10), 5269-5273.

Nicholas, T.J., Cheng, Z., Ventura, M., Mealey, K., Eichler, E.E. and Akey, J.M., (2009) The genomic architecture of segmental duplications and associated copy number variants in dogs. *Genome research*, 19(3), 491-9.

Nickerson, D.A., Tobe, V.O. and Taylor, S.L., (1997) PolyPhred: automating the detection and genotyping of single nucleotide substitutions using fluorescence-based resequencing. *Nucleic acids research*, 25(14), 2745-2751.

Olshen, A.B., Venkatraman, E.S., Lucito, R. and Wigler, M., (2004) Circular binary segmentation for the analysis of array-based DNA copy number data. *Biostatistics (Oxford, England)*, 5(4), 557-72.

Olson, M.S., Robertson, A.L., Takebayashi, N., Silim, S., Schroeder, W.R. and Tiffin, P., (2010) Nucleotide diversity and linkage disequilibrium in balsam poplar (Populus balsamifera). *The New phytologist*, 186(2), 526-36.

Out, A.A., Minderhout, I.J.H.M. van, Goeman, J.J., *et al.*, (2009) Deep sequencing to reveal new variants in pooled DNA samples. *Human mutation*, 30(12), 1703-1712.

Ouyang, S. and Buell, C.R., (2004) The TIGR Plant Repeat Databases: a collective resource for the identification of repetitive sequences in plants. *Nucleic acids research*, 32(Database issue), D360-3.

Pinkel, D., Segraves, R., Sudar, D., *et al.*, (1998) High resolution analysis of DNA copy number variation using comparative genomic hybridization to microarrays. *Nature genetics*, 20(2), 207-11.

Price, A.L., Jones, N.C. and Pevzner, P.A., (2005) De novo identification of repeat families in large genomes. *Bioinformatics (Oxford, England)*, 21 Suppl 1, i351-8.

Ramírez-Soriano, A. and Nielsen, R., (2009) Correcting estimators of theta and Tajima's D for ascertainment biases caused by the single-nucleotide polymorphism discovery process. *Genetics*, 181(2), 701-10.

Rand, D.M. and Kann, L.M., (1996) Excess amino acid polymorphism in mitochondrial DNA: contrasts among genes from Drosophila, mice, and humans. *Molecular biology and evolution*, 13(6), 735-48.

Ray, D.A. and Batzer, M.A., (2011) Reading TE leaves: New approaches to the identification of transposable element insertions. *Genome research*, 21(6), 813-20.

Remington, D.L., Thornsberry, J.M., Matsuoka, Y., Wilson, L.M., Whitt, S.R., Doebley, J., Kresovich, S., Goodman, M.M. and Buckler, E.S., (2001) Structure of linkage disequilibrium and phenotypic associations in the maize genome. *Proceedings of the National Academy of Sciences of the United States of America*, 98(20), 11479-84.

Rinaldi, C., Kohler, A., Frey, P., *et al.*, (2007) Transcript profiling of poplar leaves upon infection with compatible and incompatible strains of the foliar rust Melampsora larici-populina. *Plant physiology*, 144(1), 347-66.

Risch, N. and Merikangas, K., (1996) The future of genetic studies of complex human diseases. *Science (New York, N.Y.)*, 273(5281), 1516-7.

Rogers, L.A. and Campbell, Malcolm M., (2004) The genetic control of lignin deposition during plant growth and development. *New Phytologist*, 164(1), 17-30.

Rohde, A., Storme, Véronique, Jorge, V., *et al.*, (2010) Bud set in poplar - genetic dissection of a complex trait in natural and hybrid populations. *New Phytologist*, 189(1), 106-121.

Sarni, F., Grand, C. and Boudet, A M, (1984) Purification and properties of cinnamoyl-CoA reductase and cinnamyl alcohol dehydrogenase from poplar stems (Populus X euramericana). *European journal of biochemistry / FEBS*, 139(2), 259-65.

Sattler, S.E., Saathoff, A.J., Haas, E.J., Palmer, N.A., Funnell-Harris, D.L., Sarath, G. and Pedersen, J.F., (2009) A nonsense mutation in a cinnamyl alcohol dehydrogenase gene is responsible for the Sorghum brown midrib6 phenotype. *Plant physiology*, 150(2), 584-95.

Sebat, J., Lakshmi, B., Troge, J., *et al.*, (2004) Large-scale copy number polymorphism in the human genome. *Science (New York, N.Y.)*, 305(5683), 525-8.

Sham, P., Bader, J.S., Craig, I., O Donovan, M. and Owen, M., (2002) DNA Pooling: a tool for large-scale association studies. *Nature reviews. Genetics*, 3(11), 862-871.

Shendure, J. and Ji, H., (2008) Next-generation DNA sequencing. *Nature biotechnology*, 26(10), 1135-45.

Shi, R., Sun, Y.-H., Li, Q., Heber, S., Sederoff, R. and Chiang, V.L., (2010) Towards a systems approach for lignin biosynthesis in Populus trichocarpa: transcript abundance and specificity of the monolignol biosynthetic genes. *Plant & cell physiology*, 51(1), 144-163.

Sjödin, A., Bylesjö, M., Skogström, O., Eriksson, D., Nilsson, P., Rydén, P., Jansson, Stefan and Karlsson, J., (2006) UPSC-BASE--Populus transcriptomics online. *The Plant journal : for cell and molecular biology*, 48(5), 806-17.

Smith, S.M., Pryor, A.J. and Hulbert, S.H., (2004) Allelic and haplotypic diversity at the rp1 rust resistance locus of maize. *Genetics*, 167(4), 1939-47.

Smulders, M.J.M., Cottrell, J.E., Lefèvre, F., *et al.*, (2008) Structure of the genetic diversity in black poplar (Populus nigra L.) populations across European river systems: Consequences for conservation and restoration. *Forest Ecology and Management*, 255(5-6), 1388-1399.

Springer, N.M. and Stupar, R.M., (2007) Allelic variation and heterosis in maize: how do two halves make more than a whole? *Genome research*, 17(3), 264-75.

Springer, N.M., Ying, K., Fu, Y., *et al.*, (2009) Maize inbreds exhibit high levels of copy number variation (CNV) and presence/absence variation (PAV) in genome content. *PLoS genetics*, 5(11), e1000734.

Stephens, M., Sloan, J.S., Robertson, P.D., Scheet, P. and Nickerson, D.A., (2006) Automating sequence-based detection and genotyping of SNPs from diploid samples. *Nature genetics*, 38(3), 375-81.

Stephens, M., Smith, N.J. and Donnelly, P., (2001) A new statistical method for haplotype reconstruction from population data. *American journal of human genetics*, 68(4), 978-89.

Stupar, R.M. and Springer, N.M., (2006) Cis-transcriptional variation in maize inbred lines B73 and Mo17 leads to additive expression patterns in the F1 hybrid. *Genetics*, 173(4), 2199-210.

Sudmant, P.H., Kitzman, J.O., Antonacci, F., *et al.*, (2010) Diversity of human copy number variation and multicopy genes. *Science (New York, N.Y.)*, 330(6004), 641-6.

Tajima, F., (1989) Statistical method for testing the neutral mutation hypothesis by DNA polymorphism. *Genetics*, 123(3), 585-595.

Terwilliger, J.D. and Hiekkalinna, T., (2006) An utter refutation of the "fundamental theorem of the HapMap". *European journal of human genetics : EJHG*, 14(4), 426-37.

Tuskan, G.A., Difazio, S., Jansson, S, *et al.*, (2006) The genome of black cottonwood, Populus trichocarpa (Torr. & Gray). *Science (New York, N.Y.)*, 313(5793), 1596-604.

Tuzun, E., Sharp, A.J., Bailey, J.A., *et al.*, (2005) Fine-scale structural variation of the human genome. *Nature genetics*, 37(7), 727-32.

Untergasser, A., Nijveen, H., Rao, X., Bisseling, Ton, Geurts, R. and Leunissen, J.A.M., (2007) Primer3Plus, an enhanced web interface to Primer3. *Nucleic acids research*, 35(Web Server issue), W71-74.

VanLiere, J.M. and Rosenberg, N.A., (2008) Mathematical properties of the r2 measure of linkage disequilibrium. *Theoretical population biology*, 74(1), 130-7.

Vanholme, R., Morreel, K., Ralph, J. and Boerjan, Wout, (2008) Lignin engineering. *Current opinion in plant biology*, 11(3), 278-285.

Ventura, M., Catacchio, C.R., Alkan, C., *et al.*, (2011) Gorilla genome structural variation reveals evolutionary parallelisms with chimpanzee. *Genome research*, 21(10), 1640-9.

Volik, S., Zhao, S., Chin, K., *et al.*, (2003) End-sequence profiling: sequence-based analysis of aberrant genomes. *Proceedings of the National Academy of Sciences of the United States of America*, 100(13), 7696-701.

Walter, M.H., Grima-Pettenati, J., Grand, C., Boudet, A M and Lamb, C.J., (1988) Cinnamyl-alcohol dehydrogenase, a molecular marker specific for lignin synthesis: cDNA cloning and mRNA induction by fungal elicitor. *Proceedings of the National Academy of Sciences of the United States of America*, 85(15), 5546-50.

Weigel, D. and Mott, R., (2009) The 1001 genomes project for Arabidopsis thaliana. *Genome biology*, 10(5), 107.

Weng, J.-K. and Chapple, C., (2010) The origin and evolution of lignin biosynthesis. *The New phytologist*, 187(2), 273-85.

Weng, J.-K., Li, X., Bonawitz, N.D. and Chapple, C., (2008) Emerging strategies of lignin engineering and degradation for cellulosic biofuel production. *Current opinion in biotechnology*, 19(2), 166-72.

Yang, L. and Bennetzen, Jeffrey L, (2009) Distribution, diversity, evolution, and survival of Helitrons in the maize genome. *Proceedings of the National Academy of Sciences of the United States of America*, 106(47), 19922-7.

Yoon, S., Xuan, Z., Makarov, V., Ye, K. and Sebat, J., (2009) Sensitive and accurate detection of copy number variants using read depth of coverage. *Genome research*, 19(9), 1586-92.

You, F.M., Huo, N., Gu, Y.Q., Luo, M.-C., Ma, Y., Hane, D., Lazo, G.R., Dvorak, J. and Anderson, O.D., (2008) BatchPrimer3: a high throughput web application for PCR and sequencing primer design. *BMC bioinformatics*, 9, 253.

Youn, B., Camacho, R., Moinuddin, S.G.A., Lee, Choonseok, Davin, L.B., Lewis, N.G. and Kang, C., (2006) Crystal structures and catalytic mechanism of the

Arabidopsis cinnamyl alcohol dehydrogenases AtCAD5 and AtCAD4. *Organic & biomolecular chemistry*, 4(9), 1687-97.

Zhang, H.B., Zhao, X., Ding, X., Paterson, A.H. and Wing, R.A., (1995) Preparation of megabase-size DNA from plant nuclei. *The Plant Journal*, 7(1), 175-184.

Acknowledgments

I would like to express my gratitude to my supervisor Prof. Michele Morgante for providing me with the opportunity to complete my PhD thesis at the Institute of Applied Genomics and for his expert guidance during these last three years.

A very special thanks goes out to my co-supervisor Dr. Fabio Marroni for his invaluable teaching, for his helpfulness and friendship, and for sharing with me his "*ginial*" ideas.

I would also like to thank all my colleagues of the Institute of Applied Genomics for their great support and for the friendly atmosphere.

Last but not least, I wish to thank my family and Michele for giving me always their support.

The work described in the present thesis has been supported by the European Commission within the Seventh Framework Programme for Research, Project Energypoplar (FP7-211917).